

Characterizing the SLOPE Trade-off: A Variational Perspective and the Donoho–Tanner Limit

Zhiqi Bu^{*†} Jason M. Klusowski[‡] Cynthia Rush[§] Weijie J. Su[¶]

May 28, 2021

Abstract

Sorted ℓ_1 regularization has been incorporated into many methods for solving high-dimensional statistical estimation problems, including the SLOPE estimator in linear regression. In this paper, we study how this relatively new regularization technique improves variable selection by characterizing the optimal SLOPE trade-off between the false discovery proportion (FDP) and true positive proportion (TPP) or, equivalently, between measures of type I error and power. Assuming a regime of linear sparsity and working under Gaussian random designs, we obtain an upper bound on the optimal trade-off for SLOPE, showing its capability of breaking the Donoho–Tanner power limit. To put it into perspective, this limit is the highest possible power that the Lasso, which is perhaps the most popular ℓ_1 -based method, can achieve even with arbitrarily strong effect sizes. Next, we derive a tight lower bound that delineates the fundamental limit of sorted ℓ_1 regularization in optimally trading the FDP off for the TPP. Finally, we show that on any problem instance, SLOPE with a certain regularization sequence outperforms the Lasso, in the sense of having a smaller FDP, larger TPP and smaller ℓ_2 estimation risk simultaneously. Our proofs are based on a novel technique that reduces a variational calculus problem to a class of infinite-dimensional convex optimization problems and a very recent result from approximate message passing theory.

1 Introduction

Reconstructing the signal from noisy linear measurements is vital in many disciplines, including statistical learning, signal processing, and biomedical imaging. In many modern applications where the number of explanatory variables often exceeds the number of measurements, the signal is often believed—or, wished—to be sparse in the sense that most of its entries are zero or approximately zero. Put differently, this means that a majority of the explanatory variables are simply irrelevant to the response of interest.

Accordingly, a host of methods have been developed to tackle these problems by leveraging the sparsity of signals in high-dimensional linear regression. These methods often rely on, among

^{*} Author names are listed alphabetically.

[†] Graduate Group in Applied Mathematics and Computational Science, University of Pennsylvania. Email: zbu@sas.upenn.edu

[‡] Department of Operations Research and Financial Engineering, Princeton University. Email: jason.klusowski@princeton.edu

[§] Department of Statistics, Columbia University. Email: cynthia.rush@columbia.edu

[¶] Department of Statistics, University of Pennsylvania. Email: suw@wharton.upenn.edu

others, the concept of *regularization* to constrain the search space of the unknown signals. Perhaps the most influential instantiation of this concept is ℓ_1 regularization, which gives rise to the Lasso method (Tibshirani, 1996). The optimal amount of regularization, however, hinges on the sparsity level of the signal. Intuitively speaking, if the sparsity level is low, then more regularization should be imposed, and vice versa (see, for example, Abramovich et al. (2006)).

This intuition necessitates the development of a regularization technique that is adaptive to the sparsity level of signals, which is typically unknown in practical problems. To achieve this desired adaptivity, Bogdan et al. (2015) introduced *sorted ℓ_1 regularization*. This new regularization technique turns into a method called SLOPE in the setting of a linear regression model

$$\mathbf{y} = \mathbf{X}\boldsymbol{\beta} + \mathbf{w}, \tag{1.1}$$

where \mathbf{X} is the $n \times p$ design matrix, $\boldsymbol{\beta} \in \mathbb{R}^p$ are the regression coefficients, $\mathbf{y} \in \mathbb{R}^n$ is the response, and $\mathbf{w} \in \mathbb{R}^n$ is the noise term. Explicitly, SLOPE estimates the coefficients by solving the convex programming problem

$$\arg \min_{\mathbf{b}} \frac{1}{2} \|\mathbf{y} - \mathbf{X}\mathbf{b}\|^2 + \sum_{i=1}^p \lambda_i |b_{(i)}|, \tag{1.2}$$

where $|b_{(1)}| \geq \dots \geq |b_{(p)}|$ are the order statistics in absolute value of $\mathbf{b} = (b_1, \dots, b_p)$ and $\lambda_1 \geq \dots \geq \lambda_p \geq 0$ (with at least one strict inequality) are the regularization parameters. The sorted ℓ_1 penalty, $\sum_{i=1}^p \lambda_i |b_{(i)}|$, is a norm, and the optimization problem for SLOPE is, therefore, convex (see also Figueiredo and Nowak (2016)). As an important feature, the sorted ℓ_1 norm penalizes larger entries more heavily than smaller ones. Indeed, this regularization technique is shown to be adaptive to the degree of sparsity level and enables SLOPE to obtain optimal estimation performance for certain problems (Su and Candès, 2016). Notably, in the special case $\lambda_1 = \dots = \lambda_p$, the sorted ℓ_1 norm reduces to the usual ℓ_1 norm. Thus, the Lasso can be regarded as a special instance of SLOPE.

A fundamental question, yet to be better addressed, is how to quantitatively characterize the benefits of using the sorted ℓ_1 regularization. To explore this question, Figure 1 compares the model selection performance of SLOPE and the Lasso in terms of the *false discovery proportion* (FDP) and *true positive proportion* (TPP) or, equivalently, between measures of type I error and power. Needless to say, a model is preferred if its FDP is small while its TPP is large. As the first impression conveyed by this figure, both methods seem to undergo a trade-off between the FDP and TPP when the TPP is below a certain limit. More interestingly, while *nowhere* on the Lasso path is the TPP above a limit, which is about 0.5707 in the left plot of Figure 1 and 0.4343 in the right, SLOPE is able to pass the limit toward achieving full power. To be sure, these contrasting patterns persist even for an arbitrarily large signal-to-noise ratio. This distinction must be attributed to the flexibility of the SLOPE regularization sequence $(\lambda_1, \dots, \lambda_p)$ compared to a single value as in the Lasso case. Recognizing this message, we are tempted to ask (1) *why* the use of sorted ℓ_1 regularization brings a significant benefit over ℓ_1 regularization in the high TPP regime and, equally importantly, (2) *why* SLOPE exhibits a trade-off between the FDP and TPP just as the Lasso does in the low TPP regime.

1.1 A peek at our results

To address these two questions, in this paper we characterize the optimal trade-off of SLOPE between the TPP and FDP, uncovering several intriguing findings of sorted ℓ_1 regularization. Assuming $\text{TPP} \approx u$ for $0 \leq u \leq 1$, loosely speaking, the trade-off curve gives the smallest possible value of

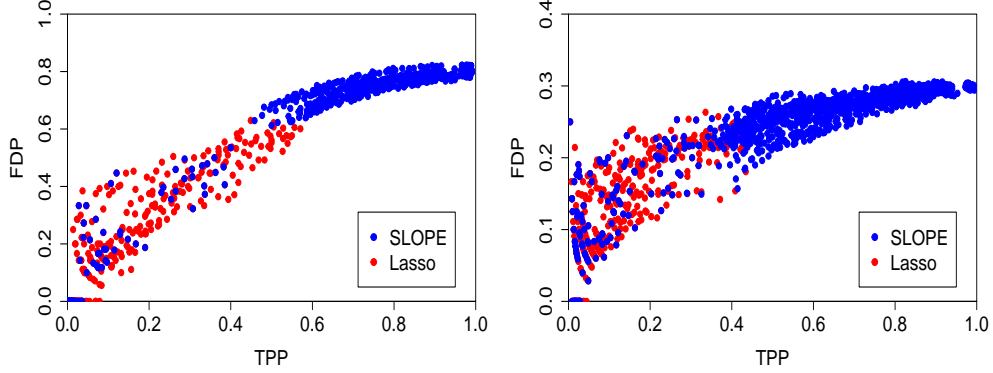


Figure 1: Comparison between SLOPE and the Lasso in terms of the TPP–FDP trade-off. Given an estimate $\hat{\beta}$, define its FDP = $\frac{|\{j:\beta_j=0 \text{ and } \hat{\beta}_j \neq 0\}|}{|\{j:\hat{\beta}_j \neq 0\}|}$ and TPP = $\frac{|\{j:\beta_j \neq 0 \text{ and } \hat{\beta}_j = 0\}|}{|\{j:\beta_j \neq 0\}|}$. The SLOPE regularization sequence $\lambda_{\lambda, r\lambda, w}$ is defined in (2.3), with varying $0 < r < 1$ and $\lambda > 0$, and $w = 0.2$ in the left plot and $w = 0.3$ in the right plot. The results of the Lasso are taken over its entire solution path, and its highest TPP is about 0.5707 in the left plot and 0.4343 in the right plot. Left: $(n, p) = (300, 1000)$, $|\{j : \beta_j \neq 0\}|/p = 0.2$, and $\mathbf{w} = \mathbf{0}$ (noiseless); right: $(n, p) = (400, 1000)$, $|\{j : \beta_j \neq 0\}|/p = 0.7$, and $\mathbf{w} = \mathbf{0}$. On both plots, non-zero entries of β are i.i.d. draws from the standard normal distribution. More specifications of the setup are detailed in Section 2. The result presents 10 independent trials.

the FDP of SLOPE using any regularization sequence in the large system limit. To prepare for a rough description of our contributions, in brief, we work in the setting where the design has i.i.d. Gaussian entries and the regression coefficients β_1, \dots, β_p are i.i.d. draws from a distribution that takes non-zero values with a certain probability. Notably, it is generally nontrivial to define false discoveries in high dimensions (G’Sell et al., 2013), which is not an issue however in the case of independent regressors. The assumption on the signal prior corresponds to the *linear sparsity* regime. In addition, we assume that both $n, p \rightarrow \infty$ and the sampling ratio n/p converges to a constant (see more detailed assumptions in Section 2). From a technical viewpoint, these assumptions allow us to make use of tools from approximate message passing (AMP) theory (Donoho et al., 2009; Bayati and Montanari, 2011).

Breaking the Donoho–Tanner power limit To explain the contrasting results presented in Figure 1, we prove that under the aforementioned assumptions, SLOPE can achieve an arbitrarily high TPP. Moving from sorted ℓ_1 regularization to ℓ_1 regularization, in stark contrast, the Lasso exhibits the Donoho–Tanner (DT) power limit when $n < p$ and the sparsity is above a certain threshold (Donoho, 2006, 2005). Informally, the DT power limit is the largest possible power that any estimate along the Lasso path can achieve in the large system limit. For example, in the setting of Figure 1 this power limit is about 0.5676 in the left plot and 0.4401 in the right plot. For SLOPE and a certain choice of the regularization sequence, interestingly, we show that the asymptotic TPP-FDP trade-off of SLOPE beyond the DT power limit is given by a simple Möbius transformation, which is shown by the blue curve in Figure 2. This Möbius transformation naturally serves as an upper bound on the (optimal) SLOPE trade-off curve above the DT power limit.

Lower bound via convex optimization Next, we address the second question by lower bounding the optimal trade-off for SLOPE, followed by a comparison between the trade-offs for the two methods in the low TPP regime. To put it into perspective, the Lasso trade-off obtained by Su et al. (2017) is plotted as the green solid curve in Figure 2. Apart from the simple fact that the SLOPE trade-off is better than or equal to the Lasso counterpart, however, it requires new tools to take into account the structure of sorted ℓ_1 regularization. To this end, we develop a technique based on a class of infinite-dimensional convex optimization problems. The resulting lower bound is shown in red in Figure 2. It is worth noting that the development of this technique presents several novel ideas that might be of independent interest for other regularization schemes.

Instance superiority of SLOPE The results illustrated so far are taken from an optimal-case viewpoint. Moving to a more practical standpoint, we are interested in comparing the two methods on a specific problem instance and, in particular, wish to find a SLOPE regularization sequence that allows SLOPE to outperform the Lasso with any given penalty parameter in terms of, for example, the TPP, the FDP, or the ℓ_2 estimation risk. Surprisingly, we prove that on any problem instance, SLOPE can dominate the Lasso according to these three indicators simultaneously. This comparison conveys the message that the flexibility of the sorted ℓ_1 regularization can turn into appreciable benefits. This result is formally stated in Theorem 3.

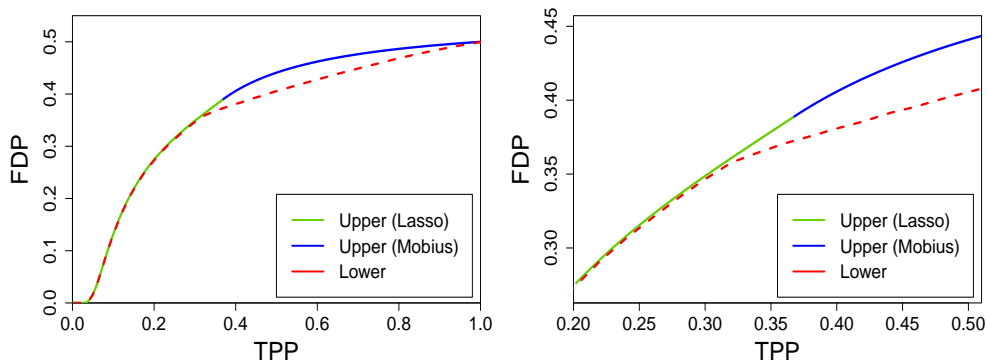


Figure 2: Illustration of the upper bound q^* and lower bound q_* for the SLOPE TPP–FDP trade-off. The right plot is the zoom-in of the left. Here $n/p = 0.3$ and $|\{j : \beta_j \neq 0\}|/p = 0.5$ (see more details in the working assumptions in Section 2). The Lasso trade-off curve shown in green is truncated at the DT power limit about 0.3669 (Su et al., 2017). The optimal SLOPE trade-off curve must lie between the two curves. Notably, the two bounds agree at $\text{TPP} = 1$.

1.2 Organization

The remainder of this paper is structured as follows. In Section 2, we present the main results of this paper. Next, Section 3 introduces the AMP machinery at a minimal level as a preparation for the proofs of our main results. In Section 4, we detail the derivation of the lower bound based on variational calculus and infinite-dimensional convex optimization. In Section 5, we specify the upper bound, especially the part given by a Möbius transformation above the DT power limit. We conclude this paper in Section 6 by proposing several future research directions. Omitted proofs are relegated to the appendix.

2 Main results

Throughout this paper, we make the following working assumptions to specify the design matrix $\mathbf{X} \in \mathbb{R}^{n \times p}$, regression coefficients $\boldsymbol{\beta} \in \mathbb{R}^p$, and noise $\mathbf{w} \in \mathbb{R}^n$ in the linear model (1.1), as well as the SLOPE regularization sequence $\boldsymbol{\lambda} = (\lambda_1, \dots, \lambda_p)$. To obviate any ambiguity, we consider a sequence of problems indexed by (n, p) with both n, p tending to infinity.

- (A1) The matrix \mathbf{X} has i.i.d. $\mathcal{N}(0, 1/n)$ entries. The sampling ratio n/p converges to a constant $\delta > 0$.
- (A2) The entries of $\boldsymbol{\beta}$ are i.i.d. copies of a random variable Π satisfying $\mathbb{P}(\Pi \neq 0) = \epsilon$ for a constant $0 < \epsilon < 1$ and $\mathbb{E}(\Pi^2 \max\{0, \log \Pi\}) < \infty$. The noise vector \mathbf{w} consists of i.i.d. copies of a random variable W with bounded second moment $\sigma^2 := \mathbb{E}(W^2) < \infty$.
- (A3) The SLOPE regularization sequence $\boldsymbol{\lambda}(p) = (\lambda_1, \dots, \lambda_p)$ is the order statistics of p i.i.d. realizations of a (nontrivial) non-negative random variable Λ .

Moreover, we assume that $\mathbf{X}, \boldsymbol{\beta}$, and \mathbf{w} are independent. Notice that the sparsity level of $\boldsymbol{\beta}$ is about ϵp and that each column of \mathbf{X} has approximately a unit ℓ_2 norm. The noise variance σ^2 can equal 0, meaning that our results apply to both noisy and noiseless settings. In (A3), by “nontrivial” we mean that Λ is not always equal to 0. As an aside, SLOPE is reduced to the Lasso if the distribution of Λ is a unit probability mass at some positive value.

The working assumptions are mainly driven by their necessity in AMP theory (Donoho et al., 2009; Bayati and Montanari, 2011), which enables the use of the recent analysis of an AMP algorithm when applied to solve SLOPE (Hu and Lu, 2019; Bu et al., 2020). Regarding (A2), the condition $\mathbb{P}(\Pi \neq 0) = \epsilon$, which implies linear sparsity of the regression coefficients, is not required for AMP theory. Rather, this condition is only made so that the TPP and FDP are well-defined. Besides, the merit of the linear sparsity regime has been increasingly recognized in the high-dimensional literature (Mousavi et al., 2018; Weng et al., 2018; Su, 2018; Sur et al., 2019; Wang et al., 2019).

2.1 Bounds on the SLOPE trade-off

Our main result is the characterization of a trade-off curve that teases apart asymptotically achievable TPP and FDP pairs from the asymptotically unachievable pairs for SLOPE¹. For any estimate $\widehat{\boldsymbol{\beta}}$, recall that its FDP and TPP are defined as

$$\text{FDP} = \frac{|\{j : \beta_j = 0 \text{ and } \widehat{\beta}_j \neq 0\}|}{|\{j : \widehat{\beta}_j \neq 0\}|}, \quad \text{TPP} = \frac{|\{j : \beta_j \neq 0 \text{ and } \widehat{\beta}_j \neq 0\}|}{|\{j : \beta_j \neq 0\}|},$$

with the convention $0/0 = 0$. When it comes to the SLOPE estimator, we use $\text{TPP}(\boldsymbol{\beta}, \boldsymbol{\lambda})$ and $\text{FDP}(\boldsymbol{\beta}, \boldsymbol{\lambda})$ to denote its TPP and FDP, respectively.

Our main results are stated in the following two theorems, which give lower and upper bounds on the optimal SLOPE trade-off. Taken together, they demonstrate a fundamental separation between asymptotically achievable TPP–FDP pairs and the unachievable pairs over all signal priors Π and SLOPE regularization sequences $\boldsymbol{\lambda}$. Note that both the upper bound q^* and lower bound q_* are defined on $[0, 1]$ and completely determined by ϵ and δ . The expression for q^* is given in (2.7), while q_* is detailed in Section 4.

¹R code to reproduce the results, e.g., to calculate q_* and q^* , is available at https://github.com/woodyx218/SLOPE_AMP.

Theorem 1 (Lower bound). *Under the working assumptions, namely (A1), (A2), and (A3), the following inequality holds with probability tending to one:*

$$\text{FDP}(\boldsymbol{\beta}, \boldsymbol{\lambda}) \geq q_{\star}(\text{TPP}(\boldsymbol{\beta}, \boldsymbol{\lambda}); \delta, \epsilon) - 0.0001.$$

Theorem 2 (Upper bound). *For any $0 \leq u \leq 1$, there exist a signal prior Π and a SLOPE regularization prior Λ satisfying the working assumptions such that the following inequalities hold with probability tending to one:*

$$\text{FDP}(\boldsymbol{\beta}, \boldsymbol{\lambda}) \leq q^{\star}(\text{TPP}(\boldsymbol{\beta}, \boldsymbol{\lambda}); \delta, \epsilon) + 0.0001 \quad \text{and} \quad |\text{TPP}(\boldsymbol{\beta}, \boldsymbol{\lambda}) - u| \leq 0.0001.$$

Remark 2.1. Above, 0.0001 can be replaced by an arbitrarily small positive constant. The probability is taken with respect to the randomness in the design matrix, regression coefficients, noise, and SLOPE regularization sequence in the large system limit $n, p \rightarrow \infty$. In relating to the assumptions made previously, this theorem holds even for $\sigma^2 = 0$, the noiseless case.

The proofs of Theorem 1 and Theorem 2 are given in Section 4 and Section 5, respectively. Most notably, our proof of Theorem 1 starts by formulating the problem of finding a tight lower bound as a calculus of variations problem. Relying on several novel elements, we further reduce this problem to a class of infinite-dimensional convex programs.

On the one hand, Theorem 1 says that it is impossible to achieve high power and a low FDP simultaneously using any sorted ℓ_1 regularization sequences, and this trade-off is specified by q_{\star} . On the other hand, Theorem 2 demonstrates that SLOPE can achieve at least the same trade-off as that given by q^{\star} by specifying a prior Π and a regularization sequence $\boldsymbol{\lambda}$. Indeed, the proof of this theorem is constructive in that we will show that SLOPE can come arbitrarily close to any point on the curve q^{\star} in Section 5. Another important observation from Theorem 2 is that SLOPE can achieve any power levels, which is not necessarily the case for ℓ_1 regularization-based methods as we show in Section 2.2.

Informally, let q_{SLOPE} denote the optimal SLOPE trade-off curve. That is, $q_{\text{SLOPE}}(u)$ is asymptotically the minimum possible value of the FDP under the constraint that the TPP is about u , over all possible SLOPE regularization sequences (see formal definition in Section 3). Combining the two theorems above, we readily see that the optimal SLOPE trade-off must be sandwiched between q^{\star} and q_{\star} :

$$q_{\star}(u) \leq q_{\text{SLOPE}}(u) \leq q^{\star}(u)$$

for all $0 \leq u \leq 1$. Consequently, the sharpness of the approximation to the SLOPE trade-off rests on the gap between the two curves. Figure 3 illustrates several examples of the two curves for various pairs of ϵ, δ . Importantly, the plots show that the two bounds are very close to each other, thereby demonstrating tightness of our bounds. Furthermore, a closer look at the plots reveals that the two curves seem to coincide exactly when the TPP is below a certain value. In this regard, the SLOPE trade-off might have been uncovered exactly in this regime of TPP. Future investigation is required to obtain a fine-grained comparison between the two curves.

To be complete, we remark that the message conveyed by these two theorems does not contradict earlier results established for FDR control of SLOPE (Bogdan et al., 2013a, 2015; Brzyski et al., 2019; Kos and Bogdan, 2020). The crucial difference between the two sides arises from the linear sparsity assumed in the present paper, which is a clear departure from the much lower sparsity level considered in the literature. In this regard, our results complement the literature by extending our understanding of the inferential properties of the SLOPE method to an uncharted regime.

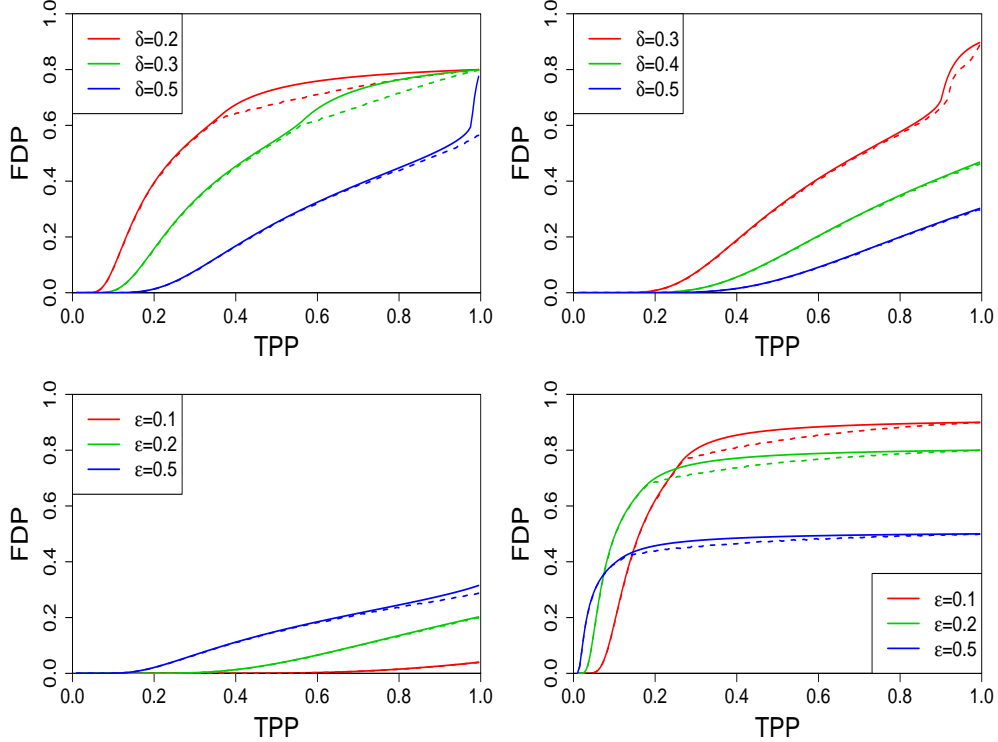


Figure 3: Examples of the SLOPE trade-off bounds q^* and q_* for different (δ, ϵ) pairs. Top-left: $\epsilon = 0.2$; top-right: $\epsilon = 0.1$; bottom-left: $\delta = 0.9$; bottom-right: $\delta = 0.1$. For a given δ , note that the trade-off for SLOPE is not monotone with respect to ϵ , which is a departure from the Lasso counterpart (see Su et al. (2017, Figure 4)). Numerically, the upper and lower bounds seem to coincide when the TPP is below a threshold (see more details in Figure 5).

2.2 Breaking the Donoho–Tanner power limit

To better appreciate the trade-off results presented in Theorem 2 for SLOPE, it is instructive to compare them with the TPP and FDP trade-off for the Lasso, which is arguably the most popular method leveraging ℓ_1 regularization.

To put it into perspective, first recall some results concerning the optimal trade-off between the TPP and FDP for the Lasso. A surprising fact is that under the working assumptions,² the Lasso cannot achieve full power even with an arbitrarily large signal-to-noise ratio when $\delta < 1$ (that is, \mathbf{X} is “fat”) and the sparsity ratio ϵ is above a threshold, which we denote by $\epsilon^*(\delta)$. The dependence of this value on δ is specified by the parametric equations

$$\delta = \frac{2\phi(s)}{2\phi(s) + s(2\Phi(s) - 1)}, \quad \epsilon^* = \frac{2\phi(s) - 2s\Phi(-s)}{2\phi(s) + s(2\Phi(s) - 1)} \quad (2.1)$$

for $s > 0$.³ For simplicity, henceforth (δ, ϵ) is said to be in the *supercritical* regime if $\delta < 1, \epsilon > \epsilon^*(\delta)$. Otherwise, it is in the *subcritical* regime when $\delta < 1, \epsilon \leq \epsilon^*(\delta)$, or $\delta \geq 1$ (that is, \mathbf{X} is “thin”).

²Note that, in the case of the Lasso, (A3) is replaced by the assumption that $\lambda > 0$ is a constant.

³In the compressed sensing literature, ϵ^* corresponds to the sparsity level where the Donoho–Tanner phase transition occurs (Donoho and Tanner, 2009b,a).

In the supercritical regime, Su et al. (2017) proved that the highest achievable TPP of the Lasso, denoted u_{DT}^* , takes the form

$$u_{\text{DT}}^*(\delta, \epsilon) := 1 - \frac{(1 - \delta)(\epsilon - \epsilon^*)}{\epsilon(1 - \epsilon^*)} < 1. \quad (2.2)$$

Throughout the paper, u_{DT}^* is referred to as the *DT power limit*. For completeness, in the subcritical regime the Lasso can achieve any power level. As such, we formally set $u_{\text{DT}}^*(\delta, \epsilon) = 1$ when $\delta < 1$, $\epsilon \leq \epsilon^*(\delta)$, or $\delta \geq 1$.

This existing result, in conjunction with Theorem 2, immediately gives the following contrasting result concerning the Lasso and SLOPE. We use $\text{TPP}_{\text{Lasso}}(\boldsymbol{\beta}, \lambda)$ and $\text{FDP}_{\text{Lasso}}(\boldsymbol{\beta}, \lambda)$ to denote, respectively, the TPP and FDP of the Lasso with penalty parameter λ . Likewise, we use $\text{TPP}_{\text{SLOPE}}(\boldsymbol{\beta}, \boldsymbol{\lambda})$ and $\text{FDP}_{\text{SLOPE}}(\boldsymbol{\beta}, \boldsymbol{\lambda})$ to denote those of SLOPE.

Corollary 2.2 (SLOPE breaks the DT power limit). *In the supercritical regime, the following conclusions hold under the working assumptions:*

- (a) *The power of the Lasso satisfies $\text{TPP}_{\text{Lasso}}(\boldsymbol{\beta}, \lambda) < u_{\text{DT}}^*$ with probability tending to one.*
- (b) *For any $0 \leq u < 1$, there exist a SLOPE regularization prior Λ and a signal prior Π such that $\text{TPP}_{\text{SLOPE}}(\boldsymbol{\beta}, \boldsymbol{\lambda}) > u$ with probability tending to one.*

For illustration, Figure 1 in the introduction reflects this distinction between SLOPE and the Lasso with $u_{\text{DT}}^*(0.4, 0.7) = 0.4401$ in the left plot. Another illustration is Figure 1 right plot and Figure 4, which is vertically truncated at $u_{\text{DT}}^*(0.3, 0.2) = 0.5676$.

Corollary 2.2 highlights the benefit of using sorted ℓ_1 regularization over the less flexible ℓ_1 regularization in terms of power. This sharp distinction persists no matter how large the effect sizes are and, therefore, it must be attributed to the flexibility of the SLOPE regularization sequence. As is well-known, the Lasso selects no more than n variables. Worse, a significant proportion of false variables are always interspersed on the Lasso path in the linear sparsity regime and, therefore, even though the Lasso can select up to $n > k$ variables, it would always miss a fraction of true variables, thereby imposing a limit on the power. In contrast, SLOPE does not bear the constraint that $\|\widehat{\boldsymbol{\beta}}\|_0 \leq n$ owing to the flexibility of its regularization sequence. In fact, the corresponding constraint for SLOPE is that the number of *unique* non-zero entries is no more than n (Su and Candès, 2016). This flexibility allows SLOPE to have arbitrarily high power regardless of the regime (δ, ϵ) belongs to.

Moving forward, we ask which regularization prior Λ and signal prior Π are “flexible” enough to enable SLOPE to break the DT power limit. To achieve desired flexibility, interestingly, it only requires a simple two-level regularization sequence for SLOPE. Consider the following *two-level* SLOPE regularization prior: given constants $a > b \geq 0$ and $0 < w < 1$, let $\Lambda_{a,b,w} = a$ with probability w and otherwise $\Lambda_{a,b,w} = b$. The SLOPE regularization sequence drawn from this prior takes the form

$$\boldsymbol{\lambda}_{a,b,w} := \left(\underbrace{a, a, \dots, a}_{\text{about } wp}, \underbrace{b, b, \dots, b}_{\text{about } (1-w)p} \right). \quad (2.3)$$

Next, for any $M > 0$ and $0 \leq \epsilon' \leq 1$, define the following signal prior:

$$\Pi_M(\epsilon') := \begin{cases} M, & \text{w.p. } \epsilon' \\ M^{-1}, & \text{w.p. } \epsilon - \epsilon' \\ 0, & \text{w.p. } 1 - \epsilon. \end{cases} \quad (2.4)$$

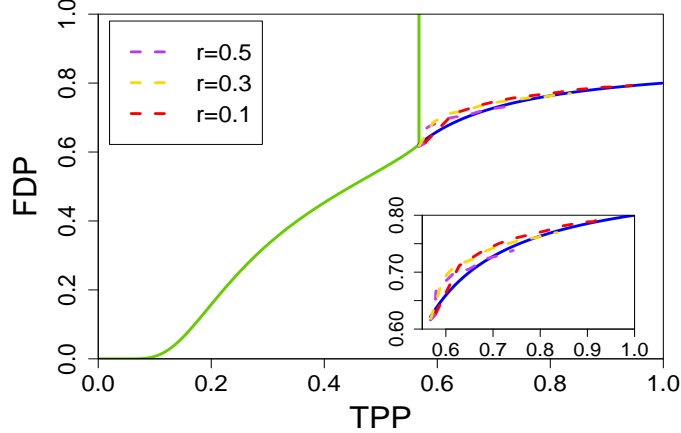


Figure 4: The Möbius part of the SLOPE trade-off upper bound q^* . The solid curve denotes the upper bound specified by $(\delta, \epsilon) = (0.3, 0.2)$. The numerical pairs of the TPP and FDP are obtained from experiments that are specified by the following parameters: $n = 300, p = 1000, \sigma^2 = 0$, signal prior $\Pi_M(\epsilon^*/\epsilon)$ with $M = 10000$ in (2.4) (note that $\epsilon^*(0.3) = 0.087$), and regularization prior $\lambda_{\sqrt{M}, r\sqrt{M}, w}$ in (2.3) with varying w . Each pair is averaged over 50 independent trials.

Henceforth in this paper, denote by $\beta_M(\epsilon')$ the regression coefficients sampled from $\Pi_M(\epsilon')$.

Now we are ready to state the following result, which shows that SLOPE with the two-level regularization sequence can approach any point on the Möbius transformation (2.5) arbitrarily close. This result also partially specifies the upper bound q^* in Theorem 2 in the supercritical regime:

$$q^*(u; \delta, \epsilon) = \frac{\epsilon(1 - \epsilon)u - \epsilon^*(1 - \epsilon)}{\epsilon(1 - \epsilon^*)u - \epsilon^*(1 - \epsilon)} \quad (2.5)$$

for $u_{\text{DT}}^* \leq u \leq 1$ (above the DT power limit). Note that this function takes the form of a *Möbius transformation*. Notably, taking $u = 1$ gives $q^*(1; \delta, \epsilon) = \frac{(\epsilon - \epsilon^*)(1 - \epsilon)}{\epsilon(1 - \epsilon^*) - \epsilon^*(1 - \epsilon)} = 1 - \epsilon$.

Proposition 2.3. *For any $u_{\text{DT}}^* \leq u \leq 1$ in the supercritical regime, there exist w such that $\lambda_{a,b,w}$ and $\beta_M(\epsilon^*/\epsilon)$ make SLOPE approach the point $(u, q^*(u))$ in the sense*

$$\lim_{M \rightarrow \infty} \lim_{n, p \rightarrow \infty} (\text{TPP}(\beta_M(\epsilon^*/\epsilon), \lambda_{a,b,w}), \text{FDP}(\beta_M(\epsilon^*/\epsilon), \lambda_{a,b,w})) \rightarrow (u, q^*(u)),$$

where $a = \sqrt{M}, b = r\sqrt{M}$ for a certain value $0 \leq r \leq 1$.

Figure 4 provides a numerical example that corroborates this proposition.

This result in fact implies Theorem 2 for $u_{\text{DT}}^* \leq u \leq 1$ in the supercritical regime. Note that the first limit $\lim_{n, p \rightarrow \infty}$ is taken in the sense of convergence in probability. See more details in its proof in Section 5.1. It is worthwhile to mention that the three-component mixture (2.4) is considered in Su et al. (2017) for the construction of favorable priors under sparsity constraint (see a generalization in Wang et al. (2020b)). This mixture prior is used to ensure that the effect sizes are either very strong or very weak. In particular, Proposition 2.3 remains true if M and $1/M$ are replaced by any value diverging to infinity and any value converging to 0, respectively.

2.3 Below the Donoho–Tanner power limit

Next, we continue to interpret Theorem 1 and Theorem 2, but with a focus on the regime below the DT power limit.

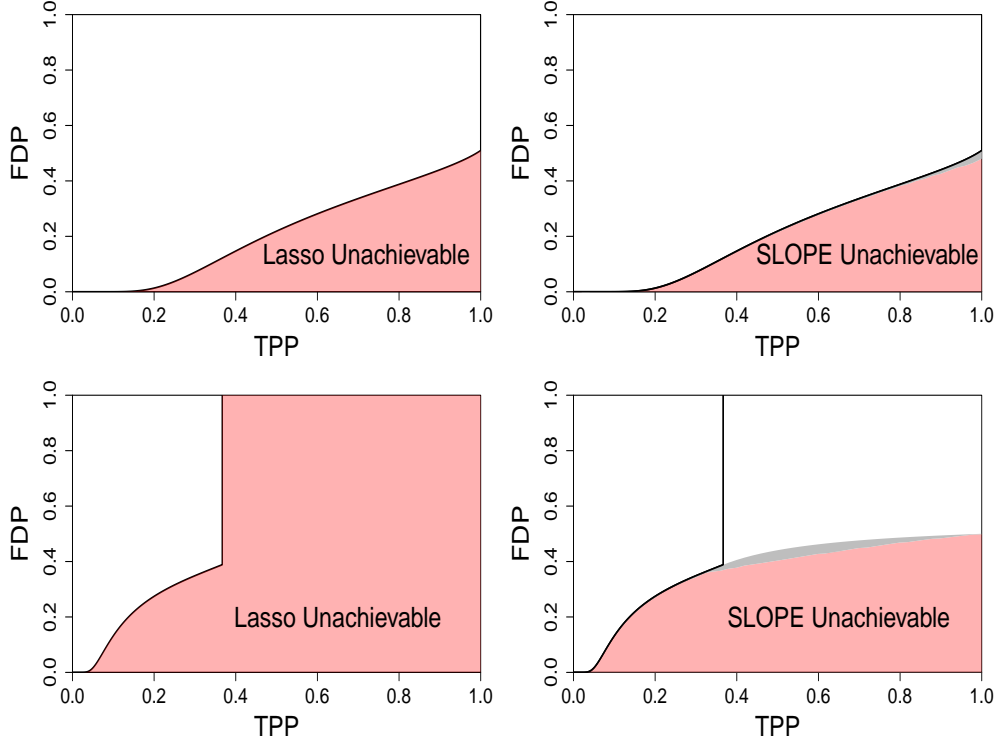


Figure 5: Examples of the TPP–FDP trade-off curve, with $(\delta, \epsilon) = (0.3, 0.2)$ on the top panel and $(0.3, 0.5)$ on the bottom. The left plot is the Lasso trade-off curve and the right plot describes the SLOPE trade-off gain. Neither the Lasso nor SLOPE can approach the red regions. The gray regions are sandwiched by the upper and lower bounds on the SLOPE trade-off.

First of all, the two right plots of Figure 5 show that the lower bound and the upper bound are very close to each other when $0 \leq \text{TPP} \leq u_{\text{DT}}^*$ (recall that $u_{\text{DT}}^* = 1$ in the subcritical regime). As a matter of fact, the upper bound in this regime is given by Su et al. (2017), which showed that under the working assumptions, there exists a function $q_{\text{Lasso}}^*(\cdot; \delta, \epsilon)$ such that

$$\text{FDP}_{\text{Lasso}}(\boldsymbol{\beta}, \lambda) \geq q_{\text{Lasso}}^*(\text{TPP}_{\text{Lasso}}(\boldsymbol{\beta}, \lambda); \delta, \epsilon) - 0.0001$$

holds with probability tending to one as $n, p \rightarrow \infty$. Moreover, q_{Lasso}^* is tight in the sense that the Lasso can come arbitrarily close to any point on this curve by specifying a prior and a penalty parameter (see refined results in Wang et al. (2020b)). Recognizing that the Lasso is an instance of SLOPE, the tightness of q_{Lasso}^* allows us to set $q^*(u) = q_{\text{Lasso}}^*(u)$ for $0 \leq u \leq u_{\text{DT}}^*$. For information, letting $t^*(u)$ be the largest positive root of the equation

$$\frac{2(1 - \epsilon) [(1 + x^2)\Phi(-x) - x\phi(x)] + \epsilon(1 + x^2) - \delta}{\epsilon [(1 + x^2)(1 - 2\Phi(-x)) + 2x\phi(x)]} = \frac{1 - u}{1 - 2\Phi(-x)}, \quad (2.6)$$

we have

$$q^*(u; \delta, \epsilon) = \begin{cases} q_{\text{Lasso}}^*(u; \delta, \epsilon) = \frac{2(1-\epsilon)\Phi(-t^*(u))}{2(1-\epsilon)\Phi(-t^*(u)) + \epsilon u}, & \text{if } u \leq u_{\text{DT}}^*(\delta, \epsilon), \\ \frac{\epsilon(1-\epsilon)u - \epsilon^*(1-\epsilon)}{\epsilon(1-\epsilon^*)u - \epsilon^*(1-\epsilon)}, & \text{if } u > u_{\text{DT}}^*(\delta, \epsilon). \end{cases} \quad (2.7)$$

Above, $\phi(\cdot)$ and $\Phi(\cdot)$ are the probability density function and cumulative distribution function of the standard normal distribution, respectively.

Returning to the lower bound, in stark contrast, the situation becomes much more challenging. To be sure, to obtain a lower bound requires a good understanding of the superiority of sorted ℓ_1 regularization over its usual ℓ_1 counterpart. From a theoretical viewpoint, a major difficulty in the analysis of SLOPE arises from the *non-separability* of sorted ℓ_1 regularization. Note that the non-separability results from the sorting operation in the penalty term $\sum_{i=1}^p \lambda_i |b|_{(i)}$ in the SLOPE optimization program (1.2). To tackle this technical issue, in this paper we formulate the SLOPE trade-off as a calculus of variations problem and further cast it into infinite-dimensional convex optimization problems (see more details in Section 4).

In a nutshell, the flexibility of the SLOPE regularization sequence seems to only bring up limited improvement on the trade-off between the TPP and FDP below the DT power limit. However, the two right plots of Figure 5 present a noticeable departure between the two bounds when the TPP is slightly below u_{DT}^* . This departure is not an artifact of our analysis. Indeed, in Section 5.3 we provide a problem instance whose asymptotic TPP and FDP trade-off falls strictly between the upper bound and the lower bound:

$$q_*(u) + 0.0001 < \text{FDP} < q^*(u) - 0.0001$$

and $\text{TPP} \approx u < u_{\text{DT}}^*$ with probability tending to one.

In passing, it is worthwhile mentioning that the performance in the high power regime is likely to carry more weight. In this sense, SLOPE overall outperforms the Lasso in terms of the trade-off between the TPP and FDP.

2.4 Instance-superiority of SLOPE

An important but less-emphasized point is that the above-mentioned comparison between the two methods is over the *lower envelope* of all the instance-specific problems. In this regard, it would be too quick to conclude that the flexibility of the penalty sequence does not gain any benefits for SLOPE, even at points where $q_*(u)$ may be very close to $q_{\text{Lasso}}^*(u)$. Under the working hypotheses, indeed, we can formally prove that SLOPE is superior to the Lasso in the sense that we can always find a SLOPE regularization prior that strictly improves the Lasso on the same linear regression problem in terms of both model selection and estimation. Below, we let $\hat{\beta}$ denote the SLOPE or the Lasso estimate, and use the subscript to distinguish between the two methods.

Theorem 3. *Under the working assumptions, namely (A1), (A2), and (A3), given any bounded signal prior Π and any Lasso regularization parameter $\lambda > 0$, there exists a SLOPE regularization Λ such that the following inequalities hold simultaneously with probability tending to one:*

$$(a) \text{TPP}_{\text{SLOPE}}(\beta, \lambda) > \text{TPP}_{\text{Lasso}}(\beta, \lambda);$$

- (b) $\text{FDP}_{\text{SLOPE}}(\boldsymbol{\beta}, \boldsymbol{\lambda}) < \text{FDP}_{\text{Lasso}}(\boldsymbol{\beta}, \lambda)$;
(c) $\|\widehat{\boldsymbol{\beta}}_{\text{SLOPE}}(\boldsymbol{\beta}, \boldsymbol{\lambda}) - \boldsymbol{\beta}\|^2 < \|\widehat{\boldsymbol{\beta}}_{\text{Lasso}}(\boldsymbol{\beta}, \lambda) - \boldsymbol{\beta}\|^2$.

This theorem shows that SLOPE can outperform the Lasso from both the model selection and the estimation viewpoints. The proof strategy of this theorem leverages a simple form of SLOPE regularization sequences that admits two distinct values (see (2.3)). Due to space constraints, we relegate the proof of this theorem to Appendix A. It is somewhat surprising that such a simple two-level sequence can already exploit the benefits of using SLOPE over the Lasso. Having said this, from a practical standpoint it is not entirely clear how to select the optimal SLOPE penalty sequence to outperform the Lasso. We leave this important direction for future research.

As an aside, we remark that SLOPE has been shown to achieve the asymptotically exact minimax estimation when the sparsity level is much lower than considered in the present paper, largely owing to the adaptivity of sorted ℓ_1 regularization (Su and Candès, 2016). When it comes to the Lasso, however, cross validation is needed to select a penalty parameter that enables the Lasso to achieve similar estimation performance, which however is not exact as the constant is not sharp (Bellec et al., 2018).

3 Preliminaries for Proofs

In this section, we collect some preliminary results about SLOPE and AMP theory that allow us to get analytic expression of the TPP and FDP asymptotically. Informally speaking, the AMP theory given in Bu et al. (2020, Theorem 3) and Hu and Lu (2019, Theorem 1) characterizes the *asymptotic* joint distribution of the SLOPE estimator $\widehat{\boldsymbol{\beta}}$ and the true regression coefficients $\boldsymbol{\beta}$. Notably, since $\widehat{\boldsymbol{\beta}}$ depends on $(\boldsymbol{\beta}, \boldsymbol{\lambda})$, when studying asymptotic properties of $\widehat{\boldsymbol{\beta}}$, we will work with their asymptotic distributions (Π, Λ) . In this way, we drop the dependence on finite-sample quantities like n, p and the sparsity level $|\{j : \beta_j \neq 0\}|$ and instead work with asymptotic quantities such as (δ, ϵ) henceforth.

To be specific, under pseudo-Lipschitz functions (see Bu et al. (2020, Definition 3.1)) on $(\widehat{\boldsymbol{\beta}}, \boldsymbol{\beta})$, the asymptotic distribution of the SLOPE (including the Lasso) estimator $\widehat{\boldsymbol{\beta}}$, which we denote as $\widehat{\Pi}$, can be described as

$$\widehat{\Pi} \stackrel{\mathcal{D}}{=} \eta_{\Pi + \tau Z, A\tau}(\Pi + \tau Z), \quad (3.1)$$

where Z is an independent standard normal and the superscript \mathcal{D} means "in distribution". We will refer to η (to be introduced in (3.5)) as the *limiting scalar function*, and (τ, A) is the unique solution to the *state evolution* and the *calibration* equations

$$\tau^2 = \sigma^2 + \frac{1}{\delta} \mathbb{E} \left(\eta_{\Pi + \tau Z, A\tau}(\Pi + \tau Z) - \Pi \right)^2, \quad (3.2)$$

$$\Lambda \stackrel{\mathcal{D}}{=} A\tau \left(1 - \frac{1}{\delta} \mathbb{E} \left(\eta'_{\Pi + \tau Z, A\tau}(\Pi + \tau Z) \right) \right). \quad (3.3)$$

In order to discuss properties of the limiting scalar function η , we first introduce the SLOPE proximal operator on $(\mathbf{y}, \boldsymbol{\theta}) \in \mathbb{R}^p \times \mathbb{R}^p$, where $\boldsymbol{\theta}$ is proportional to $\boldsymbol{\lambda}$ and $\theta_1 \geq \theta_2 \geq \dots \geq \theta_p \geq 0$ with at least one inequality. We define the proximal operator as

$$\text{prox}_J(\mathbf{y}; \boldsymbol{\theta}) := \arg \min_{\mathbf{b} \in \mathbb{R}^p} \left\{ \frac{1}{2} \|\mathbf{y} - \mathbf{b}\|^2 + J_{\boldsymbol{\theta}}(\mathbf{b}) \right\}, \quad (3.4)$$

where $J_{\boldsymbol{\theta}}(\mathbf{b}) = \sum_{i=1}^p \theta_i |b|_{(i)}$. In the Lasso case when the penalty parameter is a constant, the proximal operator reduces to the soft-thresholding function:

$$\text{prox}_J(\mathbf{y}; \theta) = \eta_{\text{soft}}(\mathbf{y}; \theta) := \text{sign}(\mathbf{y}) \cdot \max\{|\mathbf{y}| - \theta, 0\}.$$

Generally speaking, the SLOPE proximal operator in (3.4) is *adaptive* and *non-separable*, in the sense that an element of the output generally will depend on all elements of the input. As a concrete example, we obtain via Algorithm 1 that

$$\begin{aligned} & \text{prox}_J([20, 13, 10, 6, 4]; [12, 10, 5, 5, 5]) \\ &= \eta_{\text{soft}}([20, 13, 10, 6, 4]; [12, 9, 6, 5, 5]) = [8, 4, 4, 1, 0]. \end{aligned}$$

On the one hand, the adaptivity arises from the fact that larger penalties are applied to larger elements of the input. On the other hand, for example, two elements of input $[13, 10]$ are not directly thresholded by the penalty $[10, 5]$, but rather an averaging step is triggered by the existence of the other inputs, which giving an effective threshold of $[9, 6]$.

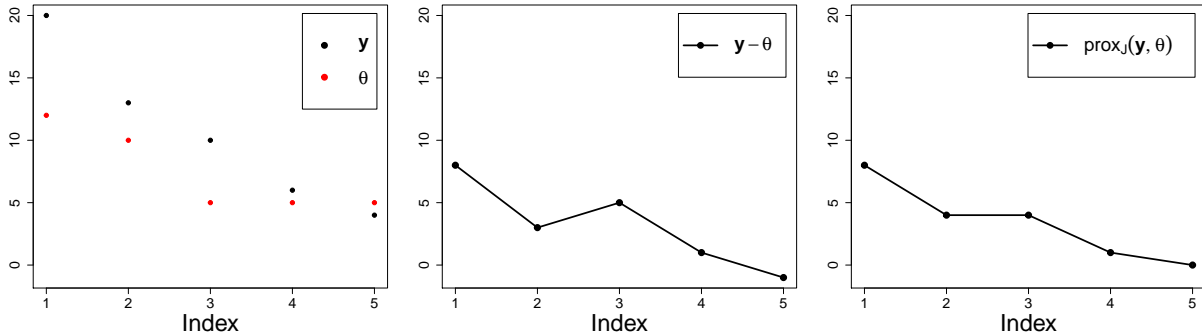


Figure 6: Illustration of how the SLOPE proximal operator can be interpreted as using an effective threshold. The leftmost figure plots two vectors \mathbf{y} and $\boldsymbol{\theta}$. The middle image plots their difference $\mathbf{y} - \boldsymbol{\theta}$ and the rightmost image plots the output of the proximal operator $\text{prox}_J(\mathbf{y}; \boldsymbol{\theta})$.

Although the SLOPE proximal operator given in (3.4) is non-separable, nevertheless, as introduced in Hu and Lu (2019, Proposition 1), the SLOPE proximal operator is *asymptotically separable*: for sequences $\{\boldsymbol{\theta}(p)\}$ and $\{\mathbf{v}(p)\}$ growing in p with empirical distributions that weakly converge to distributions Θ and V , respectively, there exists a limiting scalar function η (determined by Θ and V) such that as $p \rightarrow \infty$,

$$\frac{1}{p} \|\text{prox}_J(\mathbf{v}(p); \boldsymbol{\theta}(p)) - \eta_{V, \Theta}(\mathbf{v}(p))\|^2 \rightarrow 0. \quad (3.5)$$

The work in Hu and Lu (2019) discusses many properties of this limiting scalar function, η . Indeed, it can be shown to be odd, increasing, Lipschitz continuous with constant 1 and that it applies coordinate-wise to $\mathbf{v}(p)$ (hence it is separable; see Hu and Lu (2019, Proposition 2)). In more details, $\eta_{V, \Theta}(x)$ takes a scalar input, x , and performs soft-thresholding with a penalty adaptive to x in a way that depends on V and Θ , meaning the input-dependent penalty $\lambda_{V, \Theta}(x)$ such that $\eta_{V, \Theta}(x) = \eta_{\text{soft}}(x; \lambda_{V, \Theta}(x))$. More details on the adaptive penalty function that relates the SLOPE proximal operator to the soft-thresholding function can be found in Appendix C.

We now discuss in more detail the so-called state evolution and calibration equations given in (3.2) and (3.3). We refer to \mathbf{A} , which is defined implicitly via (3.3), as the *normalized penalty distribution*. Notice that \mathbf{A} only differs from the original penalty distribution Λ by a constant factor. In fact, there exists a one-to-one mapping between \mathbf{A} and Λ by Bu et al. (2020, Proposition 2.6), allowing one to analyze in either regime flexibly. In particular, when it is clear from the context, we will use (Π, Λ) and (π, \mathbf{A}) interchangeably since there exists a bijective calibration between the original problem instance and the normalized one. Moreover, for a fixed Π , the quantity $\tau(\mathbf{A})$ can be uniquely derived from (3.2) and, as shown in Bu et al. (2020, Corollary 3.4), it can be used to characterize the estimation error via $\|\widehat{\boldsymbol{\beta}} - \boldsymbol{\beta}\|/p \rightarrow \delta(\tau^2 - \sigma^2)$. In this work, we will use τ as a factor to define the *normalized prior*,

$$\pi(\Pi, \mathbf{A}) := \Pi/\tau(\Pi, \Lambda).$$

We refer the interested readers to Appendix B for a discussion of many nice properties of the fixed point recursion for the state evolution and the calibration mappings, (3.2) and (3.3), such as the explicit form of the divergence η' .

Under the characterization of asymptotic SLOPE distribution of (3.1), we define $\text{FDP}^\infty(\Pi, \Lambda)$ and $\text{TPP}^\infty(\Pi, \Lambda)$ as the large system limits of FDP and TPP. The proof of convergence in probability is given in the next lemma.

Lemma 3.1. *Under the working assumptions, namely (A1), (A2), and (A3), the SLOPE estimator $\widehat{\boldsymbol{\beta}}(\boldsymbol{\lambda})$ with the penalty sequence $\boldsymbol{\lambda}$ satisfies*

$$\begin{aligned} \text{FDP}(\boldsymbol{\beta}, \boldsymbol{\lambda}) &= \frac{|\{j : \widehat{\beta}_j \neq 0, \beta_j = 0\}|}{|\{j : \widehat{\beta}_j \neq 0\}|} \xrightarrow{P} \text{FDP}^\infty(\Pi, \Lambda) := \frac{(1 - \epsilon) \mathbb{P}\left(\eta_{\pi+Z, \mathbf{A}}(Z) \neq 0\right)}{\mathbb{P}\left(\eta_{\pi+Z, \mathbf{A}}(\pi + Z) \neq 0\right)}, \\ \text{TPP}(\boldsymbol{\beta}, \boldsymbol{\lambda}) &= \frac{|\{j : \widehat{\beta}_j \neq 0, \beta_j \neq 0\}|}{|\{j : \beta_j \neq 0\}|} \xrightarrow{P} \text{TPP}^\infty(\Pi, \Lambda) := \mathbb{P}\left(\eta_{\pi+Z, \mathbf{A}}(\pi^* + Z) \neq 0\right), \end{aligned} \quad (3.6)$$

where superscript P denotes convergence in probability, Z is a standard normal independent of Π , and (τ, \mathbf{A}) is the unique solution to the state evolution (3.2) and calibration (3.3). Furthermore, $\pi = \Pi/\tau$ is the normalized prior distribution, and $\Pi^* := (\Pi | \Pi \neq 0)$ is the signal prior distribution of the non-zero elements. We denote its normalized version as $\pi^* := \Pi^*/\tau$.

We give the proof of Lemma 3.1 in Appendix D.1, as an extension of Bogdan et al. (2013a, Theorem B.1).

Following the notions of FDP^∞ and TPP^∞ given in Lemma 3.1, we mathematically define the SLOPE trade-off curve as the envelope of all achievable SLOPE $(\text{TPP}^\infty, \text{FDP}^\infty)$ pairs:

$$q_{\text{SLOPE}}(u; \delta, \epsilon) := \inf_{(\Pi, \Lambda): \text{TPP}^\infty(\Pi, \Lambda) = u} \text{FDP}^\infty(\Pi, \Lambda).$$

To study the SLOPE trade-off, we will make use of a critical concept, the *zero-threshold* $\alpha(\Pi, \Lambda)$, which will be defined in Definition 4.1. Using the zero threshold, the limiting values in (3.6) can be simplified to

$$\begin{aligned} \text{TPP}^\infty(\Pi, \Lambda) &= \mathbb{P}(|\pi^* + Z| > \alpha(\Pi, \Lambda)), \\ \text{FDP}^\infty(\Pi, \Lambda) &= \frac{2(1 - \epsilon)\Phi(-\alpha(\Pi, \Lambda))}{2(1 - \epsilon)\Phi(-\alpha(\Pi, \Lambda)) + \epsilon \cdot \text{TPP}^\infty(\Pi, \Lambda)}. \end{aligned} \quad (3.7)$$

Note from the equations above that for fixed $\text{TPP}^\infty = u$, the formula of FDP^∞ is decreasing in α . Therefore we consider the maximum of feasible zero-thresholds,

$$\alpha^*(u) := \sup_{(\Pi, \Lambda): \text{TPP}^\infty = u} \alpha(\Pi, \Lambda),$$

in order to derive the minimum FDP^∞ on the SLOPE trade-off

$$q_{\text{SLOPE}}(u; \delta, \epsilon) := \frac{2(1 - \epsilon)\Phi(-\alpha^*(u))}{2(1 - \epsilon)\Phi(-\alpha^*(u)) + \epsilon u}. \quad (3.8)$$

4 Lower bound of SLOPE trade-off

The main purpose of this section is to provide a lower bound q_* for q_{SLOPE} . We accomplish this by (equivalently) giving an upper bound for $\alpha^*(u)$ for *fixed* u , which we denote as $t_*(u)$. As we shall see, in contrast to Lasso, our derivation for SLOPE requires non-standard tools from the calculus of variations and quadratic programming.

To construct the upper bound $t_*(u)$, we examine the state evolution (3.2), which gives

$$\tau^2 \geq \frac{1}{\delta} \mathbb{E} \left(\eta_{\Pi+Z, A\tau}(\Pi + \tau Z) - \Pi \right)^2 = \frac{\tau^2}{\delta} \mathbb{E} \left(\eta_{\pi+Z, A}(\pi + Z) - \pi \right)^2.$$

Rearranging the above inequality yields the state evolution condition

$$E(\Pi, \Lambda) := \mathbb{E} \left(\eta_{\pi+Z, A}(\pi + Z) - \pi \right)^2 \leq \delta. \quad (4.1)$$

Here the quantity $E(\Pi, \Lambda)$ can be viewed as the asymptotic mean squared error between the SLOPE estimator and the truth, scaled by $1/\tau^2$, since $\|\hat{\beta} - \beta\|/p \rightarrow \tau^2 E(\Pi, \Lambda)$ in probability by Bu et al. (2020, Corollary 3.4).

Before we proceed, we first introduce an important (scalar) quantity that governs the sparsity, the TPP, and the FDP of the SLOPE estimator and will be used throughout the paper.

Definition 4.1. *Let (Π, Λ) be a pair of prior and penalty distributions (or, equivalently, the normalized (π, A)) and suppose $\alpha(\Pi, \Lambda)$ is a positive number such that $\eta_{\pi+Z, A}(x) = 0$ if and only if $|x| \leq \alpha(\Pi, \Lambda)$. Then we say that $\alpha = \alpha(\Pi, \Lambda)$ is the zero-threshold.*

Intuitively, the zero-threshold is a positive threshold, below which, the input is mapped to zero. Note that the necessary condition (4.1) sets the feasible domain of (π, A) pairs and thus prescribes limits to the zero-threshold α . In the Lasso case, the zero-threshold is indeed equivalent to the normalized penalty scalar A ; but in SLOPE, it is a quantity derived from the normalized penalty distribution A in a highly nontrivial manner (see Proposition C.5 for details).

Next, we state another useful definition. Recall from Section 3 that the limiting scalar function η of SLOPE is separable and assigns a different penalty to different inputs. We therefore define the *effective penalty function* accordingly.

Definition 4.2. *Given a normalized pair of prior and penalty (π, A) , the effective penalty function $\hat{A}_{\text{eff}}: \mathbb{R} \rightarrow \mathbb{R}_+$ is a function such that*

$$\eta_{\text{soft}}(x; \hat{A}_{\text{eff}}(x)) = \eta_{\pi+Z, A}(x).$$

It is not hard to show that \widehat{A}_{eff} is well-defined. In fact, given $\eta_{\pi+Z, A}$, we can represent \widehat{A}_{eff} via the zero-threshold from Definition 4.1, namely,

$$\widehat{A}_{\text{eff}}(x) = \begin{cases} x - \eta_{\pi+Z, A}(x) & \text{if } x > \alpha(\pi, A), \\ -x + \eta_{\pi+Z, A}(x) & \text{if } x < -\alpha(\pi, A), \\ \alpha(\pi, A) & \text{if } |x| < \alpha(\pi, A). \end{cases}$$

Equipped with this effective penalty function, we can rewrite the state evolution condition (4.1) as

$$F_{\alpha}[\widehat{A}_{\text{eff}}, p_{\pi^*}] := \mathbb{E} \left(\eta_{\text{soft}}(\pi + Z; \widehat{A}_{\text{eff}}(\pi + Z)) - \pi \right)^2 \leq \delta,$$

in which the functional objective F_{α} is defined on the effective penalty function \widehat{A}_{eff} as well as the probability density function of π^* . Note here that π^* and π determine each other uniquely since $\pi^* := \pi|\pi| \neq 0$. We provide an explicit expression for $F_{\alpha}[\widehat{A}_{\text{eff}}, p_{\pi^*}]$ in (G.1).

Since the constraint (3.2) remains the same if π is replaced by $|\pi|$, we assume $\pi \geq 0$ without loss of generality. We minimize $F_{\alpha}[\widehat{A}_{\text{eff}}, p_{\pi^*}]$ over the functional space of $(\widehat{A}_{\text{eff}}, p_{\pi^*})$ through a relaxed variational problem:

$$\begin{aligned} & \min_{A_{\text{eff}}, \rho \geq 0} F_{\alpha}[A_{\text{eff}}, \rho] \\ \text{s.t. } & A_{\text{eff}}(\alpha) \geq \alpha, A'_{\text{eff}}(z) \geq 0 \text{ for all } z \geq \alpha, \\ & \int_0^{\infty} \rho(t) dt = 1, \int_0^{\infty} [\Phi(t - \alpha) + \Phi(-t - \alpha)] \rho(t) dt = u. \end{aligned} \quad (4.2)$$

Here the function A_{eff} is implicitly defined on $[\alpha, \infty)$ as $A_{\text{eff}}(z) = \alpha$ for $0 \leq z < \alpha$ and ρ is a probability measure defined on $[0, \infty)$. We remark that the constraints for A_{eff} in problem (4.2) are derived from the properties of \widehat{A}_{eff} in Appendix C, i.e. $A'_{\text{eff}} \geq 0$ comes from Fact C.3 and the boundary condition $A_{\text{eff}}(\alpha) \geq \alpha$ comes from Proposition C.5. Because some additional properties of \widehat{A}_{eff} may have been excluded in the relaxation, these constraints are only necessary and may not be sufficient. Therefore,

$$\min_{(\widehat{A}_{\text{eff}}, p_{\pi^*})} F_{\alpha}[\widehat{A}_{\text{eff}}, p_{\pi^*}] \geq \min_{(A_{\text{eff}}, \rho)} F_{\alpha}[A_{\text{eff}}, \rho],$$

with the inequality possibly being strict, provided the first optimization problem (4.1) is solved subject to (i) \widehat{A}_{eff} corresponds to the effective penalty in the limiting scalar function; and (ii) p_{π^*} is a probability density function such that $\text{TPP}^{\infty} = \mathbb{P}(|\pi^* + Z| > \alpha) = u$.

Leveraging the above relaxation (4.2), in order to lower bound q_{SLOPE} in (3.8), we can analogously define the maximum feasible zero-threshold $\alpha^*(u)$ and upper bound it with $t_{\star}(u)$ as follows:

$$\alpha^*(u) := \sup \left\{ \alpha : \min_{(\Pi, \Lambda)} F_{\alpha}[\widehat{A}_{\text{eff}}, p_{\pi^*}] \leq \delta \right\} \leq t_{\star}(u) := \sup \left\{ \alpha : \min_{(A_{\text{eff}}, \rho)} F_{\alpha}[A_{\text{eff}}, \rho] \leq \delta \right\}. \quad (4.3)$$

With these definitions in place, we are now in a position to describe the procedure to find the optimal prior and the optimal penalty in problem (4.2), given $\text{TPP}^{\infty} = u$ and $\alpha(\Pi, \Lambda) = \alpha$.

4.1 Optimal prior is three-point prior

To solve problem (4.2), we must search over all possible distributions π^* , which is generally infeasible. To overcome this obstacle, we use the concept of extreme points (i.e. points that do not lie on the line connecting any other two points of the same set) to show that the optimal π^* for problem (4.2) is a two-point distribution, having probability mass at only two non-negative (and possibly infinite) values (t_1, t_2) . In doing so, we significantly reduce the search domain, from infinite dimensional to two-dimensional. Because π has an additional point mass at 0, the optimal prior π (that can achieve minimum FDP when accompanied with the properly chosen penalty) is a three-point prior taking values at $(0, t_1, t_2)$. We recall that the two-point π^* is consistent to the Lasso result in Su et al. (2017, Section 2.5), where the optimal π^* is the infinity-or-nothing distribution with $t_1 = 0^+, t_2 = \infty$.

To see that π^* admits a two-point form, suppose that $(A_{\text{eff}}^*, \rho^*)$ is the global minimum of problem (4.2). Then clearly ρ^* is also the global minimum of the following linear problem (4.4) with linear constraints.

$$\begin{aligned} \min_{\rho \geq 0} \quad & F_\alpha[A_{\text{eff}}^*, \rho] \\ \text{s.t.} \quad & \int_0^\infty \rho(t) dt = 1, \int_0^\infty [\Phi(t - \alpha) + \Phi(-t - \alpha)] \rho(t) dt = u. \end{aligned} \tag{4.4}$$

Intuitively, since there are two constraints, we need two parameters (which will be t_1, t_2) to characterize the minimum. We formalize this intuition in the next lemma (proved in Appendix G) and show that ρ^* indeed takes the form of a sum of two Dirac delta functions.

Lemma 4.3. *If ρ^* is a global minimum of problem (4.4), then*

$$\rho^*(t) = p_1 \delta(t - t_1) + p_2 \delta(t - t_2)$$

for some constants p_1, p_2, t_1, t_2 , and $p_1 + p_2 = 1, p_1, p_2 \geq 0$.

The above specific form of the optimal ρ^* allows us to search over all (t_1, t_2) , each pair of which uniquely corresponds to either a single-point prior $\rho(t; t_1, t_2) = \delta(t - t_1)$ if $t_1 = t_2$, or a two-point prior by

$$\begin{aligned} \rho(t; t_1, t_2) &= p_1 \delta(t - t_1) + p_2 \delta(t - t_2), \\ p_1(t_1, t_2) &= \frac{u - [\Phi(t_2 - \alpha) + \Phi(-t_2 - \alpha)]}{[\Phi(t_1 - \alpha) + \Phi(-t_1 - \alpha)] - [\Phi(t_2 - \alpha) + \Phi(-t_2 - \alpha)]}, \\ p_2(t_1, t_2) &= 1 - p_1(t_1, t_2), \end{aligned} \tag{4.5}$$

where the last two equations come from the constraints in problem (4.4).

In light of Lemma 4.3, each pair (t_1, t_2) forms a different instantiation of problem (4.2), which will be problem (4.6) and whose optimal penalty is denoted by $A_{\text{eff}}^*(\cdot; t_1, t_2)$ so as to be explicitly dependent on (t_1, t_2) . Before we proceed to optimize the penalty $A_{\text{eff}}(\cdot; t_1, t_2)$, we assure the skeptical reader that, doing a grid search on (t_1, t_2) and considering the minimal value of all programs (4.6) parameterized by (t_1, t_2) to be equivalent to the minimal value of problem (4.2), is indeed a valid approach. This claim is theoretically grounded by noting that $F_\alpha[A_{\text{eff}}^*(\cdot; t_1, t_2), \rho(\cdot; t_1, t_2)]$ is continuous in (t_1, t_2) . Continuity can be seen from a perturbation analysis of the optimal value in problem (4.6). In our case, the perturbation analysis is not hard since the constraint is independent of (t_1, t_2) and F_α depends on A_{eff}^* in a strongly-convex manner: a small perturbation in (t_1, t_2) only

results in a small perturbation in A_{eff}^* and thus in $F_\alpha[A_{\text{eff}}^*(\cdot; t_1, t_2), \rho(\cdot; t_1, t_2)]$. We refer the curious reader to a line of perturbation analysis for such optimization problems in Bonnans and Shapiro (2013); Shapiro (1992); Bonnans and Shapiro (1998).

4.2 Characterizing optimal penalty analytically

By Lemma 4.3, we reduce the multivariate non-convex problem (4.2) to a set of univariate convex problems (4.6) over A_{eff} . In this section, we describe the optimal penalty function $A_{\text{eff}}^*(\cdot; t_1, t_2)$, which is the solution to the problem below:

$$\begin{aligned} \min_{A_{\text{eff}}} \quad & F_\alpha[A_{\text{eff}}, \rho(\cdot; t_1, t_2)] \\ \text{s.t.} \quad & A_{\text{eff}}(\alpha) \geq \alpha, \quad A'_{\text{eff}}(z) \geq 0 \text{ for all } z \geq \alpha. \end{aligned} \tag{4.6}$$

This is a quadratic problem with a non-holonomic constraint. To see this, we can expand the objective functional F_α from (G.1) and split it into a functional integral that involves A_{eff} and other terms which do not, i.e.

$$\begin{aligned} F_\alpha[A_{\text{eff}}, \rho(\cdot; t_1, t_2)] = \int_\alpha^\infty L(z, A_{\text{eff}}) dz &+ \epsilon p_1 t_1^2 [\Phi(\alpha - t_1) - \Phi(-\alpha - t_1)] \\ &+ \epsilon p_2 t_2^2 [\Phi(\alpha - t_2) - \Phi(-\alpha - t_2)]. \end{aligned}$$

This split changes our objective functional from $F_\alpha[A_{\text{eff}}, \rho(\cdot; t_1, t_2)]$ to the new functional $\int_\alpha^\infty L(z, A_{\text{eff}}) dz$ with

$$\begin{aligned} L(z, A_{\text{eff}}) : &= 2(1 - \epsilon)(z - A_{\text{eff}}(z))^2 \phi(z) \\ &+ \epsilon p_1 \left((z - t_1 - A_{\text{eff}}(z))^2 \phi(z - t_1) + (-z - t_1 + A_{\text{eff}}(z))^2 \phi(-z - t_1) \right) \\ &+ \epsilon p_2 \left((z - t_2 - A_{\text{eff}}(z))^2 \phi(z - t_2) + (-z - t_2 + A_{\text{eff}}(z))^2 \phi(-z - t_2) \right). \end{aligned} \tag{4.7}$$

We will numerically optimize the functional $\int_\alpha^\infty L(z, A_{\text{eff}}) dz$ together with the constraints in problem (4.6). In addition, although we cannot derive the analytic form of $A_{\text{eff}}^*(\cdot; t_1, t_2)$ from problem (4.6), we can still analytically characterize it at points z where the monotonicity constraint is non-binding (that is, when $A_{\text{eff}}^*(\cdot; t_1, t_2)$ is strictly increasing in a neighborhood of z), as shown in Appendix E.1.

4.3 Searching over optimal penalty numerically

To solve the functional optimization problem (4.6), we approximate it by a discrete optimization problem via Euler's finite difference method. Specifically, we approximate the function $L(z, A_{\text{eff}})$ (and hence F_α) on a discretized uniform grid of z and solve the resulting quadratic programming problem with linear constraints.

To this end, we denote vectors $\mathbf{z} = [\alpha, \alpha + \Delta z, \alpha + 2\Delta z, \dots, \alpha + m\Delta z]$ and $\mathbf{A} = [A_{\text{eff}}(\alpha), A_{\text{eff}}(\alpha + \Delta z), \dots, A_{\text{eff}}(\alpha + m\Delta z)]$ for some small Δz and large m . Then problem (4.6) is discretized into the

convex quadratic program

$$\begin{aligned} \min_{\mathbf{A}_{\text{eff}}} \quad & \bar{F}_\alpha(\mathbf{A}; t_1, t_2) \\ \text{s.t.} \quad & \begin{pmatrix} 1 & 0 & 0 & \cdots & 0 \\ -1 & 1 & 0 & \cdots & 0 \\ 0 & -1 & 1 & \cdots & 0 \\ \cdots & \cdots & \cdots & \cdots & \cdots \\ 0 & \cdots & 0 & -1 & 1 \end{pmatrix} \mathbf{A} \geq \begin{pmatrix} \alpha \\ 0 \\ \vdots \\ 0 \end{pmatrix}, \end{aligned} \quad (4.8)$$

in which the new objective $\bar{F}_\alpha(\mathbf{A}; t_1, t_2)$ (derived in (G.2) and also presented below) is the discretized objective of $F_\alpha[\mathbf{A}_{\text{eff}}, \rho(\cdot; t_1, t_2)]$ from problem (4.6).

As $\Delta z \rightarrow 0$ and $m \rightarrow \infty$, problem (4.8) recovers problem (4.6) by well-known convergence theory for Euler's finite difference method. To simplify the exposition, we write the objective of problem (4.8) in matrix and vector notation as follows:

$$\begin{aligned} \mathbf{Q} &= \text{diag} \left(2(1 - \epsilon)\phi(\mathbf{z}) + \epsilon \sum_{j=1,2} p_j [\phi(\mathbf{z} - t_j) + \phi(-\mathbf{z} - t_j)] \right), \\ \mathbf{d} &= 2(1 - \epsilon)\mathbf{z}\phi(\mathbf{z}) + \epsilon \sum_{j=1,2} p_j [(z - t_j)\phi(\mathbf{z} - t_j) + (z + t_j)\phi(\mathbf{z} + t_j)], \end{aligned}$$

and observe that

$$\bar{F}_\alpha(\mathbf{A}; t_1, t_2) = (\mathbf{A}^\top \mathbf{Q} \mathbf{A} - 2\mathbf{A}^\top \mathbf{d})\Delta z + \epsilon \sum_{j=1,2} p_j t_j^2 [\Phi(\alpha - t_j) - \Phi(-\alpha - t_j)].$$

The discretized problem (4.8) is equivalent to a standard quadratic programming problem, whose objective is the discrete version of $\int_\alpha^\infty L(z, \mathbf{A}_{\text{eff}})dz$ in (4.7),

$$\begin{aligned} \min_{\mathbf{A}} \quad & \frac{1}{2} \mathbf{A}^\top \mathbf{Q} \mathbf{A} - \mathbf{A}^\top \mathbf{d} \\ \text{s.t.} \quad & \begin{pmatrix} 1 & 0 & 0 & \cdots & 0 \\ -1 & 1 & 0 & \cdots & 0 \\ 0 & -1 & 1 & \cdots & 0 \\ \cdots & \cdots & \cdots & \cdots & \cdots \\ 0 & \cdots & 0 & -1 & 1 \end{pmatrix} \mathbf{A} \geq \begin{pmatrix} \alpha \\ 0 \\ \vdots \\ 0 \end{pmatrix}. \end{aligned} \quad (4.9)$$

4.4 Solving the quadratic program

Here we briefly discuss our numerical approach to solving the quadratic program (4.9). Generally speaking, quadratic programming problems do not admit closed-form solutions. However, they can be efficiently solved by classical numerical methods, including the interior point method (Dikin, 1967; Sra et al., 2012), active set method (Murty and Yu, 1988; Ferreau et al., 2014) and other dual methods (Goldfarb and Idnani, 1983; Frank and Wolfe, 1956). In this work, we use the dual method in Goldfarb and Idnani (1983), as implemented in the R library `quadprog`, to solve (4.9).

We remark that problem (4.9) is not the only way to discretize problem (4.6) and we now mention other approaches, which can result in better discretization accuracy. The discretization of

problem (4.6) contains two parts: (i) a numerical integration to approximate the objective and (ii) a numerical differentiation to approximate the constraints.

When formulating the quadratic programming problem (4.9), we chose to apply the left endpoint rule to approximate the objective integral $\int_{\alpha}^{\infty} L(z, A_{\text{eff}}) dz$ in (4.7) by $(\mathbf{A}^{\top} \mathbf{Q} \mathbf{A} - 2\mathbf{A}^{\top} \mathbf{d}) \Delta z$, as well as the backward finite difference (with first-order accuracy) to describe the constraint $A'_{\text{eff}}(z) \geq 0$. Alternatively, one can use different numerical quadratures to approximate the integral $\int_{\alpha}^{\infty} L(z, A_{\text{eff}}) dz$ or use a change of variable to approximate a different integral. We can also apply different finite differences to discretize the monotonicity constraint in problem (4.6).

4.4.1 Numerical integration to approximate the objective

More specifically, for the approximation of the objective in problem (4.6), we can alternatively apply numerical quadratures such as the trapezoid rule, Simpson's rule, or Gauss-Laguerre quadrature (Salzer and Zucker, 1949) to improve the numerical integration for $\int_{\alpha}^{\infty} L(z, A_{\text{eff}}) dz$. On the other hand, we may use a change of variable $z = \frac{x}{1-x} + \alpha$ to transform the integral $\int_{\alpha}^{\infty} L(z) dz$ over an infinite interval $[\alpha, \infty)$ to the integral $\int_0^1 L\left(\frac{x}{1-x} + \alpha\right) \frac{dx}{(1-x)^2}$ over a finite interval $[0, 1]$. This new integral can then be approximated by the same left endpoint rule (or other rules) but with different \mathbf{Q} and \mathbf{d} .

4.4.2 Numerical differentiation to approximate the constraints

As for the monotonicity constraint $A'_{\text{eff}}(z) \geq 0$, we may alternatively use other difference methods, e.g. the central difference, or higher-order accuracies. Doing so will result in a different matrix that left-multiplies \mathbf{A} in the constraint of (4.9).

In conclusion, different numerical integration and differentiation schemes will lead to other formulations of the quadratic programming that are different from (4.9). We do not pursue these additional numerical aspects in the present work.

4.5 Summary

To summarize everything so far, the procedure of finding the lower bound $q_{\star}(u)$ involves the following steps: fixing $\text{TPP}^{\infty} = u$, we search over a line of zero-thresholds $\{\alpha\}$; for each α , we search over a two-dimensional finite grid of (t_1, t_2) , each pair defining a standard quadratic programming problem (4.9); we then solve the quadratic problem and reject (t_1, t_2) if the minimal value of the equivalent problem (4.8) is larger than δ ; if all (t_1, t_2) are rejected, then the current zero-threshold α is too large to be valid. We set the largest valid zero-threshold as $t_{\star}(u)$ in (4.3) and write the lower bound of the FDP^{∞} as $q_{\star}(u) = \frac{2(1-\epsilon)\Phi(-t_{\star}(u))}{2(1-\epsilon)\Phi(-t_{\star}(u))+\epsilon u}$.

4.6 Differences between SLOPE and Lasso

We end this section by discussing why deriving the SLOPE trade-off is fundamentally more complicated than the Lasso case. We highlight that the variational problem (4.2) is *non-convex*, even though it is convex with respect to each variable A_{eff} and ρ (i.e. it is bi-convex but non-convex). Generally speaking, approximate solutions to non-convex problems are not accompanied by theoretical guarantees, except for some special cases. Our bi-convex problem (4.2) cannot be solved by alternating descent, namely, fixing one variable, optimizing over the other and then alternating.

Furthermore, our constraints only add another layer of complexity to the problem: in particular, the monotonicity constraint of A_{eff} is non-holonomic (i.e. the constraint $A'_{\text{eff}} \geq 0$ does not depend explicitly on A_{eff}).

More precisely, the difficulty in directly solving the problem (4.2) is two-fold. The first difficulty lies in the search for the optimal penalty. For the Lasso case, the penalty distribution A and the penalty function \widehat{A}_{eff} are not adaptive to the input and hence they both equal the zero-threshold α . Therefore, we can perform a grid search on $A \in \mathbb{R}$ and simply optimize over ρ . However, for SLOPE, the penalty \widehat{A}_{eff} is a *function* and hence it is intractable to search over the SLOPE penalty function space. The functional form of the penalty is the reason we must rely on the calculus of variations to study the associated optimization problem.

To demonstrate the second difficulty, we again consider the convex problem (4.4), which is over the probability density function ρ , assuming the optimal penalty A_{eff}^* has been obtained. In the Lasso case, it was shown in Su et al. (2017, Equation (C.2)) that the optimal π^* is the infinity-or-nothing distribution: $\mathbb{P}(\pi^* = 0) = 1 - \epsilon'$ and $\mathbb{P}(\pi^* = \infty) = \epsilon'$. In other words, given A_{eff}^* , we can easily derive the optimal ρ . However, a key concavity result in Su et al. (2017, Lemma C.1), which holds for Lasso and determines the optimal π^* , unfortunately breaks in SLOPE. Therefore, the optimal form of π^* is inaccessible for SLOPE with existing tools, even if the optimal penalty A_{eff}^* is known.

5 Upper bound of SLOPE trade-off

In this section, we rigorously analyze the SLOPE trade-off upper boundary curve q^* (defined in (2.7)). As stated in Theorem 2, q^* takes two forms: below the DT power limit, i.e. when $\text{TPP}^\infty < u_{\text{DT}}^*$ for u_{DT}^* defined in (2.2), we have $q^* = q_{\text{Lasso}}^*$, and beyond the DT power limit, q^* is a Möbius curve.

We start by giving some intuition for why the domain of q^* is the entire interval $[0, 1]$, whereas, the Lasso trade-off curve is only defined on $[0, u_{\text{DT}}^*)$. Intuitively, SLOPE is capable of overcoming the DT power limit and achieving 100% TPP since it is possible for SLOPE estimators to select all p features, hence, by the definition of TPP (see Section 2.1), one can find a completely dense SLOPE estimator whose TPP is automatically 1. This is not true for the Lasso, since it can select *at most* n out of p features. The corresponding constraint for the SLOPE estimator follows from the AMP calibration in (3.3) (discussed in detail in Appendix B), namely it says that the number of *unique absolute values* in the entries of the SLOPE estimator is at most n out of p . However, this does not directly constrain the sparsity of SLOPE estimator, and thus it can still be dense. In other words, the SLOPE estimator always satisfies

$$\text{number of unique non-zero magnitude } |\widehat{\beta}_i| \text{ in } \widehat{\beta}(p) \leq n. \quad (5.1)$$

Notice that, in the Lasso sub-case, the above implies a direct sparsity constraint $|\{i : \widehat{\beta}_i \neq 0\}| \leq n$ as just discussed, since all non-zero entries in Lasso have unique magnitudes.

With this intuition, we are prepared to prove Theorem 2 and show that q^* indeed serves as an upper bound of q_{SLOPE} . Following Proposition 2.3, we have the tightness of q^* when $u \geq u_{\text{DT}}^*$. We will further discuss the proof of Proposition 2.3 in Section 5.1, but leave the full details for Appendix D.4. The tightness of q^* when $u < u_{\text{DT}}^*$ follows from the existing tightness result on the Lasso trade-off (see Su et al. (2017, Section 2.5)), since the Lasso is a sub-case of SLOPE and q^* matches the Lasso trade-off curve for $u < u_{\text{DT}}^*$. Hence, we have the corollary below.

Corollary 5.1. *For any $0 \leq u \leq 1$, there exists an $\epsilon' \in [0, \epsilon^*/\epsilon]$, and values $r(u) \in [0, 1]$ and $w(u) \in [0, 1]$, both depending on u , such that the penalty $\boldsymbol{\lambda} = \boldsymbol{\lambda}_{\sqrt{M}, r(u)\sqrt{M}, w(u)}$ (defined in (2.3)) and the prior $\boldsymbol{\beta}_M(\epsilon')$ (defined in (2.4)) make SLOPE approach the point $(u, q^*(u))$ in the sense*

$$\lim_{M \rightarrow \infty} \lim_{n, p \rightarrow \infty} (\text{TPP}(\boldsymbol{\beta}_M(\epsilon'), \boldsymbol{\lambda}), \text{FDP}(\boldsymbol{\beta}_M(\epsilon'), \boldsymbol{\lambda})) \rightarrow (u, q^*(u)).$$

Moreover, when $u < u_{\text{DT}}^*$, we can set $r(u) = 1$, without specifying $w(u)$, and $\epsilon' = \epsilon'(u)$ will also depend on u . When $u \geq u_{\text{DT}}^*$, we fix $\epsilon' = \epsilon^*/\epsilon$ and set $r(u)$ via (5.2) and $w(u)$ via (5.3) below.

An interesting aspect of this result is that there are two different strategies for attaining $q^*(u)$, depending on whether $\text{TPP}^\infty = u$ is above or below the DT power limit. In both cases, we use a two-level penalty $\boldsymbol{\lambda}_{\sqrt{M}, r(u)\sqrt{M}, w(u)}$ and a sparse prior (see (2.4)) with very small and very large non-zeros. However, when $\text{TPP}^\infty = u < u_{\text{DT}}^*$, the strategy for attaining $q^*(u)$ is to vary the proportion of strong signals (which equals $\epsilon\epsilon'$ and ϵ' varies with u), but when $u \geq u_{\text{DT}}^*$, sharpness in the Möbius part of q^* is attained by keeping the sequence of priors fixed and instead tuning the ratio between strong and weak penalties.

The sharpness result of Corollary 5.1 shows that over the entire domain, q^* is arbitrarily closely achievable, thus, $q^*(u)$ must serve as the upper bound of the minimum FDP^∞ , $q_{\text{SLOPE}}(u)$, hence we have completed the proof of Theorem 2.

5.1 Möbius upper bound is achievable

In this section, we will sketch the proof of Proposition 2.3, which is used to prove Corollary 5.1 in the regime $u \geq u_{\text{DT}}^*$. To complement Proposition 2.3 and Corollary 5.1, for concreteness, we give a specific prior and penalty pair in (2.5) that approaches $q^*(u)$ when $u \geq u_{\text{DT}}^*$. The fully rigorous proof of Proposition 2.3, together with the derivation of (r, w) , is given in Appendix D.4.

Before we sketch the proof, we will provide some intuition for what makes the specific choice of priors and penalties behave effectively in terms of reducing the FDP^∞ while still driving TPP^∞ to 1, in order that we are able to approach $q^*(u)$ for all $u \geq u_{\text{DT}}^*$.

First, for fixed $\text{TPP}^\infty = u$, we can reduce the FDP^∞ through a smart use of the priors defined in (2.4), where many elements equal 0 exactly, while some non-zero elements are small (equal to $1/M$) and others large (equal to M) with M tending to ∞ . This is the same strategy as was used for demonstrating the achievability of the Lasso curve in Su et al. (2017), and the intuition that we present here is based on this analysis. Mathematically speaking, for the Lasso, Su et al. (2017, Lemma C.1) revealed a concave relationship in Π between the normalized estimation error $E(\Pi, \Lambda) = \mathbb{E}(\eta_{\pi+Z, \Lambda}(\pi+Z) - \pi)^2$ in (4.1) and the sparsity $\mathbb{P}(\eta_{\pi+Z, \Lambda}(\pi+Z) \neq 0)$, which also depends on the pair (Π, Λ) . The idea is that minimizing FDP^∞ corresponds to minimizing the sparsity (this can be seen, for example, by the relationship in (5.11) where $\kappa(\Pi, \Lambda)$ denotes the sparsity). Therefore, to find a prior Π that satisfies the state evolution condition (4.1), while minimizing the sparsity, the optimal (normalized) distribution for the non-zero elements, π^* , for the Lasso case has probability masses concentrated at the endpoints of the domain, namely 0^+ and ∞ . In this way, the form of the signal prior Π contributes to reducing the FDP^∞ by mixing the weak effects β_i with the zero effects.

Combining the priors discussed above, with a special subset of the possible penalties, namely the two-level penalties defined in (2.3), we are able to reduce the FDP^∞ while still increasing the TPP^∞ to its maximum value of 1, hence attaining $q^*(u)$ for all $u \geq u_{\text{DT}}^*$. Interestingly, the fact that SLOPE

can do this, is through its penalty, which mixes the weak predictors $\widehat{\beta}_i$ and the zero predictors (see Figure 10). This mix-up is in fact triggered by the averaging step in the SLOPE proximal operator (see Algorithm 1; the averaging is determined by the sorted ℓ_1 norm in the SLOPE problem), which creates non-zero magnitudes that are shared by some predictors and hence maintains the quota of unique magnitudes in (5.1). As a consequence, the SLOPE estimator can overcome the DT power limit (and reach higher TPP^∞) without violating the uniqueness constraint (5.1) on its magnitudes.

When constructing the two-level penalties just discussed, we must choose a pair (r, w) that, respectively, defines the downweighting of the \sqrt{M} used for the smaller penalty and the proportion of penalties getting each value. Concretely speaking, in Proposition 2.3 and Corollary 5.1, we set

$$r(u) = \Phi^{-1} \left(\frac{2\epsilon - \epsilon^* - \epsilon u}{2(\epsilon - \epsilon^*)} \right) / t^*(u_{\text{DT}}^*). \quad (5.2)$$

where ϵ^* and u_{DT}^* define the DT power limit and are given in (2.1)-(2.2) and t^* is defined in (2.6). Moreover,

$$w(u) = \epsilon^* + \frac{2(1 - \epsilon^*)}{1 - r} \left[\Phi(-t^*(u_{\text{DT}}^*)) - r\Phi(-rt^*(u_{\text{DT}}^*)) - \frac{\phi(-t^*(u_{\text{DT}}^*)) - \phi(-rt^*(u_{\text{DT}}^*))}{t^*(u_{\text{DT}}^*)} \right], \quad (5.3)$$

where r in the above is shorthand for the $r(u)$ from (5.2).

Without going into details, the key reason for choosing such pair (r, w) is so that the sequence of two-level penalties have two different penalization effects: for one, the SLOPE estimator $\eta_{\pi+Z,A}(\pi+Z)$ is equivalent to a Lasso estimator $\eta_{\text{soft}}(\pi+Z; t^*(u_{\text{DT}}^*))$ in the sense of (5.4); for the other, the SLOPE estimator is equivalent to a different Lasso estimator $\eta_{\text{soft}}(\pi+Z; rt^*(u_{\text{DT}}^*))$ in the sense of (5.5).

To be precise, it can be shown that

$$\eta_{\pi+Z,A}(\pi+Z) \stackrel{P}{=} \eta_{\text{soft}}(\pi+Z; t^*(u_{\text{DT}}^*)),$$

and

$$\mathbb{E}(\eta_{\pi+Z,A}(\pi+Z) - \pi)^2 = \mathbb{E}(\eta_{\text{soft}}(\pi+Z; t^*(u_{\text{DT}}^*)) - \pi)^2, \quad (5.4)$$

so when considering the asymptotic magnitude of the elements of the SLOPE estimator, or its asymptotic estimation error (4.1), we can analyze the limiting scalar function instead using a soft-thresholding function with threshold given by $t^*(u_{\text{DT}}^*)$. Moreover, this implies that SLOPE satisfies the state evolution constraint (4.1) in a similar way to how the Lasso satisfies its corresponding state evolution constraint.

However, analysis of the asymptotic sparsity of the SLOPE estimator or of its asymptotic TPP and FDP, relies on the fact that one can prove

$$\mathbb{P}(\eta_{\pi+Z,A}(\pi+Z) \neq 0) = \mathbb{P}(\eta_{\text{soft}}(\pi+Z; rt^*(u_{\text{DT}}^*)) \neq 0), \quad (5.5)$$

Hence, again, instead of analyzing the limiting scalar function one can analyze a soft-thresholding function, but now with a smaller threshold given by $rt^*(u_{\text{DT}}^*)$ for some $0 \leq r \leq 1$ defined in (5.2). Reducing the threshold in this way functions to improve the attainable TPP–FDP over the comparable Lasso problem by allowing more elements in the estimate with non-zero values. We visualize the above claims in Figure 10(d).

Essentially, the state evolution condition (4.1) must always hold, but it uses the larger pseudo zero-threshold $t^*(u_{\text{DT}}^*)$, while inference is conducted on the true, but smaller, zero-threshold $rt^*(u_{\text{DT}}^*)$. In this way, we can extend attainability of q_{Lasso}^* to attainability q^* , while still working within the state evolution constraint (4.1).

5.2 Infinity-or-nothing prior has FDP above upper bound

The goal of this section is to provide some intuition for the Möbius form of the curve $q^*(u)$ when u is larger than the DT power limit. This will be done by demonstrating that, in the case of infinity-or-nothing priors, with a special subset of penalties, the SLOPE FDP^∞ is always above q^* in Proposition 5.2. This also motivates the achievability results of Section 5.1, as the proof given in Section 5.1 essentially tries to construct prior penalty pairs such that the inequality in Proposition 5.2 becomes an equality. While we only consider infinity-or-nothing priors here, we remark that in the Lasso case these are actually the *optimal* priors (see Su et al. (2017, Section 2.5)), meaning that they achieve the minimum FDP^∞ given TPP^∞ .

Proposition 5.2. *Assuming that β is sampled i.i.d. from (2.4), for any $\epsilon' \in [0, 1]$ and set $M \rightarrow \infty$, and that λ is the order statistics of i.i.d. realization of a non-negative Λ with $\mathbb{P}(\Lambda = \max \Lambda) \geq \epsilon\epsilon'$, the following inequality holds with probability tending to one:*

$$\text{FDP}(\beta_M(\epsilon'), \lambda) \geq q^*(\text{TPP}(\beta_M(\epsilon'), \lambda); \delta, \epsilon) - 0.0001.$$

Proof of Proposition 5.2. As in Section 4, we assume $\pi \geq 0$ without loss of generality since the analysis holds if we replace π by $|\pi|$. Consider a *subset of priors*, namely the infinity-or-nothing priors: for some $\epsilon' \in [0, 1]$,

$$\pi_\infty(\epsilon') = \begin{cases} \infty & \text{w.p. } \epsilon\epsilon', \\ 0 & \text{w.p. } 1 - \epsilon\epsilon'. \end{cases} \quad (5.6)$$

Although the infinity-or-nothing prior in (5.6) does not satisfy the assumption (A2) that $\mathbb{P}(\Pi \neq 0) = \mathbb{P}(\pi \neq 0) = \epsilon$, this does not affect our discussion⁴.

In fact, as demonstrated by Lemma 5.3 below, for infinity-or-nothing priors, the state evolution constraint (4.1) guarantees that $\epsilon' \leq \epsilon^*/\epsilon$. Since ϵ^* is the same for the Lasso and SLOPE, this means that the maximum proportion of ∞ signals in the infinity-or-nothing prior is the same for both as well.

Lemma 5.3. *Under assumptions in Proposition 5.2, we must have $\epsilon' \in [0, \epsilon^*/\epsilon]$.*

The proof of Lemma 5.3 is given in Appendix D.3. It turns out that the DT threshold ϵ^* plays an important role in understanding the relationship between the sparsity and TPP^∞ . Before illustrating this relationship, we introduce the concept of *sparsity*. In a finite dimension, the sparsity of SLOPE estimator is $|\{j : \widehat{\beta}_j \neq 0\}|$. However, as $p \rightarrow \infty$, the count of non-zeros will also go to infinity, meaning a quantity like $\lim_p |\{j : \widehat{\beta}_j \neq 0\}|$ is not well-defined. Therefore we introduce the *asymptotic sparsity* of the SLOPE estimator via the distributional characterization in (3.1), denoting the limit in probability by plim ,

$$\kappa(\Pi, \Lambda) := \mathbb{P}(\eta_{\pi+Z, \Lambda}(\pi + Z) \neq 0) = \mathbb{P}(\widehat{\Pi} \neq 0) = \text{plim} |\{j : \widehat{\beta}_j \neq 0\}|/p. \quad (5.7)$$

Making use of the DT threshold $\epsilon^*(\delta)$, we show in Lemma 5.4 that the sparsity $\kappa(\Pi, \Lambda)$ sets an upper bound on achievable TPP^∞ .

⁴The infinity-or-nothing prior can be approximated arbitrarily closely by a sequence of priors that satisfy the assumption. For example, let $M \rightarrow \infty$ and consider $\pi_M(\epsilon')$ defined in (2.4).

Lemma 5.4. Consider SLOPE based on the pair (Π, Λ) with Π from (2.4) and set $M \rightarrow \infty$. Then with the asymptotic sparsity $0 \leq \kappa(\Pi, \Lambda) < 1$, we have $\text{TPP}^\infty(\Pi, \Lambda) \leq u^*(\kappa(\Pi, \Lambda); \epsilon, \delta)$ where

$$u^*(\kappa; \epsilon, \delta) := \begin{cases} 1 - \frac{(1-\kappa)(\epsilon-\epsilon^*)}{\epsilon(1-\epsilon^*)}, & \text{if } \delta < 1 \text{ and } \epsilon > \epsilon^*(\delta), \\ 1, & \text{otherwise.} \end{cases} \quad (5.8)$$

Proof of Lemma 5.4. We will only prove $\text{TPP}^\infty(\Pi, \Lambda) \leq 1 - \frac{(1-\kappa)(\epsilon-\epsilon^*)}{\epsilon(1-\epsilon^*)}$ when $\delta < 1$ and $\epsilon > \epsilon^*(\delta)$. We note that the bound on u^* given in (5.8) when $\delta \geq 1$ or $\epsilon \leq \epsilon^*(\delta)$ is trivial since, by definition, $\text{TPP}^\infty(\Pi, \Lambda) \leq 1$.

As $M \rightarrow \infty$ in (2.4), the prior π converges to the infinity-or-nothing priors $\pi_\infty(\epsilon')$ in (5.6). In addition, $\pi^* = \pi_\infty(\epsilon'/\epsilon)$. By the intermediate value theorem, there must exist some $\epsilon' \in [0, 1]$ such that

$$\begin{aligned} \text{TPP}^\infty(\Pi, \Lambda) &= \mathbb{P}(|\pi^* + Z| > \alpha) = (1 - \epsilon') \mathbb{P}(|Z| > \alpha) + \epsilon' \mathbb{P}(|\infty + Z| > \alpha) \\ &= 2(1 - \epsilon')\Phi(-\alpha) + \epsilon'. \end{aligned}$$

Here the first equality is given by (3.7) and $\alpha \equiv \alpha(\Pi, \Lambda)$ is the zero-threshold in Definition 4.1. The second equality follows from substituting the infinity-or-nothing π^* . Therefore, the asymptotic sparsity in (5.7) is

$$\kappa(\Pi, \Lambda) = \mathbb{P}(|\pi + Z| > \alpha) = (1 - \epsilon) \mathbb{P}(|Z| > \alpha) + \epsilon \text{TPP}^\infty = 2(1 - \epsilon\epsilon')\Phi(-\alpha) + \epsilon\epsilon',$$

where the first equality follows by the definition of the zero-threshold in Definition 4.1, the second uses that $\text{TPP}^\infty(\Pi, \Lambda) = \mathbb{P}(|\pi^* + Z| > \alpha)$, and the third is the result from the previous equation.

Some rearrangement gives

$$\Phi(-\alpha) = \frac{\kappa(\Pi, \Lambda) - \epsilon\epsilon'}{2(1 - \epsilon\epsilon')}, \quad \text{and} \quad \text{TPP}^\infty(\Pi, \Lambda) = \frac{(1 - \epsilon')(\kappa(\Pi, \Lambda) - \epsilon\epsilon')}{1 - \epsilon\epsilon'} + \epsilon'. \quad (5.9)$$

Simple calculus shows that the $\text{TPP}^\infty(\Pi, \Lambda)$ in (5.9) is an increasing function of ϵ' . To see this, notice that the derivative is $\frac{(1-\epsilon)(1-\kappa)}{(1-\epsilon\epsilon')^2} \geq 0$. Given that $\epsilon' \leq \epsilon^*/\epsilon$ by Lemma 5.3, we have

$$\text{TPP}^\infty(\Pi, \Lambda) \leq \frac{(1 - \frac{\epsilon^*}{\epsilon})(\kappa(\Pi, \Lambda) - \epsilon \cdot \frac{\epsilon^*}{\epsilon})}{1 - \epsilon \cdot \frac{\epsilon^*}{\epsilon}} + \frac{\epsilon^*}{\epsilon} = 1 - \frac{(1 - \kappa)(\epsilon - \epsilon^*)}{\epsilon(1 - \epsilon^*)}.$$

□

In fact, Lemma 5.4 is an extension of Su et al. (2017, Lemma C.2) (restated in Corollary 2.2(a)), which claims that, in the Lasso case, for all priors including those are not infinity-or-nothing, $\text{TPP}^\infty \leq u^*(\delta; \epsilon, \delta)$. In particular, we remark that $u^*(\delta; \epsilon, \delta)$ is equivalent to $u_{\text{DT}}^*(\delta, \epsilon)$, since any Lasso estimator has an asymptotic sparsity no larger than δ .

As an immediate consequence of Lemma 5.4, we can reversely set a lower bound on the sparsity $\kappa(\Pi, \Lambda)$ given $\text{TPP}^\infty(\Pi, \Lambda)$. This is achieved by inverting the mapping in (5.8) and setting $u^* = \text{TPP}^\infty$:

$$\kappa(\Pi, \Lambda) \geq 1 - \frac{\epsilon(1 - \text{TPP}^\infty(\Pi, \Lambda))(1 - \epsilon^*)}{\epsilon - \epsilon^*}. \quad (5.10)$$

Finally, leveraging the lower bound on the sparsity, we can minimize the FDP^∞ by minimizing the sparsity $\kappa(\Pi, \Lambda)$, since by definition

$$\text{FDP}^\infty(\Pi, \Lambda) = 1 - \frac{\epsilon \cdot \text{TPP}^\infty(\Pi, \Lambda)}{\kappa(\Pi, \Lambda)}. \quad (5.11)$$

Plugging (5.10) into (5.11), we finish the proof that $\text{FDP}^\infty \geq q^*(\text{TPP}^\infty)$ for the SLOPE when we restrict the priors to be infinity-or-nothing: with $\text{TPP}^\infty = u$,

$$\text{FDP}^\infty(\Pi, \Lambda) \geq q^*(u; \delta, \epsilon) := 1 - \frac{\epsilon u}{1 - \frac{\epsilon(1-u)(1-\epsilon^*)}{\epsilon - \epsilon^*}} = \frac{\epsilon u(1 - \epsilon) - \epsilon^*(1 - \epsilon)}{\epsilon u(1 - \epsilon^*) - \epsilon^*(1 - \epsilon)}.$$

□

5.3 Gap between upper and lower bounds

Considering Figure 2, we observe that the upper and lower boundary curves, q_* and q^* , can be visually and numerically close to each other, especially when $\text{TPP}^\infty < u_{\text{DT}}^*$. One may wonder whether these boundaries actually coincide below the DT power limit. We answer this question in the negative and show analytically that there may exist pairs of $(\text{TPP}^\infty, \text{FDP}^\infty)$ with the FDP^∞ strictly below $q^*(\text{TPP}^\infty)$ when $\text{TPP}^\infty < u_{\text{DT}}^*$. In other words, there are instances where $(\text{TPP}^\infty, \text{FDP}^\infty)$ points lie between the boundary curves q_* and q^* .

We note that, for the Lasso trade-off at $(u, q^*(u))$, the zero-threshold $\alpha(\Pi, \lambda) = t^*(u)$ (defined in (2.6)) exactly and the state evolution constraint (4.1) is binding, i.e. $E(\Pi, \lambda) = \delta$ (see Su et al. (2017, Lemma C.4, Lemma C.5)).

Fixing $\text{TPP}^\infty = u$, our strategy (detailed in Appendix E) is to construct (π, Λ) for SLOPE such that $\alpha(\pi, \Lambda) = t^*(u)$ as well but the state evolution constraint (4.1) is not binding, i.e. $E(\Pi, \Lambda) < \delta$. If such a construction succeeds, we can use a strictly larger zero-threshold than $t^*(u)$ that can increase until $E(\Pi, \Lambda) > \delta$. Then, by using a larger zero-threshold, the SLOPE FDP^∞ is guaranteed to be strictly smaller than $q^*(\text{TPP}^\infty)$ by (3.7). Thus we will complete the proof that $q_*(u) < q^*(u)$ for some $u < u_{\text{DT}}^*$.

To construct (π, Λ) satisfying $\alpha(\pi, \Lambda) = t^*(u)$ with $E(\Pi, \Lambda) < \delta$, we leverage our empirical observation that the optimal priors π^* , in the sense of problem (4.2), which achieves the lower bound q_* , are oftentimes either infinity-or-nothing or constant. This motivates us to consider constant priors $\pi^* = t_1$, for some constant t_1 (i.e. $p_1 = 1, t_1 = t_2$ in (4.5)), and hence

$$\pi = \begin{cases} t_1 & \text{w.p. } \epsilon, \\ 0 & \text{w.p. } 1 - \epsilon. \end{cases}$$

In fact, conditioning on $\alpha(\Pi, \Lambda) = t^*$ and $\text{TPP}^\infty = u$, the constant $t_1(u)$ is uniquely determined by (3.7):

$$\mathbb{P}(|t_1 + Z| > t^*(u)) = u,$$

where Z is a standard normal.

Next, we use a common tool in the calculus of variations, known as the Euler-Lagrange equation (detailed in Appendix E.2), to construct an effective penalty function $A_{\text{eff}}(z)$ analytically on the

interval $[0, \infty)$. The explicit form of $A_{\text{eff}}(z)$ is defined in (E.1) with $\alpha = t^*$. We emphasize that the constructed A_{eff} may not be a feasible SLOPE penalty function in the sense that it may violate the constraints in problem (4.6); however, if A_{eff} is increasing, then the optimal SLOPE effective penalty must be A_{eff} , as it is the minimizer of the unconstrained version of problem (4.6) and clearly satisfies the constraints. In the case that A_{eff} is feasible, we compare $E(\Pi, \Lambda) = F_{t^*(u)}[A_{\text{eff}}, p_{t_1}]$ with δ to determine whether $q^*(u) > q_*(u)$.

We now give a concrete example, which is elaborated in Appendix E.3. When $\delta = 0.3, \epsilon = 0.2, \Pi^* = 4.9006, \text{TPP}^\infty = u_{\text{DT}}^* = 0.5676$, the maximum Lasso zero-threshold $t^*(u_{\text{DT}}^*) = 1.1924$ and the minimum Lasso $\text{FDP}^\infty = 0.6216$. We can construct the SLOPE penalty A_{eff} that has the same zero-threshold and achieves $E(\Pi, \Lambda) = 0.2773 < \delta$. We can further construct the SLOPE penalty with larger zero-threshold, up to 1.2567, eventually have the SLOPE $\text{FDP}^\infty = 0.5954$, which is much smaller than the minimum Lasso FDP^∞ . In fact, our method can construct SLOPE penalty that outperforms the Lasso trade-off for any $\text{TPP}^\infty \in (0.5283, 1]$, as shown in Figure 14.

6 Discussion

In this paper, we have investigated the possible advantages of employing sorted ℓ_1 regularization in model selection instead of the usual ℓ_1 regularization. Focusing on SLOPE, which instantiates sorted ℓ_1 regularization, our main results are presented by lower and upper bounds on the trade-off between false and true positive rates. On the one hand, the two tight bounds together demonstrate that type I and type II errors cannot both be small simultaneously using the SLOPE method with any regularization sequences, no matter how large the effect sizes are. This is the same situation as the Lasso (Su et al., 2017), which instantiates ℓ_1 regularization. More importantly, our results on the other hand highlight several benefits of using sorted ℓ_1 regularization. First, SLOPE is shown to be capable of achieving arbitrarily high power, thereby breaking the DT power limit. For comparison, the Lasso cannot pass the DT power limit in the supercritical regime, no matter how strong the effect sizes are. Second, moving to the regime below the DT power limit, we provide a problem instance where the SLOPE TPP and FDP trade-off is strictly better than the Lasso. Third, we introduce a comparison theorem which shows that any solution along the Lasso path can be dominated by a certain SLOPE estimate in terms of both the TPP and FDP and the estimation risk. In other words, the flexibility of sorted ℓ_1 regularization can always improve on the usual ℓ_1 regularization in the instance-specific setting.

The assumptions underlying the above-mentioned results include the random designs that have independent Gaussian entries and linear sparsity. In the venerable literature on high-dimensional regression, however, a more common sparsity regime is sublinear regimes where k/p tends to zero. As such, it is crucial to keep in mind the distinction in the sparsity regime when interpreting the results in this paper. From a technical viewpoint, our assumptions here enable the use of tools from AMP theory and in particular a very recent technique for tackling non-separable penalties. To obtain the lower bound, moreover, we have introduced several novel elements that might be useful in establishing trade-offs for estimators using other penalties.

In closing, we propose several directions for future research. Perhaps the most pressing question is to obtain the exact optimal trade-off for SLOPE. Regarding this question, a closer look at Figure 3 and Figure 5 suggests that our lower and upper bounds seem to coincide exactly when the TPP is small. If so, part of the optimal trade-off would already be specified. Having shown the advantage of SLOPE over the Lasso, a question of practical importance is to develop an approach to selecting

regularization sequences for SLOPE to realize these benefits. Next, we would welcome extensions of our results to other methods using sorted ℓ_1 regularization, such as the group SLOPE (Brzyski et al., 2019). For this purpose, our optimization-based technique for the variational calculus problems would likely serve as an effective tool. Recognizing that we have made heavy use of the two-level regularization sequences in many of our results, one is tempted to examine the possible benefits of using multi-level sequences for SLOPE (Zhang and Bu, 2021). Finally, a challenging question is to investigate the SLOPE trade-off under correlated design matrices; the recent development by Celentano et al. (2020) in AMP theory can be a stepping stone for this highly desirable generalization.

Acknowledgments

Weijie Su was supported in part by NSF through CAREER DMS-1847415 and CCF-1934876, an Alfred Sloan Research Fellowship, and the Wharton Dean’s Research Fund. Cynthia Rush was supported by NSF through CCF-1849883, the Simons Institute for the Theory of Computing, and NTT Research. Jason M. Klusowski was supported in part by NSF through DMS-2054808 and HDR TRIPODS DATA-INSPIRE DCCF-1934924.

References

- F. Abramovich, Y. Benjamini, D. L. Donoho, and I. M. Johnstone. Adapting to unknown sparsity by controlling the false discovery rate. *The Annals of Statistics*, 34(2):584–653, 2006.
- M. Bayati and A. Montanari. The dynamics of message passing on dense graphs, with applications to compressed sensing. *IEEE Transactions on Information Theory*, 57(2):764–785, 2011.
- P. C. Bellec, G. Lecué, and A. B. Tsybakov. SLOPE meets lasso: improved oracle bounds and optimality. *The Annals of Statistics*, 46(6B):3603–3642, 2018.
- M. Bogdan, E. v. d. Berg, W. Su, and E. Candès. Statistical estimation and testing via the sorted ℓ_1 norm. *arXiv preprint arXiv:1310.1969*, 2013a.
- M. Bogdan, E. van den Berg, W. Su, and E. J. Candès. Supplementary materials for statistical estimation and testing via the sorted ℓ_1 norm. Available at https://statweb.stanford.edu/~candes/publications/downloads/SortedL1_SM.pdf, 2013b.
- M. Bogdan, E. Van Den Berg, C. Sabatti, W. Su, and E. J. Candès. SLOPE—Adaptive variable selection via convex optimization. *The Annals of Applied Statistics*, 9(3):1103, 2015.
- J. F. Bonnans and A. Shapiro. Optimization problems with perturbations: A guided tour. *SIAM review*, 40(2):228–264, 1998.
- J. F. Bonnans and A. Shapiro. *Perturbation analysis of optimization problems*. Springer Science & Business Media, 2013.
- D. Brzyski, A. Gossmann, W. Su, and M. Bogdan. Group SLOPE—Adaptive selection of groups of predictors. *Journal of the American Statistical Association*, 114(525):419–433, 2019.

- Z. Bu, J. M. Klusowski, C. Rush, and W. J. Su. Algorithmic analysis and statistical estimation of SLOPE via approximate message passing. *IEEE Transactions on Information Theory*, 67(1): 506–537, 2020.
- M. Celentano, A. Montanari, and Y. Wei. The lasso with general gaussian designs with applications to hypothesis testing. *arXiv preprint arXiv:2007.13716*, 2020.
- I. Dikin. Iterative solution of problems of linear and quadratic programming. In *Doklady Akademii Nauk*, volume 174, pages 747–748. Russian Academy of Sciences, 1967.
- D. Donoho and J. Tanner. Counting faces of randomly projected polytopes when the projection radically lowers dimension. *Journal of the American Mathematical Society*, 22(1):1–53, 2009a.
- D. Donoho and J. Tanner. Observed universality of phase transitions in high-dimensional geometry, with implications for modern data analysis and signal processing. *Philosophical Transactions of the Royal Society A: Mathematical, Physical and Engineering Sciences*, 367(1906):4273–4293, 2009b.
- D. L. Donoho. Neighborly polytopes and sparse solutions of underdetermined linear equations. 2005.
- D. L. Donoho. High-dimensional centrally symmetric polytopes with neighborliness proportional to dimension. *Discrete & Computational Geometry*, 35(4):617–652, 2006.
- D. L. Donoho, A. Maleki, and A. Montanari. Message-passing algorithms for compressed sensing. *Proceedings of the National Academy of Sciences*, 106(45):18914–18919, 2009.
- H. J. Ferreau, C. Kirches, A. Potschka, H. G. Bock, and M. Diehl. qpoads: A parametric active-set algorithm for quadratic programming. *Mathematical Programming Computation*, 6(4):327–363, 2014.
- M. Figueiredo and R. Nowak. Ordered weighted l1 regularized regression with strongly correlated covariates: Theoretical aspects. In *Artificial Intelligence and Statistics*, pages 930–938. PMLR, 2016.
- M. Frank and P. Wolfe. An algorithm for quadratic programming. *Naval research logistics quarterly*, 3(1-2):95–110, 1956.
- D. Goldfarb and A. Idnani. A numerically stable dual method for solving strictly convex quadratic programs. *Mathematical programming*, 27(1):1–33, 1983.
- M. G. G’Sell, T. Hastie, and R. Tibshirani. False variable selection rates in regression. *arXiv preprint arXiv:1302.2303*, 2013.
- H. Hu and Y. M. Lu. Asymptotics and optimal designs of SLOPE for sparse linear regression. In *2019 IEEE International Symposium on Information Theory (ISIT)*, pages 375–379. IEEE, 2019.
- R. Johnsonbaugh and W. E. Pfaffenberger. *Foundations of mathematical analysis*. Courier Corporation, 2012.
- A. Kolmogorov. *Introductory real analysis*.

- M. Kos and M. Bogdan. On the asymptotic properties of SLOPE. *Sankhya A*, 82(2):499–532, 2020.
- A. Mousavi, A. Maleki, and R. G. Baraniuk. Consistent parameter estimation for lasso and approximate message passing. *The Annals of Statistics*, 46(1):119–148, 2018.
- K. G. Murty and F.-T. Yu. *Linear complementarity, linear and nonlinear programming*, volume 3. Citeseer, 1988.
- W. Rudin et al. *Principles of mathematical analysis*, volume 3. McGraw-hill New York, 1976.
- H. E. Salzer and R. Zucker. Table of the zeros and weight factors of the first fifteen laguerre polynomials. *Bulletin of the American Mathematical Society*, 55(10):1004–1012, 1949.
- A. Shapiro. Perturbation analysis of optimization problems in banach spaces. *Numerical Functional Analysis and Optimization*, 13(1-2):97–116, 1992.
- S. Sra, S. Nowozin, and S. J. Wright. *Optimization for machine learning*. MIT Press, 2012.
- W. Su and E. J. Candès. SLOPE is adaptive to unknown sparsity and asymptotically minimax. *The Annals of Statistics*, 44(3):1038–1068, 2016.
- W. Su, M. Bogdan, and E. J. Candès. False discoveries occur early on the lasso path. *The Annals of Statistics*, 45(5):2133–2150, 2017.
- W. J. Su. When is the first spurious variable selected by sequential regression procedures? *Biometrika*, 105(3):517–527, 2018.
- P. Sur, Y. Chen, and E. J. Candès. The likelihood ratio test in high-dimensional logistic regression is asymptotically a rescaled chi-square. *Probability Theory and Related Fields*, 175(1-2):487–558, 2019.
- R. Tibshirani. Regression shrinkage and selection via the lasso. *Journal of the Royal Statistical Society: Series B (Statistical Methodology)*, 58(1):267–288, 1996.
- H. Wang, Y. Yang, Z. Bu, and W. Su. The complete lasso tradeoff diagram. *Advances in Neural Information Processing Systems*, 33, 2020a.
- H. Wang, Y. Yang, and W. J. Su. The price of competition: Effect size heterogeneity matters in high dimensions. *arXiv preprint arXiv:2007.00566*, 2020b.
- S. Wang, H. Weng, and A. Maleki. Does SLOPE outperform bridge regression? *arXiv preprint arXiv:1909.09345*, 2019.
- H. Weng, A. Maleki, and L. Zheng. Overcoming the limitations of phase transition by higher order analysis of regularization techniques. *Annals of Statistics*, 46(6A):3099–3129, 2018.
- Y. Zhang and Z. Bu. Efficient designs of slope penalty sequences in finite dimension. *The 24th International Conference on Artificial Intelligence and Statistics*, 2021.

A When does SLOPE outperform Lasso?

When studying the SLOPE tradeoff curve, we consider results that hold true for all combinations of signal prior distribution and penalty distribution, (Π, Λ) . In this section, we will instead look at instances of *fixed* bounded signal prior distributions.

Although the SLOPE trade-off upper bound q^* is no better than the Lasso one q_{Lasso}^* when $\text{TPP}^\infty < u_{\text{DT}}^*(\delta)$, as has been studied extensively in the previous sections of the paper, it is still possible that for a *fixed* prior distribution Π , the SLOPE can outperform Lasso using a smart choice of penalty vector. We emphasize that such cases are important, since in the real-world, the ground truth prior of the signal is indeed unknown but fixed. In fact, we will demonstrate that the SLOPE can always outperform Lasso in terms of the TPP, the FDP, the mean squared error (MSE).

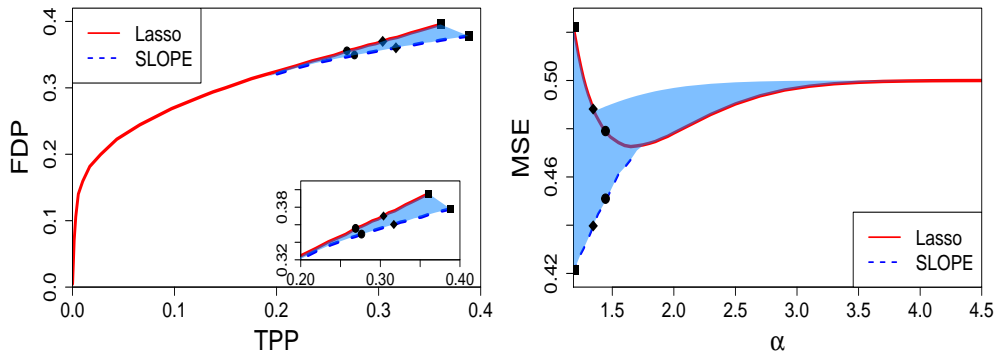


Figure 7: SLOPE outperforms the Lasso below the DT power limit. The red line is the Lasso paths when Π is Bernoulli(ϵ), $\delta = 0.3$, $\epsilon = 0.5$, and $\sigma = 0$. The blue region is the SLOPE $(\text{TPP}^\infty, \text{FDP}^\infty)$, produced by $\Theta(\ell, \alpha_L, 0.1)$ where $\alpha_L \in (\alpha_0, \infty)$ is the zero-threshold shared by the Lasso and the SLOPE for all $\ell \geq \alpha_L$. The blue dashed line is the boundary of blue region. The black dots on the red line are specific $(\text{TPP}^\infty, \text{FDP}^\infty, \text{MSE})$ by the Lasso, while the dots on the blue dashed line correspond to the Lasso dots by shape.

The proofs we provide only consider the two-level SLOPE penalty sequences of the form $\lambda = \theta_{\lambda_1, \lambda_2, w}$ as in (2.3). Despite the simplicity of the penalty sequence, we are already able to leverage the advantages of the flexibility of the SLOPE penalty relative to the Lasso. We moreover believe that the advantages of the SLOPE over the Lasso could be even greater when more general SLOPE penalty sequences are considered, though we leave this to future work.

To be specific, we consider a Lasso pair (Π_L, Λ_L) and aim to construct a corresponding SLOPE pair (Π_S, Λ_S) that outperforms the Lasso, under the requirement that $\Pi_L = \Pi_S = \Pi$. We will demonstrate that, for any fixed bounded Π , each Lasso penalty Λ_L can be dominated by some two-level SLOPE penalty distributions Λ_S , in the sense that the SLOPE produces strictly better $(\text{TPP}^\infty, \text{FDP}^\infty)$ and MSE. We further demonstrate a method to search for such dominating SLOPE penalties Λ_S and then we reinforce these ideas with simulation results.

The theoretical result of this section can be found in Theorem 3. In specific, we demonstrate that switching from Lasso to the simple two-level SLOPE can achieve better TPP^∞ , better FDP^∞ and better MSE at the same time. The full proof is in Appendix F and we discuss the ideas of proof here.

In the following, we work in the normalized A or α regime (given by the AMP calibration (3.3);

see also the interpretations below that equation) instead of the Λ or λ regime. The minimum $\alpha \in \mathbb{R}_+$ such that the corresponding the Lasso penalty $\lambda(\alpha)$ is non-negative, is denoted α_0 . We denote the normalized prior $\pi_L := \Pi/\tau_L < \Pi/\tau_S := \pi_S$ and their non-zero conditional distribution as π_L^*, π_S^* respectively. Here τ_L, τ_S are computed from the state evolution (3.2) of the Lasso and the SLOPE.

The high-level idea of the proof is, for any Lasso penalty A_L , to find a SLOPE penalty distribution A_S which has

- (1) the same zero-threshold $\alpha(\pi_S, A_S) = \alpha(\pi_L, A_L)$ (defined in Definition 4.1);
- (2) a smaller τ_S than the Lasso τ_L (from Equation (4.1));
- (3) a larger sparsity $\kappa(\Pi, A_S)$ than $\kappa(\Pi, A_L)$ (defined in Equation (5.7)).

To see why such A_S is dominating, we can show (2) together with Bu et al. (2020, Corollary 3.4), restated in (F.1), implies that the SLOPE MSE is strictly smaller than the Lasso MSE.

Further results follow from the definitions of TPP and FDP: by (3.7), we get

$$\text{TPP}^\infty(\Pi, A_S) = \mathbb{P}(|\pi_S^* + Z| > A_L) > \mathbb{P}(|\pi_L^* + Z| > A_L) = \text{TPP}^\infty(\Pi, A_L),$$

where we have used the equal zero-threshold condition (1). Finally, we finish the proof for the FDP $^\infty$ result by using (5.11) as well as the sparsity condition (3).

Using the above conditions as the searching criteria, we have designed an algorithm that, for any fixed prior Π and for each Lasso penalty $A_L = \alpha_L$, finds a superior two-level SLOPE penalty $A_S = \Theta_{\ell, \alpha_L, w}$ by searching over (ℓ, w) . As presented in Figure 7, the SLOPE (TPP $^\infty$, FDP $^\infty$) with two-level penalties outperforms the Lasso path.

B Detailed preliminary results of SLOPE AMP

In this section, we introduce the proximal operator of SLOPE, its limiting form (known as the limiting scalar function, on which the SLOPE AMP algorithm is based), and the SLOPE AMP theory relating to the state evolution and calibration equations.

B.1 SLOPE proximal operator

We start with the definition of the proximal operator. For input $\mathbf{y} \in \mathbb{R}^p$, define the **proximal operator** of a function $f : \mathbb{R}^p \rightarrow \mathbb{R}$ as

$$\text{prox}_f(\mathbf{y}) := \arg \min_{\mathbf{b} \in \mathbb{R}^p} \left\{ \frac{1}{2} \|\mathbf{y} - \mathbf{b}\|^2 + f(\mathbf{b}) \right\}.$$

For SLOPE, the proximal operator uses $f(\mathbf{b}) = J_\theta(\mathbf{b}) := \sum_{i=1}^p \theta_i |b_{(i)}|$ for some penalty vector θ and as discussed in Bogdan et al. (2015), the SLOPE proximal operator can be computed by Algorithm 1⁵.

For the Lasso, the relevant proximal operator uses $f(\mathbf{b}) = \theta \|\mathbf{b}\|_1$ and is known as the soft-thresholding function, which we will denote as $\eta_{\text{soft}} : \mathbb{R}^p \times \mathbb{R}_+ \rightarrow \mathbb{R}^p$. Namely, for any index

⁵The SLOPE proximal operator can be computed by R library SLOPE.

Algorithm 1 Solving $\text{prox}_J(\mathbf{s}; \boldsymbol{\theta})$ by (Bogdan et al., 2015, Algorithm 3)

- (1). **Sorting:** Sort $|\mathbf{s}|$ in decreasing order, returning $\text{sort}(|\mathbf{s}|)$;
- (2). **Differencing:** Calculate a difference sequence, \mathbf{S} , defined as

$$\mathbf{S} = \text{sort}(|\mathbf{s}|) - \boldsymbol{\theta};$$

- (3). **Averaging:** Repeatedly average out strictly increasing subsequences in \mathbf{S} until none remains. We refer to the decreasing sequence after all the averaging as $\text{AVE}(\mathbf{S})$, and reassign

$$\mathbf{S} = \text{AVE}(\mathbf{S});$$

- (4). **Truncating:** Set negative values in the difference sequence to 0 and reassign

$$\mathbf{S} = \max(\mathbf{S}, 0);$$

- (5). **Restoring:** Restore the order and the sign of \mathbf{s} from step (1) to \mathbf{S} . Now \mathbf{S} with the restored order and sign is the final output.
-

$i \in \{1, 2, \dots, p\}$, the soft-thresholding function is defined as

$$[\text{prox}_{\theta\|\cdot\|_1}(\mathbf{y})]_i = [\eta_{\text{soft}}(\mathbf{y}; \theta)]_i := \begin{cases} y_i - \theta, & \text{if } y_i > \theta, \\ y_i + \theta, & \text{if } y_i < -\theta, \\ 0, & \text{otherwise.} \end{cases}$$

Note that the Lasso proximal operator is indeed *separable*, meaning that any element of its output depends only on the corresponding element of its input. This generally does not hold for the SLOPE proximal operator, which renders the analysis of SLOPE much more difficult. Nevertheless, the SLOPE proximal operator is an *asymptotically separable* function (as discussed in (3.5)) and enables the analysis of the input-dependent penalty, which is detailed in Appendix C.

In what follows, we denote $\text{prox}_J(\mathbf{v}; \boldsymbol{\lambda})$ as the SLOPE proximal operator $\text{prox}_{J_{\boldsymbol{\lambda}}}(\mathbf{v})$.

B.2 SLOPE AMP algorithm

Under the working assumptions (see (A1) \sim (A3) in Section 2) and using the SLOPE proximal operator, the SLOPE optimization problem (1.2) can be solved by the following AMP algorithm with any initial conditions (Bu et al. (2020)):

$$\begin{aligned} \boldsymbol{\beta}^{t+1} &= \text{prox}_J(\mathbf{X}^\top \mathbf{z}^t + \boldsymbol{\beta}^t; \boldsymbol{\alpha}\tau_t), \\ \mathbf{z}^{t+1} &= \mathbf{y} - \mathbf{X}\boldsymbol{\beta}^{t+1} + \frac{\mathbf{z}^t}{\delta} \left[\nabla \text{prox}_J(\mathbf{X}^\top \mathbf{z}^t + \boldsymbol{\beta}^t; \boldsymbol{\alpha}\tau_t) \right], \end{aligned}$$

where ∇ denotes the divergence and $(\boldsymbol{\alpha}, \tau_t)$ is defined in the equations known as the state evolution and the calibration, which we will describe shortly.

It has been shown in (Bu et al., 2020, Theorem 2) that asymptotically $\boldsymbol{\beta}^t$ converges to the true minimizer $\widehat{\boldsymbol{\beta}}$. In addition, for uniformly pseudo-Lipschitz sequence functions ϕ_p , we have from (Bu et al., 2020, Theorem 3) that

$$\text{plim}_p \phi_p(\widehat{\boldsymbol{\beta}}, \boldsymbol{\beta}) = \lim_t \text{plim}_p \mathbb{E}_Z[\phi_p(\text{prox}_J(\boldsymbol{\beta} + \tau_t \mathbf{Z}; \boldsymbol{\alpha}(p)\tau_t), \boldsymbol{\beta})].$$

Loosely speaking, AMP theory characterizes the SLOPE estimator by

$$\widehat{\boldsymbol{\beta}} \stackrel{\mathcal{D}}{\approx} \text{prox}_J(\boldsymbol{\beta} + \tau \mathbf{Z}; \boldsymbol{\alpha}\tau),$$

whose empirical distribution weakly converges to $\eta_{\Pi + \tau Z, A\tau}(\Pi + \tau Z)$ and we describe (A, τ) below.

B.3 State evolution of SLOPE AMP

Rigorously speaking, the **state evolution** for SLOPE is

$$\tau^2 = \sigma^2 + \frac{1}{\delta} \mathbb{E} (\eta_{\Pi + \tau Z; A\tau}(\Pi + \tau Z) - \Pi)^2 = \sigma^2 + \frac{\tau^2}{\delta} \mathbb{E} (\eta_{\pi + Z; A}(\pi + Z) - \pi)^2, \quad (\text{B.1})$$

which can be solved iteratively via

$$\tau_{t+1}^2 = F(\tau_t, A\tau_t) = \sigma^2 + \frac{1}{\delta} \mathbb{E} (\eta_{\Pi + \tau_t Z; A\tau_t}(\Pi + \tau_t Z) - \Pi)^2,$$

From the algorithmic perspective of AMP, we use the finite approximation of the state evolution,

$$\tau^2 = F(\tau, \boldsymbol{\alpha}\tau) := \sigma^2 + \frac{1}{\delta} \mathbb{E} \langle [\text{prox}_J(\boldsymbol{\beta} + \tau \mathbf{Z}; \boldsymbol{\alpha}\tau) - \boldsymbol{\beta}]^2 \rangle, \quad (\text{B.2})$$

which can be recursively solved from the fixed point recursion $\tau_{t+1}^2(p) = F(\tau_t(p), \boldsymbol{\alpha}\tau_t(p))$ for each vector $\boldsymbol{\alpha} \in \mathbb{R}^p$. Here $\langle \mathbf{u} \rangle = \sum_{i=1}^p u_i/p$. Furthermore, this state evolution enjoys nice convergence properties: it is shown in (Bu et al., 2020, Theorem 1) that $\{\tau_t\}$ converges monotonically to a unique fixed point τ , under any initial condition.

B.4 Calibration of SLOPE AMP

For finite p , we have seen that the state evolution term τ depends on Π and $\boldsymbol{\alpha}$. Therefore fixing Π , we can view $\tau(\boldsymbol{\alpha})$ as a function of $\boldsymbol{\alpha}$ and then gives the **calibration** mapping of the SLOPE penalty $\boldsymbol{\lambda} \in \mathbb{R}^p$ through (Bu et al., 2020, Lemma 2.2),

$$\boldsymbol{\lambda}(\boldsymbol{\alpha}) = \boldsymbol{\alpha}\tau \left(1 - \frac{1}{\delta p} \mathbb{E} (\nabla \text{prox}_J(\boldsymbol{\Pi} + \tau \mathbf{Z}; \boldsymbol{\alpha}\tau)) \right), \quad (\text{B.3})$$

where the divergence of the proximal operator is defined as

$$\nabla \text{prox}_J(\mathbf{v}; \boldsymbol{\alpha}\tau) := \text{diag} \left(\frac{\partial}{\partial v_1}, \frac{\partial}{\partial v_2}, \dots \right) \cdot \text{prox}_J(\mathbf{v}; \boldsymbol{\alpha}\tau).$$

There are certain critical observations given by (Bu et al., 2020, Lemma 2.1) and (Su and Candès, 2016, Proofs of Fact 3.2 and 3.3) that explain the divergence term as

$$\nabla \text{prox}_J(\mathbf{v}; \boldsymbol{\alpha}\tau) = \|\text{prox}_J(\mathbf{v}; \boldsymbol{\alpha}\tau)\|_0^*,$$

where $\|\mathbf{x}\|_0^*$ counts the *unique* non-zero magnitudes in the vector \mathbf{x} . E.g. $\|(2, -1, 1, 0)\|_0^* = 2$. This norm reduces to ℓ_0 norm in the Lasso case, where all non-zero elements in $\text{prox}_J(\mathbf{v}; \boldsymbol{\alpha}\tau)$ have unique magnitudes. Therefore we can express (B.3) as

$$\boldsymbol{\lambda}(\boldsymbol{\alpha}) = \boldsymbol{\alpha}\tau \left(1 - \frac{1}{n} \mathbb{E} \|\text{prox}_J(\boldsymbol{\Pi} + \tau \mathbf{Z}; \boldsymbol{\alpha}\tau)\|_0^* \right). \quad (\text{B.4})$$

In the asymptotic case, the calibration lies between the original penalty distribution Λ and the normalized penalty A , to which the empirical distributions of $\{\boldsymbol{\lambda}\}$ and $\{\boldsymbol{\alpha}\}$ converge weakly:

$$\begin{aligned}\Lambda &\stackrel{\mathcal{D}}{=} A\tau \left(1 - \frac{1}{\delta} \lim_{p \rightarrow \infty} \frac{1}{p} \mathbb{E} \|\text{prox}_J(\boldsymbol{\Pi} + \tau \mathbf{Z}; \mathbf{A}(p)\tau)\|_0^* \right) \\ &= A\tau \left(1 - \frac{1}{\delta} \mathbb{P} \left(\eta_{\pi+Z;A}(\pi + Z) \in \mathcal{U}(\eta_{\pi+Z;A}(\pi + Z)) \right) \right),\end{aligned}\tag{B.5}$$

where $\mathcal{U}(\cdot)$ is defined by

$$\mathcal{U}(\eta) := \left\{ h \in \mathbb{R}_+ : \mathbb{P}(|\eta| = h) = 0 \right\}.$$

This quantity represents the portion of the probability space on which $|\eta_{\pi+Z;A}(\pi + Z)|$ has zero probability mass. In addition, $\mathbb{P}(\eta \in \mathcal{U}(\eta))$ is the asymptotic proportion of *unique* non-zeros in the SLOPE estimator η . For example, if η follows a Bernoulli-Gaussian distribution with 30% probability being zero, then $\mathcal{U} = (0, \infty)$, since the only point mass is concentrated at 0 and $\mathbb{P}(\eta \in \mathcal{U}(\eta)) = 0.7$.

C Bridging SLOPE and soft-thresholding

In this section we describe a connection between the SLOPE proximal operator and the Lasso proximal operator, i.e. the soft-thresholding function. This connection is built on top of the concept of **effective penalty** in Definition 4.2, which allows one to **reduce** the SLOPE proximal operator to the soft-thresholding function with an input-dependent penalty. In analyzing both bounds of the SLOPE trade-off, q_* and q^* , we use this technique so that we can study the much more amenable soft-thresholding function in place of the SLOPE proximal operator.

Here we use ‘ $\text{prox}_J(\mathbf{v}; \boldsymbol{\alpha})$ ’ to denote the SLOPE proximal operator and η_{soft} to denote the soft-thresholding function, both defined in Section 3. Note that unlike the soft-thresholding function, the SLOPE proximal operator does not have an explicit formula (nor does its limiting form given by the limiting scalar function η), however it can be efficiently computed by Algorithm 1. Recall that the SLOPE penalty vector $\boldsymbol{\alpha}$ is decreasing and non-negative. The first result we present in this section says that in finite dimension, we can always design an effective penalty $\widehat{\boldsymbol{\alpha}}(\mathbf{v}, \boldsymbol{\alpha})$, such that applying prox_J on penalty $\boldsymbol{\alpha}$ is equivalent to applying elementwise soft-thresholding on $\widehat{\boldsymbol{\alpha}}$.

Fact C.1. *For any $\boldsymbol{\alpha}, \mathbf{v} \in \mathbb{R}^p$, there exists $\widehat{\boldsymbol{\alpha}} \in \mathbb{R}^p$ such that*

$$\text{prox}_J(\mathbf{v}; \boldsymbol{\alpha}) = \eta_{\text{soft}}(\mathbf{v}; \widehat{\boldsymbol{\alpha}}).$$

Proof of Fact C.1. For $\mathbf{v} \geq 0$, the soft-thresholding operator is $\eta_{\text{soft}}(\mathbf{v}; \widehat{\boldsymbol{\alpha}}) = \max(\mathbf{v} - \widehat{\boldsymbol{\alpha}}, 0)$. Note that $\mathbf{v} \geq 0$ implies $\text{prox}_J(\mathbf{v}; \boldsymbol{\alpha}) \geq 0$ and $[\text{prox}_J(\mathbf{v}; \boldsymbol{\alpha})]_i \leq v_i$ for every i . Then we can simply design $\widehat{\boldsymbol{\alpha}}$ by setting $\widehat{\boldsymbol{\alpha}} = \mathbf{v} - \text{prox}_J(\mathbf{v}; \boldsymbol{\alpha})$. More generally, for any \mathbf{v} , we can set $\widehat{\boldsymbol{\alpha}} = |\mathbf{v}| - \text{prox}_J(|\mathbf{v}|; \boldsymbol{\alpha})$ (c.f. (Hu and Lu, 2019, Proposition 2)). \square

We notice that there are possibly multiple valid designs of $\widehat{\boldsymbol{\alpha}}$. An example would be

$$\text{prox}_J([6, 5, 3, 2, 1]; [5, 2, 2, 2, 2]) = [2, 2, 1, 0, 0] = \eta_{\text{soft}}([6, 5, 3, 2, 1]; \widehat{\boldsymbol{\alpha}}),\tag{C.1}$$

and both $\widehat{\boldsymbol{\alpha}} = [4, 3, 2, 2, 1]$ or $[4, 3, 2, 2, 2]$ give the desired result.

We remark that the asymptotic version of the above fact is established in (Hu and Lu, 2019, Proposition 1 and Algorithm 1). However, we emphasize that although the construction of $\hat{\alpha}$ is trivial once $\text{prox}_J(\mathbf{v}; \boldsymbol{\alpha})$ is known beforehand, it is difficult to derive $\hat{\alpha}$ in general: $\text{prox}_J(\mathbf{v}; \boldsymbol{\alpha})$ has no explicit form and its computation is complicated, as can be seen in Algorithm 1. Nevertheless, certain useful properties of the effective penalty $\hat{\alpha}$ can be extracted.

Fact C.2. *Suppose \mathbf{v} is sorted in decreasing absolute values, then $\hat{\alpha}$ agrees with $\boldsymbol{\alpha}$ at the non-zero entries of $\text{prox}_J(\mathbf{v}; \boldsymbol{\alpha})$ where the proximal operation takes no averaging.*

Proof of Fact C.2. From Algorithm 1, for each entry of \mathbf{v} , one may think of prox_J as either applying a soft-thresholding or applying a soft-thresholding followed by an averaging. \square

In the example given in (C.1), the subsequence $[3, 2, 1]$ of \mathbf{v} experiences the soft-thresholding with respect to the penalty subsequence $[2, 2, 2]$; on the other hand, the subsequence $[6, 5]$ experiences the soft-thresholding with respect to the penalty subsequence $[5, 2]$ (resulting in $[1, 3]$) then the averaging (resulting in $[2, 2]$); this output is equivalent to $[6, 5]$ experiencing the soft-thresholding with respect to the effective penalty subsequence $[4, 3]$ instead of the actual penalty subsequence $[5, 2]$.

In other words, if v_i is indeed penalized by α_i without averaging, then the effective penalty $\hat{\alpha}_i$ agrees with the actual penalty α_i .

The above result generally does not hold when v is not sorted in decreasing magnitudes. For instance,

$$\text{prox}_J([3, 5, -6]; [5, 2, 2]) = [1, 2, -2] = \eta_{\text{soft}}([3, 5, -6]; [2, 3, 4]).$$

Nevertheless, we show that larger input (in magnitude) matches with larger penalties.

Fact C.3. *Suppose \mathbf{v} is sorted in decreasing absolute values, so is $\hat{\alpha}$. Then larger input will have larger effective penalty.*

Proof of Fact C.3. For the simplicity of discussion, we assume $\mathbf{v} \geq 0$. Then we have $\text{prox}_J(\mathbf{v}; \boldsymbol{\alpha}) = \max(\text{AVE}(\mathbf{v} - \boldsymbol{\alpha}), 0)$ where $\text{AVE}(\cdot)$ is the averaging operator in Algorithm 1. For indices where the averaging does not take place on the sequence $\mathbf{v} - \boldsymbol{\alpha}$, we have $\hat{\alpha}_i = \alpha_i$ from Fact C.2. Clearly $\hat{\alpha}$ is decreasing on these indices as $\boldsymbol{\alpha}$ is decreasing by the definition of the sorted ℓ_1 norm. For indices where the averaging does take place, say the averaged magnitude is $c := [\text{prox}_J(\mathbf{v}; \boldsymbol{\alpha})]_I$ for some set of indices I , then $\hat{\alpha}_i = v_i - [\text{prox}_J(\mathbf{v}; \boldsymbol{\alpha})]_i = v_i - c$ (by Fact C.1), which is decreasing in i since \mathbf{v}_I is a decreasing subsequence. \square

Now that we have derived some properties of the sequence $\hat{\alpha}$ as a whole, we will focus on a particular point of the sequence. Before we move on, we introduce a quantile-related concept.

Definition C.4. *For a vector $\mathbf{v} \in \mathbb{R}^p$, we denote the k -th largest element in absolute values as $\mathbf{v}_{(k)}$. For a distribution V , we denote $V_{(\mathbf{k})}$ as the **upper \mathbf{k} -quantile** with $\mathbf{k} \in [0, 1]$:*

$$\mathbb{P}(|V| \geq V_{(\mathbf{k})}) = \mathbf{k}.$$

For example, $V_{(0.25)}$ is the upper quartile of $|V|$; $V_{(0.5)}, V_{(0)}, V_{(1)}$ are the median, maximum and minimum of $|V|$ respectively.

We show an asymptotic result that $\boldsymbol{\alpha}$ and $\hat{\alpha}$ agree at a specific point closely related to the zero-threshold defined in Definition 4.1.

Proposition C.5. *Suppose $\mathbf{v}(p), \boldsymbol{\alpha}(p), \widehat{\boldsymbol{\alpha}}(p)$ converge weakly to distributions V, A, \widehat{A} respectively, with V being a continuous distribution whose support contains 0. Then*

$$\widehat{A}_{(\kappa)} = A_{(\kappa)} = |V|_{(\kappa)},$$

where κ is the asymptotic sparsity of the SLOPE estimator, defined in (5.7).

To see how this asymptotic result relates to the zero-threshold $\alpha(\pi, A)$ in Definition 4.1, it is helpful to consider $V = \pi + Z$ (which is continuous even if π is discrete), since the SLOPE estimator's distribution is $\widehat{\Pi} = \eta_{\pi+Z, A}(\pi + Z)$.

Proof of Proposition C.5. Then the asymptotic sparsity is

$$\kappa := \text{plim} \{|\{i : [\text{prox}_J(\mathbf{v}; \boldsymbol{\alpha})]_i \neq 0\}|/p = \mathbb{P}(\eta_{\pi+Z, A}(\pi + Z) \neq 0) = \mathbb{P}(|\pi + Z| > \alpha(\pi, A)).$$

On the other hand, from the soft-thresholding effect of $\eta_{V, A}$, we have

$$\eta_{V, A}(V) = \eta_{\text{soft}}(V; \widehat{A}),$$

and equivalently

$$\kappa = \mathbb{P}(|\eta_{V, A}(V)| \neq 0) = \mathbb{P}(\eta_{\text{soft}}(|V|; \widehat{A}) \neq 0) = \mathbb{P}(|V| > \widehat{A}),$$

which indicates

$$|V|_{(\kappa)} = \widehat{A}_{(\kappa)} = \alpha(\pi, A).$$

From the proof of Fact C.1 (also from (Hu and Lu, 2019, Proposition 2)), we know $\widehat{A}_{(\kappa)} = |V|_{(\kappa)} - \eta_{V, A}(|V|_{(\kappa)})$. Together with the above, it holds that $\eta_{V, A}(|V|_{(\kappa)}) = 0$.

Notice that $\eta_{V, A}$ is continuous, thus there must exist some interval $[|V|_{(\kappa)}, x]$ where $\eta_{V, A}$ is not constant (i.e. penalties are not averaged), because $\eta_{V, A}(|V|_{(\kappa)}) = 0$ but $\eta_{V, A}(x) > 0$. Hence by Fact C.2, we obtain $\widehat{A}_{(\kappa)} = A_{(\kappa)}$. \square

To summarize, we can reduce the non-separable SLOPE proximal operator to some separable soft-thresholding, asymptotically. In this way, we can alternatively study the effective penalty used in the soft-thresholding, instead of the implicit SLOPE proximal operator. We emphasize that Appendix C is the key to study the SLOPE TPP-FDP trade-off bounds q_\star and q^\star in Section 4 and Section 5.

D SLOPE trade-off and Möbius upper bound

In this section we provide some useful results that describe the SLOPE TPP-FDP trade-off curve beyond the Lasso phase transition. In particular, we show that the SLOPE state evolution and calibration constraints can be translated to analogous constraints based on the soft-thresholding function.

D.1 Using AMP to characterize the asymptotic TPP and FDP

In this section, we give a sketch of the proof of Lemma 3.1, which consists of justifying the use of AMP to characterize the FDP and TPP of SLOPE asymptotically.

It has been rigorously proven in (Bu et al., 2020, Theorem 3) that $\frac{1}{n} \sum_{i=1}^n \psi([\eta_{\Pi+\tau Z, A\tau}(\boldsymbol{\beta} + \tau Z)]_i, \beta_i)$ is asymptotically equal in distribution to that of $\frac{1}{n} \sum_{i=1}^n \psi(\widehat{\beta}_i, \beta_i)$, when $\psi : \mathbb{R}^2 \rightarrow \mathbb{R}$ is a pseudo-Lipschitz continuous function. We would like to use this result to analyze the FDP and TPP, where from Lemma 3.1 we see that

$$\text{FDP}(\boldsymbol{\beta}, \boldsymbol{\lambda}) = \frac{|\{j : \widehat{\beta}_j \neq 0, \beta_j = 0\}|}{|\{j : \widehat{\beta}_j \neq 0\}|} = \frac{\sum_j \varphi_V(\widehat{\beta}_j, \beta_j)}{\sum_j \varphi_V(\widehat{\beta}_j, \beta_j) + \sum_j \varphi_T(\widehat{\beta}_j, \beta_j)}, \quad (\text{D.1})$$

and

$$\text{TPP}(\boldsymbol{\beta}, \boldsymbol{\lambda}) = \frac{|\{j : \widehat{\beta}_j \neq 0, \beta_j \neq 0\}|}{|\{j : \beta_j \neq 0\}|} = \frac{\sum_j \varphi_T(\widehat{\beta}_j, \beta_j)}{\sum_j 1(\beta_j \neq 0)}, \quad (\text{D.2})$$

are determined by sums of discontinuous functions, $\varphi_V(x, y) = 1(x \neq 0)1(y = 0)$ and $\varphi_T(x, y) = 1(x \neq 0)1(y \neq 0)$, and not pseudo-Lipschitz functions. Therefore (Bu et al., 2020, Theorem 3) does not apply directly. Nevertheless, we are still able to use the characterization given by AMP, as is demonstrated in Lemma D.1. The proof of Lemma D.1 is an extension of the analogous result for the Lasso case given in (Su et al., 2017, Lemma A.1). We notice that the result of Lemma 3.1 is just that given in (D.5).

Lemma D.1. *Under the working assumptions, namely (A1), (A2), and (A3), the SLOPE estimator $\widehat{\boldsymbol{\beta}}(\boldsymbol{\lambda})$ obeys*

$$\frac{V(\boldsymbol{\lambda})}{p} := \sum_j \frac{\varphi_V(\widehat{\beta}_j, \beta_j)}{p} = \frac{|\{j : \widehat{\beta}_j \neq 0, \beta_j = 0\}|}{p} \xrightarrow{P} \mathbb{P}(\eta_{\pi+Z, A}(\pi + Z) \neq 0, \pi = 0), \quad (\text{D.3})$$

$$\frac{T(\boldsymbol{\lambda})}{p} := \sum_j \frac{\varphi_T(\widehat{\beta}_j, \beta_j)}{p} = \frac{|\{j : \widehat{\beta}_j \neq 0, \beta_j \neq 0\}|}{p} \xrightarrow{P} \mathbb{P}(\eta_{\pi+Z, A}(\pi + Z) \neq 0, \pi \neq 0), \quad (\text{D.4})$$

where Z is a standard normal independent of Π , (τ, A) is the unique solution to the state evolution (3.2) and the calibration (3.3), and $\pi = \Pi/\tau$. Consequently, we have using the representations in (D.1) and (D.2) and the definitions of $V(\boldsymbol{\lambda})$ and $T(\boldsymbol{\lambda})$ above, that

$$\text{FDP} = \frac{V(\boldsymbol{\lambda})}{V(\boldsymbol{\lambda}) + T(\boldsymbol{\lambda})} \xrightarrow{P} \text{FDP}^\infty, \quad \text{and} \quad \text{TPP} = \frac{T(\boldsymbol{\lambda})}{\sum_j 1(\beta_j \neq 0)} \xrightarrow{P} \text{TPP}^\infty. \quad (\text{D.5})$$

Proof of Lemma D.1. The analogous result for when $\widehat{\boldsymbol{\beta}}$ is a Lasso solution is proven rigorously in Bogdan et al. (2013b). Here we adapt their proof for SLOPE. The high level idea for the proof of (D.3) and (D.4) is to construct two series of pseudo-Lipschitz continuous functions

$$\varphi_{V,h}(x, y) = (1 - Q(x/h))Q(y/h) \quad \text{and} \quad \varphi_{T,h}(x, y) = (1 - Q(x/h))(1 - Q(y/h)),$$

where $Q(x) = \max\{1 - |x|, 0\}$, that approach φ_V, φ_T as $h \rightarrow 0^+$. Hence, one can then argue

$$\begin{aligned} \lim_{p \rightarrow \infty} \frac{1}{p} \sum_{i=1}^p \varphi_V(\hat{\beta}_i, \beta_i) &\stackrel{P}{=} \lim_{h \rightarrow 0} \lim_{p \rightarrow \infty} \frac{1}{p} \sum_{i=1}^p \varphi_{V,h}(\hat{\beta}_i, \beta_i) \\ &\stackrel{P}{=} \lim_{h \rightarrow 0} \mathbb{E} \varphi_{V,h} \left(\eta_{\Pi + \tau Z, A\tau}(\Pi + \tau Z), \Pi \right) \\ &= \mathbb{E} \varphi_V \left(\eta_{\Pi + \tau Z, A\tau}(\Pi + \tau Z), \Pi \right), \end{aligned}$$

where the second equality in the above employs the AMP results for the pseudo-Lipschitz continuous function $\varphi_{V,h}(\cdot, \cdot)$. The technical aspects of the proof involve making this argument rigorous. The final result follows by noticing that

$$\begin{aligned} \mathbb{E} \varphi_V \left(\eta_{\Pi + \tau Z, A\tau}(\Pi + \tau Z), \Pi \right) &= \mathbb{E} [1(\eta_{\Pi + \tau Z, A\tau}(\Pi + \tau Z) \neq 0) 1(\Pi = 0)] \\ &= \mathbb{P} \left(\eta_{\Pi + \tau Z, A\tau}(\Pi + \tau Z) \neq 0, \Pi = 0 \right) \\ &= \mathbb{P}(\eta_{\pi + Z, A}(\pi + Z) \neq 0, \pi = 0). \end{aligned}$$

Since the proof for the SLOPE results (D.3) and (D.4) are extremely similar to that of the Lasso given in (Bogdan et al., 2013b, Theorem 1), we omit the details and only point out that there are some minor differences due to the fact that the subgradient vector from the partial KKT condition of the SLOPE solution to problem (1.2) has a slightly different form compared to the analogous subgradient vector for Lasso.

Now leveraging results (D.3) and (D.4), that give

$$\begin{aligned} V(\boldsymbol{\lambda})/p &\xrightarrow{\mathbb{P}} \mathbb{P} \left(\eta_{\Pi + \tau Z, A\tau}(\Pi + \tau Z) \neq 0, \Pi = 0 \right) = \mathbb{P}(\eta_{\pi + Z, A}(\pi + Z) \neq 0, \pi = 0), \\ T(\boldsymbol{\lambda})/p &\xrightarrow{\mathbb{P}} \mathbb{P} \left(\eta_{\Pi + \tau Z, A\tau}(\Pi + \tau Z) \neq 0, \Pi \neq 0 \right) = \mathbb{P}(\eta_{\pi + Z, A}(\pi + Z) \neq 0, \pi \neq 0), \end{aligned}$$

and using that

$$\mathbb{P}(\eta_{\pi + Z, A}(\pi + Z) \neq 0, \pi = 0) = (1 - \epsilon) \mathbb{P}(\eta_{\pi + Z, A}(Z) \neq 0),$$

and

$$\mathbb{P}(\eta_{\pi + Z, A}(\pi + Z) \neq 0, \pi \neq 0) = \epsilon \mathbb{P}(\eta_{\pi + Z, A}(\pi^* + Z) \neq 0),$$

where we recall π^* is the distribution of the non-zero part of π , we finally obtain

$$\begin{aligned} \text{FDP}^\infty(\Pi, \Lambda) &= \text{plim} \frac{V(\boldsymbol{\lambda})}{V(\boldsymbol{\lambda}) + T(\boldsymbol{\lambda})} \\ &= \frac{(1 - \epsilon) \mathbb{P}(\eta_{\pi + Z, A}(Z) \neq 0)}{(1 - \epsilon) \mathbb{P}(\eta_{\pi + Z, A}(Z) \neq 0) + \epsilon \mathbb{P}(\eta_{\pi + Z, A}(\pi^* + Z) \neq 0)}, \\ \text{TPP}^\infty(\Pi, \Lambda) &= \text{plim} \frac{T(\boldsymbol{\lambda})}{|\{j : \beta_j \neq 0\}|} = \mathbb{P}(\eta_{\pi + Z, A}(\pi^* + Z) \neq 0). \end{aligned}$$

□

The result of Lemma 3.1 (and Lemma D.1) demonstrates that when studying the trade-off between the FDP and TPP asymptotically, we can work with the explicit and amenable quantities $\mathbb{P}(\eta_{\pi + Z, A}(Z) \neq 0)$ and $\mathbb{P}(\eta_{\pi + Z, A}(\pi^* + Z) \neq 0)$.

D.2 A better understanding the Donoho-Tanner threshold

In this section, we introduce an equivalent definition of the DT threshold ϵ^* , originally defined in (2.1), from a non-parametric viewpoint. This definition is necessary for our analysis of the SLOPE trade-off upper bound q^* discussed in Section 5.

To specify the threshold ϵ^* when $\delta < 1$, we consider the equation

$$2(1 - \epsilon)[(1 + x^2)\Phi(-x) - x\phi(x)] + \epsilon(1 + x^2) = \delta \quad (\text{D.6})$$

in $x > 0$. Above, $\phi(\cdot)$ and $\Phi(\cdot)$ are the probability density function and cumulative distribution function of the standard normal distribution, respectively. We demonstrate the properties of (D.6) can be found in Figure 8 and Figure 9.

The key point we will use is that this equation has a unique positive root in x if and only if $0 < \epsilon < 1$ takes a certain value $\epsilon^*(\delta)$ that depends only on δ . This unique root is $x := t^*(u_{\text{DT}}^*(\delta))$, as given by Su et al. (2017, Appendix C). Furthermore, (D.6) has two roots when $\epsilon \leq \epsilon^*$ and no root otherwise. In fact, (D.6) originates from the state evolution (4.1) for the Lasso when we consider the infinity-or-nothing priors defined in (5.6), and it can also be found in Su et al. (2017, Equation (C.5)).

In summary, (D.6) gives an equivalent representation of $\epsilon^*(\delta)$ that we will find useful in the upcoming proofs. Namely, $\epsilon^*(\delta)$ is the specific value of $0 < \epsilon < 1$ such that (D.6) has a unique root.

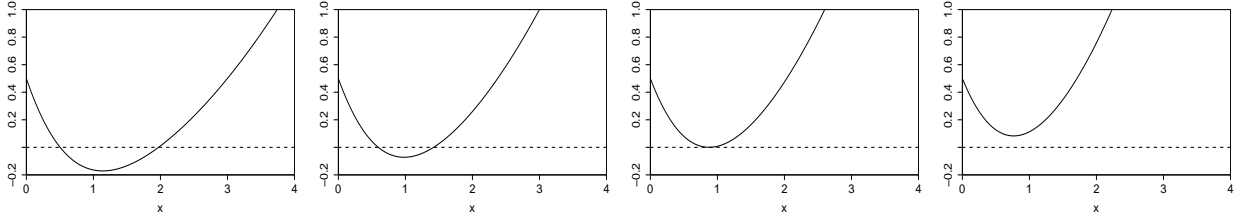


Figure 8: A plot of the function $f(x) = 2(1 - \epsilon)[(1 + x^2)\Phi(-x) - x\phi(x)] + \epsilon(1 + x^2) - \delta$ defined in (D.6) for $\delta = 0.5$ and $\epsilon \in \{0.1, 0.15, \epsilon^*(\delta) = 0.1928, 0.25\}$ (from left to right).

D.3 Proof of Lemma 5.3

Proof of Lemma 5.3. For infinity-or-nothing priors where $\pi = \infty$ with probability $\epsilon\epsilon'$ or $\pi = 0$ with probability $1 - \epsilon\epsilon'$, the state evolution constraint (4.1) gives,

$$\begin{aligned} \delta &\geq \mathbb{E} \left(\eta_{\pi+Z, A}(\pi + Z) - \pi \right)^2 \\ &= \mathbb{P}(\pi = \infty) \mathbb{E} \left(\eta_{\pi+Z, A}(\pi^* + Z) - \pi^* \right)^2 + \mathbb{P}(\pi \neq \infty) \mathbb{E} \eta_{\pi+Z, A}(Z)^2 \\ &= \epsilon\epsilon' \mathbb{E} \left(\eta_{\pi+Z, A}(\pi^* + Z) - \pi^* \right)^2 + (1 - \epsilon\epsilon') \mathbb{E} \eta_{\pi+Z, A}(Z)^2. \end{aligned} \quad (\text{D.7})$$

Using the effective penalty function \widehat{A}_{eff} defined in Definition 4.2, we can write the above as

$$\delta \geq \epsilon\epsilon' \mathbb{E} \left(\eta_{\text{soft}}(\pi^* + Z; \widehat{A}_{\text{eff}}(\pi^* + Z)) - \pi^* \right)^2 + (1 - \epsilon\epsilon') \mathbb{E} \eta_{\text{soft}}(Z; \widehat{A}_{\text{eff}}(Z))^2.$$

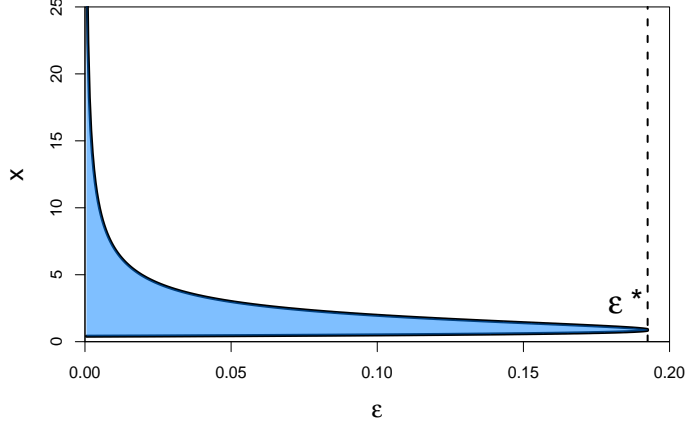


Figure 9: A plot to demonstration the roots of (D.6) with $\delta = 0.5$. Here $\epsilon^* = 0.1928$ is the dashed line and the blue area contains valid x for which the inequality in (D.6) holds for each ϵ . The black solid lines are the roots. Notice that the blue area corresponding to $\epsilon = 0.1$ corresponds to the area under the dashed line in leftmost plot of Figure 8.

Now, we denote the distribution $\widehat{A} \stackrel{\mathcal{D}}{=} \widehat{A}_{\text{eff}}(\pi + Z)$ and in what follows we study the distribution of $\widehat{A}_{\text{eff}}(\pi^* + Z)$ in more detail. Using the fact that $\pi^* + Z$ is almost surely larger than Z (since $\pi^* = \infty$) and Fact C.3, which states SLOPE assigns larger effective penalty to larger input, we conclude

$$\widehat{A}_{\text{eff}}(\pi^* + Z) \stackrel{\mathcal{D}}{=} \widehat{A} \Big| \widehat{A} > \widehat{A}_{(\epsilon\epsilon')}.$$

which, we will shortly show, is a constant. In the above, the quantity with a subscript, $\widehat{A}_{(\epsilon\epsilon')}$, is a quantile-related scalar such that $\mathbb{P}(\widehat{A} > \widehat{A}_{(\epsilon\epsilon')}) = \epsilon\epsilon'$, defined in Definition C.4. In words, the larger part of \widehat{A} (i.e. $\widehat{A} \Big| \widehat{A} > \widehat{A}_{(\epsilon\epsilon')}$) is assigned to the larger part of the input $\pi^* + Z$; and $\widehat{A} \Big| \widehat{A} \leq \widehat{A}_{(\epsilon\epsilon')}$ is assigned to the input Z . Furthermore, using the assumption that

$$\epsilon\epsilon' \leq \mathbb{P}(\Lambda = \max \Lambda) = \mathbb{P}(A = \max A), \quad (\text{D.8})$$

where the final equality follows since Λ and A only differ by a constant (see the calibration equation (3.3)), we get

$$\widehat{A} \Big| \widehat{A} \geq \widehat{A}_{(\epsilon\epsilon')} \stackrel{\mathcal{D}}{=} A \Big| A \geq A_{(\epsilon\epsilon')} = A_{(\epsilon\epsilon')} \in \mathbb{R}.$$

In the above, the first equality comes from the fact that the upper $\epsilon\epsilon'$ quantile of A is Lasso-like, following from (D.8) (hence, there is no averaging in the SLOPE proximal operator and Fact C.2 applies) and the second equality also follows from (D.8) as well.

Therefore, using that $\widehat{A}_{\text{eff}}(\pi^* + Z)$ is a constant equal to $A_{(\epsilon\epsilon')}$, the state evolution constraint becomes

$$\begin{aligned} \delta &\geq \epsilon\epsilon' \mathbb{E} \left(\eta_{\text{soft}}(\pi^* + Z; A_{(\epsilon\epsilon')}) - \pi^* \right)^2 + (1 - \epsilon\epsilon') \mathbb{E} \eta_{\text{soft}}(Z; \widehat{A}_{\text{eff}}(Z))^2 \\ &= \epsilon\epsilon' \mathbb{E} (A_{(\epsilon\epsilon')} - Z)^2 + (1 - \epsilon\epsilon') \mathbb{E} \eta_{\text{soft}}(Z; \widehat{A}_{\text{eff}}(Z))^2 \\ &= \epsilon\epsilon' (1 + A_{(\epsilon\epsilon')}^2) + (1 - \epsilon\epsilon') \mathbb{E} \eta_{\text{soft}}(Z; \widehat{A}_{\text{eff}}(Z))^2, \end{aligned} \quad (\text{D.9})$$

where the first equality follows by the definition of the soft-thresholding function and the fact that $A_{(\epsilon\epsilon')}$ is constant and the second from the fact that $Z \sim \mathcal{N}(0, 1)$.

Notice that, again by Fact C.3, $\widehat{A}_{\text{eff}}(z)$ is increasing in absolute value of z , hence

$$\widehat{A}_{\text{eff}}(Z) \leq \sup \left(\widehat{A} | \widehat{A} \leq \widehat{A}_{(\epsilon\epsilon')} \right) = \widehat{A}_{(\epsilon\epsilon')} = A_{(\epsilon\epsilon')},$$

in which the last equality holds from Fact C.2, as a consequence of

$$\lim_{x \nearrow \epsilon\epsilon'} \left| \eta_{\pi+Z, A}(\pi + Z) \right|_{(x)} = \infty > \sup_Z \left| \eta_{\pi+Z, A}(Z) \right| = \lim_{x \searrow \epsilon\epsilon'} \left| \eta_{\pi+Z, A}(\pi + Z) \right|_{(x)},$$

i.e. no averaging takes place at the quantile $\epsilon\epsilon'$ (here the limits are one-sided limits). Additionally, we observe that $\eta_{\text{soft}}(z; x)^2$ is decreasing in the scalar x . Therefore, we get

$$\mathbb{E} \eta_{\text{soft}}(Z; \widehat{A}_{\text{eff}}(Z))^2 \geq \mathbb{E} \eta_{\text{soft}}(Z; A_{(\epsilon\epsilon')})^2.$$

Applying the above bound into (D.9) and then using some simple algebra to express the soft-thresholding function, we find

$$\begin{aligned} \delta &\geq \epsilon\epsilon'(1 + A_{(\epsilon\epsilon')}^2) + (1 - \epsilon\epsilon') \mathbb{E} \eta_{\text{soft}}(Z; A_{(\epsilon\epsilon')})^2 \\ &= \epsilon\epsilon'(1 + A_{(\epsilon\epsilon')}^2) + 2(1 - \epsilon\epsilon') \left[(1 + A_{(\epsilon\epsilon')}^2) \Phi(-A_{(\epsilon\epsilon')}) - A_{(\epsilon\epsilon')} \phi(A_{(\epsilon\epsilon')}) \right]. \end{aligned} \quad (\text{D.10})$$

Following the discussion around (D.6), the above inequality can only possibly hold when $\epsilon\epsilon' \leq \epsilon^*$, or when $\epsilon' \in [0, \epsilon^*/\epsilon]$ as desired. \square

D.4 Achieving the Möbius curve of q^*

In this section we prove Proposition 2.3, or in other words, we show that with the special design of a two-level SLOPE penalty and infinity-or-nothing prior, we can approach the Möbius part of q^* arbitrarily close.

Proof of Proposition 2.3. To give the proof, we consider a specific prior $\Pi_M(\epsilon^*/\epsilon)$ as in (2.4) and let $M \rightarrow \infty$. Here ϵ^* is defined in (2.1). This is equivalent to setting the normalized prior π to the infinity-or-nothing prior $\pi_\infty(\epsilon^*/\epsilon)$, defined in (5.6) as:

$$\pi_\infty(\epsilon^*/\epsilon) = \begin{cases} \infty & w.p. \ \epsilon^*, \\ 0 & w.p. \ 1 - \epsilon^*. \end{cases} \quad (\text{D.11})$$

As for the SLOPE penalty, we consider a sub-class of two-level penalty distributions Λ that satisfy $\mathbb{P}(\Lambda = \max \Lambda) \geq \epsilon^*$, or in the notation of (2.3) we will have $w > \epsilon^*$. By setting the penalty as such, we satisfy the assumption in Proposition 5.2 and consequently we can apply the results in Lemma 5.3 and Lemma 5.4.

Now we are ready to present the proof. For any $\text{TPP}^\infty = u \geq u_{\text{DT}}^*(\delta)$, we recall from (5.9) in the proof of Lemma 5.4 that the asymptotic sparsity $\kappa(\Pi, \Lambda)$ (defined in (5.7)) satisfies

$$\kappa(\Pi, \Lambda) = 1 - \frac{\epsilon(1-u)(1-\epsilon\epsilon')}{\epsilon - \epsilon\epsilon'}. \quad (\text{D.12})$$

From (5.11), minimizing $\text{FDP}^\infty(\Pi, \Lambda)$ is equivalent to minimizing $\kappa(\Pi, \Lambda)$, which from (D.12) we see is further equivalent to maximizing ϵ' . Since Lemma 5.3 states that $\epsilon' \leq \epsilon^*/\epsilon$, we aim to achieve a sparsity with $\epsilon' = \epsilon^*/\epsilon$, namely a sparsity of

$$\kappa(\Pi, \Lambda) = 1 - \frac{\epsilon(1-u)(1-\epsilon^*)}{\epsilon - \epsilon^*}, \quad (\text{D.13})$$

which is given in (5.10) as the smallest sparsity for which $\text{TPP}^\infty \geq u$ is possible.

Therefore, we consider a specific prior $\Pi_M(\epsilon^*/\epsilon)$ as in (2.4) and let $M \rightarrow \infty$. Then the limiting normalized prior π is the infinity-or-nothing prior defined in (D.11). Next, we seek the penalty Λ that can result in the desired sparsity $\kappa(\pi, \Lambda)$ in (D.13), or equivalently, we seek the normalized version of Λ given by A , defined via the calibration equation (3.3).

To find such a penalty Λ , we consider the state evolution constraint (4.1), and emphasize that when achieving the desired sparsity, (4.1) must be satisfied by the pair (π, A) . We use the result of (D.10) and more generally, the proof of Lemma 5.3 in Appendix D.3, to give for $\epsilon' = \epsilon^*/\epsilon$,

$$(1 - \epsilon^*) \mathbb{E} \eta_{\text{soft}}(Z; A_{(\epsilon^*)})^2 + \epsilon^*(1 + A_{(\epsilon^*)}^2) \leq \mathbb{E} \left(\eta_{\pi+Z, A}(\pi + Z) - \pi \right)^2 \leq \delta, \quad (\text{D.14})$$

where again $A_{(\epsilon^*)}$ is a scalar defined in Definition C.4, i.e., it is chosen such that $\mathbb{P}(A > A_{(\epsilon^*)}) = \epsilon^*$. In particular, the first inequality above only holds with equality when $\eta_{\pi+Z, A}(Z) \stackrel{\mathcal{D}}{=} \eta_{\text{soft}}(Z; A_{(\epsilon^*)})$, which can be seen by comparing the bounds in (D.10) and (D.7).

From another direction, by the alternative definition of ϵ^* in (D.6), we have

$$(1 - \epsilon^*) \mathbb{E} \eta_{\text{soft}}(Z; x)^2 + \epsilon^*(1 + x^2) \geq \delta, \quad (\text{D.15})$$

for all $x > 0$, with the equality holding only when $x = t^*(u_{\text{DT}}^*(\delta))$, as has been discussed in Appendix D.2. We notice that (D.15) equals (D.6) since $\mathbb{E} \eta_{\text{soft}}(Z; x)^2 = 2[(1 + x^2)\Phi(-x) - x\phi(x)]$. Combining (D.14) and (D.15), we obtain

$$\delta \stackrel{(a)}{\leq} (1 - \epsilon^*) \mathbb{E} \eta_{\text{soft}}(Z; A_{(\epsilon^*)})^2 + \epsilon^*(1 + A_{(\epsilon^*)}^2) \stackrel{(b)}{\leq} \mathbb{E} \left(\eta_{\pi+Z, A}(\pi + Z) - \pi \right)^2 \stackrel{(c)}{\leq} \delta,$$

which is only valid when we meet the equality conditions for all the inequalities above. I.e, the penalty distribution A must be chosen to satisfy

$$\begin{aligned} (a) \quad & t^*(u_{\text{DT}}^*) = A_{(\epsilon^*)}; \\ (b) \quad & \eta_{\pi+Z, A}(Z) \stackrel{\mathcal{D}}{=} \eta_{\text{soft}}(Z; t^*(u_{\text{DT}}^*)); \end{aligned}$$

Notice that the condition (c) is automatically satisfied when the condition (a) is satisfied.

To design such A , it suffices to set a two-level penalty distribution $A = A_{t^*(u_{\text{DT}}^*), r t^*(u_{\text{DT}}^*), w}$ in (2.3) for carefully chosen $r(u)$ and $w(u)$, with $w(u) > \epsilon^*$. Then the condition $w(u) > \epsilon^*$ gives $A_{(\epsilon^*)} = t^*(u_{\text{DT}}^*)$ by design, thus we satisfy the condition (a). In words, the infinite input $\pi^* + Z$ is assigned to match with the first level of the two-level SLOPE penalty A .

We now turn to the more difficult condition (b) and explicitly choose $r(u)$ and $w(u)$ so that it is satisfied. Before giving the exact values of $r(u)$ and $w(u)$ and showing how they lead to satisfying condition (b), we take some time to further investigate the sparsity of the SLOPE estimator, $\kappa(\pi, A)$. Recall that the zero-threshold, defined in Definition 4.1, is the value $\alpha(\pi, A)$ such that $\eta_{\pi+Z, A}(x) = 0$

if and only if $|x| \leq \alpha(\pi, A)$ and by Proposition C.5, we know that the zero-threshold must be equal to one of the two levels of SLOPE penalty.

Now, when w is small, few input values are subjected to the larger level of the penalty and of those inputs, all will correspond to infinite signal prior elements. Thus, the zero-threshold will be the smaller level of the penalty, namely it equals $rt^*(u_{\text{DT}}^*)$ (visualized in Figure 10(a)(b)). In more details, for small $w(u)$, the value $r(u)$ controls the sparsity in the sense that

$$\kappa(\pi, A) = \mathbb{P}(|\pi + Z| > rt^*(u_{\text{DT}}^*)) = \epsilon^* + (1 - \epsilon^*) \mathbb{P}(|Z| > rt^*(u_{\text{DT}}^*)).$$

Following the above equation, there exists an one-to-one map between $\text{TPP}^\infty = u$ and $r(u)$ to achieve the desired sparsity of (D.13):

$$\begin{aligned} 1 - \frac{\epsilon(1-u)(1-\epsilon^*)}{\epsilon - \epsilon^*} &= \kappa(\pi, A) = \epsilon^* + (1 - \epsilon^*) \mathbb{P}(|Z| > rt^*(u_{\text{DT}}^*)) \\ &= \epsilon^* + 2(1 - \epsilon^*) \Phi(-rt^*(u_{\text{DT}}^*)). \end{aligned}$$

Explicitly, by rearranging the above, we conclude that the sparsity condition (D.13) is satisfied if one sets

$$r(u) = \Phi^{-1} \left(\frac{2\epsilon - \epsilon^* - \epsilon u}{2(\epsilon - \epsilon^*)} \right) / t^*(u_{\text{DT}}^*),$$

given that $rt^*(u_{\text{DT}}^*)$ is the zero-threshold. In what follows, we always aim to keep the zero-threshold at $rt^*(u_{\text{DT}}^*)$.

As w increases, more and more input values are subjected to the larger level of the penalty. Thus, the zero-threshold and sparsity will remain the same, taking as values the second level of the penalty, $rt^*(u_{\text{DT}}^*)$, and that in (D.13), respectively, until w moves above a certain bound and forces the zero-threshold to increase to the larger level of A (again by Proposition C.5 the zero-threshold can only take these two levels).

Moreover, as w increases to this bound, we observe that $\eta_{\pi+Z,A}(Z)$ becomes more similar to $\eta_{\text{soft}}(Z; t^*(u_{\text{DT}}^*))$, as demonstrated in Figure 10, and hence $\mathbb{E} \eta_{\pi+Z,A}(Z)^2$ becomes more similar to $\mathbb{E} \eta_{\text{soft}}(Z; t^*(u_{\text{DT}}^*))^2$. To observe this similarity property rigorously, notice that the quantile function of $\pi + Z$ has a sharp drop at ϵ^* since $\mathbb{P}(\pi = \infty) = \epsilon^*$, which splits the quantiles corresponding to $\infty + Z$ and to Z . Accordingly, Fact C.3 says that for the input value corresponding to the ‘infinity’ part of the signal, $\infty + Z$, since $w > \epsilon^*$, the SLOPE assigns a penalty given by the upper ϵ^* quantiles of A , namely $(A|A \geq A_{(\epsilon^*)}) = A_{(\epsilon^*)} = t^*(u_{\text{DT}}^*)$ and for the inputs corresponding to the ‘nothing’ part of the signal, Z , SLOPE assigns a penalty given by the lower $1 - \epsilon^*$ quantiles of A , denoted by

$$A^*(w) := (A|A \leq A_{(\epsilon^*)}) = A_{t^*(u_{\text{DT}}^*), rt^*(u_{\text{DT}}^*), \frac{w-\epsilon^*}{1-\epsilon^*}}.$$

Notice that what the above says is that a fraction, $\frac{w-\epsilon^*}{1-\epsilon^*}$, of the ‘nothing’ signals Z match with the large penalty $t^*(u_{\text{DT}}^*)$ and the remaining fraction match with the smaller penalty $rt^*(u_{\text{DT}}^*)$. In this way, when considering just the ‘nothing’ part of the signal, we can write $\eta_{\pi+Z,A}(Z) \stackrel{\mathcal{D}}{=} \eta_{Z,A^*(w)}(Z)$ ⁶.

We now determine the exact $w(u)$ such that $\eta_{Z,A^*(w)}(Z) \stackrel{\mathcal{D}}{=} \eta_{\text{soft}}(Z; t^*(u_{\text{DT}}^*))$, so as to satisfy condition (b). Our strategy is to select a $w(u)$ such that we are able to divide the output of

⁶Notice that, because no averaging takes place at the w -th position, $\text{prox}_J(\pi + \mathbf{Z}; \boldsymbol{\alpha}) = [\text{prox}_J(\pi^* + \mathbf{Z}; (\alpha_1, \dots, \alpha_{wp})), \text{prox}_J(\mathbf{Z}; (\alpha_{wp+1}, \dots, \alpha_p))]$, in which $[\cdot]$ means concatenation.

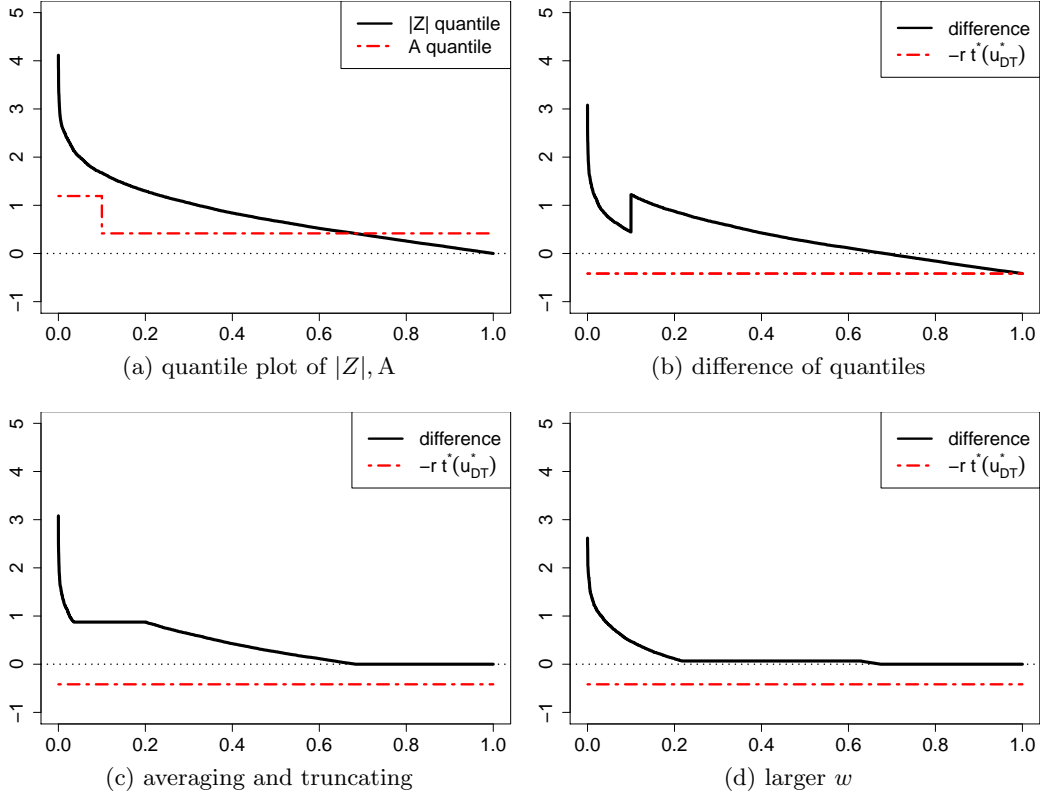


Figure 10: Fixing r and varying w within some range remains the sparsity of the SLOPE estimator (around 0.6) but forces the SLOPE proximal operator to approach the soft-thresholding. In other words, as w increases, the flat (averaged) quantile of $\eta_{\pi+Z,A}(\pi+Z)$ takes a magnitude converging to zero. This implies that $\eta_{Z,A^*}(Z) \rightarrow \eta_{\text{soft}}(Z; t^*(u_{\text{DT}}^*))$. Here $\pi = 0, \mathbf{A} = \mathbf{A}_{t^*(u_{\text{DT}}^*), rt^*(u_{\text{DT}}^*), w}, \delta = 0.3, \epsilon = 0.2, \epsilon^* = 0.087, t^*(u_{\text{DT}}^*) = 1.1924, u = 0.8176, r(u) = 0.3500, w(u) = 0.4819$.

$\eta_{Z,A^*(w)}(Z)$ into clearly non-zero, arbitrarily close to zero and zero parts, so as to look like the soft-thresholding function as desired. That we can do this is visualized in Figure 10 and follows from the fact that with the two-level penalty, there will be only one flat averaged region in the output of $\eta_{Z,A^*(w)}(Z)$, which we want to suppress to almost zero. Denoting

$$P_1 := \mathbb{P}(|Z| > t^*(u_{\text{DT}}^*)), \quad P_2 := \frac{w - \epsilon^*}{1 - \epsilon^*}, \quad \text{and} \quad P_3 := \mathbb{P}(|Z| > rt^*(u_{\text{DT}}^*)), \quad (\text{D.16})$$

we quantitatively define these three parts (clearly non-zero, close to zero, and zero) as the quantiles of $\eta_{Z,A^*(w)}(Z)$ on the probability intervals $(0, P_1)$, (P_1, P_3) and $(P_3, 1)$ respectively: i.e. we want $w(u)$ such that

$$|\eta_{Z,A^*(w)}(Z)| \stackrel{\mathcal{D}}{=} \begin{cases} \eta_{\text{soft}}(|Z|; |Z| > t^*(u_{\text{DT}}^*); t^*(u_{\text{DT}}^*)) & \text{w.p. } P_1 \\ 0.0001 & \text{w.p. } P_3 - P_1 \\ 0 & \text{w.p. } 1 - P_3 \end{cases}$$

Here 0.0001 can be an arbitrarily small positive constant, which tends to 0 as $w \nearrow w(u)$. By such a construction, we have met our goal: we have determined $w(u)$ such that $\eta_{Z, A^*(w)}(Z) \stackrel{D}{=} \eta_{\text{soft}}(Z; t^*(u_{\text{DT}}^*))$. For example, in Figure 10(d), $P_1 \approx 0.23$ and $P_3 \approx 0.68$. Given that the averaged sub-interval between P_1 and P_3 is arbitrarily close to zero, we can write the scaled conditional expectation of $|\eta_{Z, A^*(w)}(Z)|$ being on the flat region as an integral of the quantile function:

$$\begin{aligned} & \int_{P_1}^{P_2} (|Z|_{(x)} - t^*(u_{\text{DT}}^*)) dx + \int_{P_2}^{P_3} (|Z|_{(x)} - rt^*(u_{\text{DT}}^*)) dx \\ &= \int_{P_1}^{P_3} \eta_{Z, A^*(w)}(|Z|_{(x)}) dx = 0.0001(P_3 - P_1). \end{aligned}$$

Setting $w = w(u)$ and thus the right hand side to 0, and rearranging the equation,

$$\int_{P_1}^{P_3} |Z|_{(x)} dx = t^*(u_{\text{DT}}^*)(P_2 - P_1) + rt^*(u_{\text{DT}}^*)(P_3 - P_2) = t^*(u_{\text{DT}}^*)[(P_2 - P_1) + r(P_3 - P_2)],$$

where the left hand side is the scaled conditional expectation of the random variable $|Z|$ given $rt^*(u_{\text{DT}}^*) < |Z| < t^*(u_{\text{DT}}^*)$, with an explicit form as

$$\begin{aligned} \int_{P_1}^{P_3} |Z|_{(x)} dx &= \mathbb{E} \left(|Z| \middle| rt^*(u_{\text{DT}}^*) < |Z| < t^*(u_{\text{DT}}^*) \right) \mathbb{P} (rt^*(u_{\text{DT}}^*) < |Z| < t^*(u_{\text{DT}}^*)) \\ &= \mathbb{E} \left(Z \middle| rt^*(u_{\text{DT}}^*) < Z < t^*(u_{\text{DT}}^*) \right) \mathbb{P} (rt^*(u_{\text{DT}}^*) < |Z| < t^*(u_{\text{DT}}^*)) \\ &= 2\phi(rt^*(u_{\text{DT}}^*)) - 2\phi(t^*(u_{\text{DT}}^*)), \end{aligned}$$

in which the last equality holds from a direct calculation of the expectation of a two-sided truncated normal distribution. Hence, we have,

$$2\phi(rt^*(u_{\text{DT}}^*)) - 2\phi(t^*(u_{\text{DT}}^*)) = t^*(u_{\text{DT}}^*)[(P_2 - P_1) + r(P_3 - P_2)],$$

which, upon rearrangement, gives

$$P_2 = \frac{P_1 - rP_3}{1 - r} - \frac{2}{(1 - r)} \left[\frac{\phi(t^*(u_{\text{DT}}^*)) - \phi(rt^*(u_{\text{DT}}^*))}{t^*(u_{\text{DT}}^*)} \right].$$

Then, plugging in the values in (D.16), the above simplifies to

$$w(u) = \epsilon^* + \frac{2(1 - \epsilon^*)}{1 - r} \left[\Phi(-t^*(u_{\text{DT}}^*)) - r\Phi(-rt^*(u_{\text{DT}}^*)) - \frac{\phi(-t^*(u_{\text{DT}}^*)) - \phi(-rt^*(u_{\text{DT}}^*))}{t^*(u_{\text{DT}}^*)} \right].$$

We claim $w(u)$ can be uniquely determined by $r(u)$, and $w(u)$ is clearly larger than ϵ^* as the second term is positive. To see this, we study the term in the bracket and claim that its derivative over t^* is $(\phi(-t^*) - \phi(-rt^*)) / (t^*)^2$, which is negative and hence the term is larger than when $t^* = \infty$, i.e. 0.

Combining (5.2) for designing $r(u)$ and (5.3) for designing $w(u)$, we can design the two-level SLOPE penalty that, together with infinity-or-nothing prior $\pi_\infty(\epsilon^*/\epsilon)$, approaches $(u, q^*(u))$ arbitrarily close. \square

On a side note, if the w is larger than the specific choice in (5.3), i.e. when the flat quantile in Figure 10 drops below zero, the SLOPE proximal operator has the same effect as soft-thresholding and the analysis for the Lasso case follows. Consequently, TPP^∞ reduces to the interval $[0, u_{\text{DT}}^*]$. Graphically speaking, when one fixes r and increases w from 0 to 1 (similar to Figure 4), the SLOPE TPP^∞ will increase from u_{DT}^* to above, until $(\text{TPP}^\infty, \text{FDP}^\infty)$ touches the Möbius curve. Then TPP^∞ will suddenly jump below u_{DT}^* , once w is larger than (5.3), and then remain constant afterwards.

D.5 Achievable TPP–FDP region by SLOPE

The trade-off boundary curves q_* and q^* only provide information that splits the entire TPP–FDP region into two parts: the possibly achievable $(\text{TPP}^\infty, \text{FDP}^\infty)$ and the unachievable ones. See the red and non-red regions in Figure 5. Although we have shown the achievability of the upper boundary q^* via Proposition 2.3, such achievability of the curve does not directly distinguish the achievability of the regions, until the recent work on Lasso by Wang et al. (2020a) which gives a complete Lasso TPP–FDP diagram.

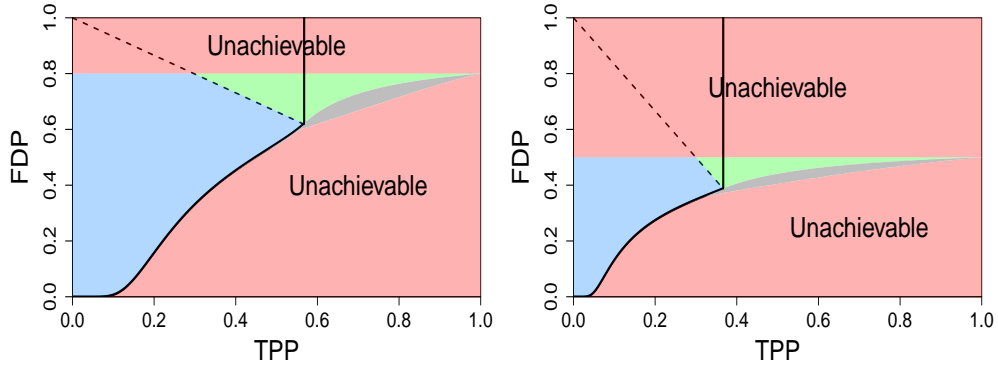


Figure 11: SLOPE TPP–FDP diagram by Proposition D.3. Left: $(\delta, \epsilon) = (0.3, 0.2)$. Right: $(\delta, \epsilon) = (0.3, 0.5)$. The red regions are $(\text{TPP}^\infty, \text{FDP}^\infty)$ pairs not achievable by SLOPE nor by the Lasso, regardless of the prior distribution or the penalty tuning. The blue regions are achievable by both the SLOPE and by the Lasso. The green region is achievable only by the SLOPE but not by the Lasso. We note that the boundary between the blue region and the green one is a line segment connection $(0,1)$ and $(u_{\text{DT}}^*, q^*(u_{\text{DT}}^*))$, same as given by Wang et al. (2020a) for the Lasso case. The gray region is where the SLOPE trade-off lies in, and thus is possibly achievable by the SLOPE but not by the Lasso.

Here we leverage the homotopy result in (Wang et al., 2020a, Lemma 3.8) to bridge from the achievability of the boundary curve to the achievability of the region. Thus we establish the actually achievable region by SLOPE.

The idea of homotopy is quite intuitive: suppose there are two curves, Curve A (our upper boundary curve q^*) and Curve B (the horizontal line $\text{FDP}^\infty = 1 - \epsilon$), and a continuous transformation f moving from Curve A to B . During the movement, f sweeps out a region whose boundaries include Curve A and B , where every single point in this region is passed by the transforming curve during the transformation. Formally, we have a homotopy lemma below.

Lemma D.2 (Lemma 3.7, Wang et al. (2020a)). *If a continuous curve is parameterized by $f : [0, 1] \times [0, 1] \rightarrow \mathbb{R}^2$ and if the four curves*

- $\mathcal{C}_1 = \{f(u, 0) : 0 \leq u \leq 1\}$,
- $\mathcal{C}_2 = \{f(u, 1) : 0 \leq u \leq 1\}$,
- $\mathcal{C}_3 = \{f(0, s) : 0 \leq s \leq 1\}$,
- $\mathcal{C}_4 = \{f(1, s) : 0 \leq s \leq 1\}$,

join together as a simple closed curve, $\mathcal{C} := \mathcal{C}_1 \cup \mathcal{C}_2 \cup \mathcal{C}_3 \cup \mathcal{C}_4$, then \mathcal{C} encloses an interior area \mathcal{D} , and $\forall (x, y) \in \mathcal{D}, \exists (u, s) \in [0, 1] \times [0, 1]$ such that $f(u, s) = (x, y)$. In other words, every point inside the region \mathcal{D} enclosed by curve \mathcal{C} is realizable by some $f(u, s)$.

Now we can show a region $\mathcal{D}_{\epsilon, \delta}$ defined below is indeed asymptotically achievable. This directly give the SLOPE TPP–FDP diagram in Figure 11.

Proposition D.3. *Any $(\text{TPP}^\infty, \text{FDP}^\infty)$ in $\mathcal{D}_{\epsilon, \delta}$ is asymptotically achievable by the SLOPE. Here $\delta < 1, \epsilon > \epsilon^*(\delta)$ and $\mathcal{D}_{\epsilon, \delta}$ is enclosed by the four curves: $\text{FDP}^\infty = 1 - \epsilon, \text{FDP}^\infty = q^*(\text{TPP}^\infty), \text{TPP}^\infty = 0$ and $\text{TPP}^\infty = 1$.*

Proof of Proposition D.3. Note that $(\text{TPP}^\infty, \text{FDP}^\infty)$ is a function of Λ, σ and Π and hence we can denote every TPP–FDP point in $[0, 1] \times [0, 1]$ as

$$g = (\text{TPP}^\infty(\Lambda, \sigma, \Pi), \text{FDP}^\infty(\Lambda, \sigma, \Pi)).$$

To characterize the boundary of the achievable region, i.e. \mathcal{C}_1 , we parameterize the (two-level) penalty distribution $\Lambda_*(u)$ and the (infinity-or-nothing) prior distribution $\Pi_*(u)$, empowered by the achievability result Corollary 5.1 (which holds for finite noise, including the noiseless case), such that

$$\begin{aligned} \text{TPP}^\infty(\Pi_*(u), \Lambda_*(u)) &= u, \\ \text{FDP}^\infty(\Pi_*(u), \Lambda_*(u)) &= q^*(u). \end{aligned}$$

Leveraging this parameterization, we define the transformation

$$f(u, s) = g(\Lambda_*(u), \tan\left(\frac{\pi s}{2}\right), \Pi_*(u)),$$

that is employed in Lemma D.2. Therefore, \mathcal{C}_1 is the curve described by q^* .

When the noise $\sigma = \infty$, clearly $\text{FDP}^\infty(\Lambda, \infty, \Pi) = 1 - \epsilon$. It follows that \mathcal{C}_2 is $\text{FDP}^\infty = 1 - \epsilon$. When $\text{TPP}^\infty = u = 0$, this is the case that the penalty $\Lambda = \infty$ and we get \mathcal{C}_3 is $\text{TPP}^\infty = 0$. When $u = 1$, we have $f(1, s) = (1, 1 - \epsilon)$. This is the case that the penalty $\Lambda = 0$ and \mathcal{C}_4 is $\text{TPP}^\infty = 1$.

We notice that $\{\mathcal{C}_1, \mathcal{C}_2, \mathcal{C}_3, \mathcal{C}_4\}$ indeed composes a closed curve. Therefore, f sweeps from \mathcal{C}_1 to \mathcal{C}_2 and each point in $\mathcal{D}_{\epsilon, \delta}$ is achievable by some $f(u, s)$ by the homotopy lemma in Lemma D.2. \square

E Lower bound not equal to upper bound

To complement Section 5.3, we give concrete examples that the upper bound q^* does not equal the lower bound q_* . Visually, in Figure 2, it is not difficult to distinguish the two bounds when $\text{TPP}^\infty \geq u_{\text{DT}}^*$. However, when $\text{TPP}^\infty < u_{\text{DT}}^*$, the difference can be rather small (see Figure 12), but we assert that, at least for some $\text{TPP}^\infty < u_{\text{DT}}^*$, the difference indeed exists and is not a result of numerical errors.

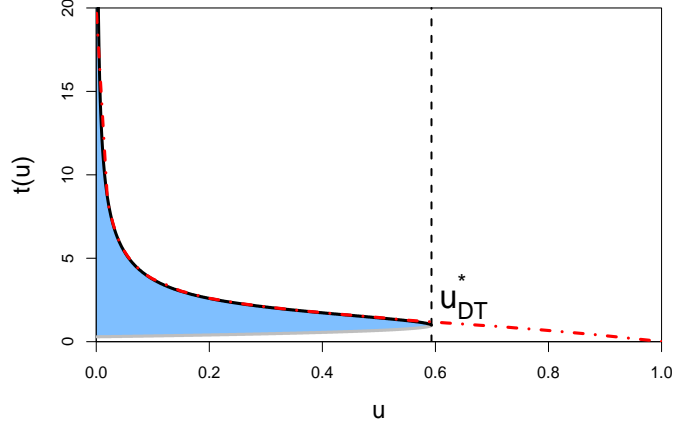


Figure 12: Demonstration of $t^*(u)$ and $t_*(u)$ with $\delta = 0.3, \epsilon = 0.2$. The blue area is valid x if (2.6) is an inequality with the left hand side being smaller than the right one; the black solid line is the larger root of (2.6), i.e. $t^*(u)$, with the support $[0, u_{DT}^*]$; the gray line is the smaller root. The red dotted line is $t_*(u)$, with support $[0, 1]$. Note that if $t^*(u) > t_*(u)$ at some u , then $q^*(u) > q_*(u)$.

E.1 Characterizing the analytic SLOPE penalty

In order to characterize the optimal SLOPE penalty analytically, we discuss the complementary slackness condition on the monotonicity constraint in problem (4.6). We start with the case when the monotonicity constraint is **not binding** (i.e. when $A'_{\text{eff}}(z) > 0$ for all $z \geq \alpha$). We apply the Euler-Lagrange Multiplier Theorem to derive the following Euler-Lagrange equation on $L(z, A_{\text{eff}})$ defined in (4.7):

$$\frac{\partial L}{\partial A_{\text{eff}}} - \frac{d}{dz} \frac{\partial L}{\partial A'_{\text{eff}}} = 0.$$

This is a necessary condition of the optimal SLOPE penalty function. Since L does not explicitly depend on A'_{eff} , the Euler-Lagrange equation gives, for the optimal SLOPE penalty function A_{eff}^* of problem (4.6),

$$\begin{aligned} \frac{\partial L}{\partial A_{\text{eff}}} &= 4(1 - \epsilon)(A_{\text{eff}}^*(z) - z)\phi(z) \\ &+ 2\epsilon \sum_{j=1,2} p_j [(A_{\text{eff}}^*(z) - (z - t_j))\phi(z - t_j) + (A_{\text{eff}}^*(z) - (z + t_j))\phi(z + t_j)] = 0. \end{aligned}$$

This equation can be significantly simplified: if we denote a function

$$H(z) := 4(1 - \epsilon)\phi(z) + 2\epsilon \sum_{j=1,2} p_j [\phi(z - t_j) + \phi(z + t_j)],$$

then the Euler-Lagrange equation above claims that

$$H(z)A_{\text{eff}}^*(z) + H'(z) = 0,$$

which is equivalent to

$$A_{\text{eff}}^*(z) = -H'(z)/H(z).$$

On the other hand, when the monotonicity constraint is **binding** (i.e. when $A'_{\text{eff}}(z) = 0$ for all $z \geq \alpha$), clearly the penalty function A_{eff}^* is a constant. In short, the optimal penalty function A_{eff}^* coincides with the function $-H'/H$ in the interval (α, ∞) when A_{eff}^* is strictly increasing and stays (piecewise) constant elsewhere; in particular, $A_{\text{eff}}^*(z) = \alpha$ on $[0, \alpha]$.

Unfortunately, the conclusion so far only gives the necessary but not sufficient condition for any penalty function to be optimal. Putting differently, the condition is not specific enough to uniquely determine A_{eff}^* and thus we have to rely on the numerical approach to find A_{eff}^* , as shown in Section 4. Nevertheless, the condition we derived above will serve as an essential tool to build up analytic SLOPE penalty in the following sections.

E.2 Analytic SLOPE penalty for two-point prior

Here we derive the optimal SLOPE penalty analytically for a special two-point prior, which can be used to prove $q_*(u) < q^*(u)$ for some u , including those below the DT power limit. We review what is known for the Lasso trade-off: fixing δ, ϵ and $\text{TPP}^\infty = u$, the maximum Lasso zero-threshold $t^*(u)$ satisfies (2.6) and the minimum Lasso FDP^∞ is achieved at such threshold (see (2.7)). If for SLOPE we can find a larger zero-threshold α than $t^*(u)$, then by the definition in (3.7):

$$\text{FDP}^\infty(\Pi, \Lambda) = \frac{2(1 - \epsilon)\Phi(-\alpha)}{2(1 - \epsilon)\Phi(-\alpha) + \epsilon u}$$

for the SLOPE must be smaller than the minimum Lasso FDP^∞ .

We first determine the prior that we want to study. We focus on a zero-or-constant prior

$$\pi = \begin{cases} t_1 & \text{w.p. } \epsilon \\ 0 & \text{w.p. } 1 - \epsilon, \end{cases}$$

whose probability density function is $p_\pi(t) = (1 - \epsilon)\delta(t) + \epsilon\delta(t - t_1)$ and clearly $\pi^* = t_1$. For the Lasso, from (3.7), we see that $\text{TPP}^\infty = u$ defines a unique t_1 by

$$\mathbb{P}(|t_1 + Z| > t^*(u)) = \Phi(t_1 - t^*) + \Phi(-t_1 - t^*) = u,$$

i.e. $t_1(u, \delta, \epsilon)$ only depends on u, δ and ϵ .

Now that we have determined the prior, we seek a feasible SLOPE penalty function A_S which allows a larger zero-threshold α with this prior: let

$$A_S(z) = \begin{cases} \alpha & \text{if } |z| < \alpha \\ \max(\alpha, -H'_{t_1}(z)/H_{t_1}(z)) & \text{if } |z| \geq \alpha, \end{cases} \quad (\text{E.1})$$

where $H_{t_1}(z)$ is the function $H(z)$ in the Appendix E.1 but specific to our new prior, i.e. $p_1 = 1, p_2 = 0, t_1 = t_2$ in (4.5): we get

$$H_{t_1}(z) = 4(1 - \epsilon)\phi(z) + 2\epsilon[\phi(z - t_1) + \phi(z + t_1)].$$

We remark that the SLOPE penalty A_S is clearly feasible for problems (4.2) and (4.6) if it is monotonically increasing. Furthermore, this monotonicity condition indeed holds true for some t_1 and α (such that A_S is increasing in z ; we will give examples shortly), for which we can show $q_*(u) < q^*(u)$.

In summary, fixing (u, δ, ϵ) , we can uniquely determine $t_1 \in \mathbb{R}$ for the two-point zero-or-constant prior and the maximum Lasso penalty $t^* \in \mathbb{R}_+$. Looking at t_1 , we can construct A_S using (E.1) on the interval $(\alpha = t^*, \infty)$. If furthermore A_S is increasing, then this non-constant penalty A_S is feasible and must outperform the constant penalty of the Lasso (which is t^*), based on the Euler-Lagrange equation discussed in Appendix E.1. In consequence, the SLOPE allows strictly larger zero-threshold α than the maximum Lasso zero-threshold t^* , until for some α we saturate the state evolution condition (4.1) by having $F_\alpha[A_S, p_{\pi^*}] = \delta$.

We give an example as follows for the framework described above.

E.3 An example of SLOPE FDP below the Lasso trade-off

As a concrete example of SLOPE FDP $^\infty$ being smaller than the minimum Lasso FDP $^\infty$, i.e. q_{Lasso}^* , we use $\delta = 0.3, \epsilon = 0.2, \sigma = 1, u = u_{\text{DT}}^*(\delta, \epsilon) = 0.56760$ by (2.2). Then the maximum Lasso zero-threshold $t^*(u)$ (or equivalently the Lasso penalty A_L) equals 1.19241 by (2.6). In this case, the Lasso FDP $^\infty = 0.62160$ by (3.7). We can compute $t_1(u, \delta, \epsilon) = 1.34864$ by (3.7).

One can check that the function $-H'_{t_1}/H_{t_1}$ as well as the penalty function A_S in (E.1) (with α set as t^*) are indeed increasing. Hence A_S is the unique optimal SLOPE penalty that satisfies the Euler-Lagrange equation. We can analytically compute the state evolution condition in problem (4.2) (see also (G.1) for the formula):

$$\begin{aligned} F_{t^*}[A_S, p_{\pi^*}] &= 2(1 - \epsilon) \int_{t^*}^{\infty} (z - A_S(z))^2 \phi(z) dz + \epsilon \left[t^2 (\Phi(t^* - t_1) - \Phi(-t^* - t_1)) \right. \\ &\quad \left. + \int_{t^*}^{\infty} \left((z - t_1 - A_S(z))^2 \phi(z - t_1) + (-z - t_1 + A_S(z))^2 \phi(-z - t_1) \right) dz \right] \\ &= \int_{t^*}^{\infty} \left[\frac{1}{2} H_t(z) A_S(z)^2 + H'_t(z) A_S(z) \right] dz + \epsilon t_1^2 (\Phi(t^* - t_1) - \Phi(-t^* - t_1)) \\ &\quad + 2(1 - \epsilon) \int_{t^*}^{\infty} z^2 \phi(z) dz + \epsilon \int_{t^*}^{\infty} (z - t_1)^2 \phi(z - t_1) dz + \epsilon \int_{t^*}^{\infty} (z + t_1)^2 \phi(z + t_1) dz. \end{aligned}$$

Using the facts that $\ddot{\phi}(z) = (z^2 - 1)\phi(z)$ and $\dot{\phi}(z) = -z\phi(z)$, we get $\frac{d}{dz} (\Phi(z) - z\phi(z)) = z^2\phi(z)$, which can be used to simplify the last three integrals:

$$\begin{aligned} F_{t^*}[A_S, p_{\pi^*}] &= \int_{t^*}^{\infty} \left[\frac{1}{2} H_t(z) A_S(z)^2 + H'_t(z) A_S(z) \right] dz \\ &\quad + \epsilon t_1^2 (\Phi(t^* - t_1) - \Phi(-t^* - t_1)) + 2(1 - \epsilon) [t^* \phi(t^*) + \Phi(-t^*)] \\ &\quad + \epsilon [(t^* - t_1) \phi(t^* - t_1) + \Phi(-t^* + t_1)] + \epsilon [(t^* + t_1) \phi(t^* + t_1) + \Phi(-t^* - t_1)]. \end{aligned}$$

Together with $A_S(z) = \max(t^*, -H'_{t_1}(z)/H_{t_1}(z))$ on (t^*, ∞) , this analytic quantity can be calculated by numerical integration to arbitrary precision, and it gives $E(\pi, A_S) = 0.27727 < \delta$. In words, at the Lasso maximum zero-threshold t^* , the SLOPE and the Lasso have the same FDP $^\infty$, but the SLOPE has a smaller normalized estimation error E in the state evolution condition (4.1). Hence, this leaves a margin to further reduce the FDP $^\infty$ before we use up the margin.

Up until now, we are working in the normalized regime on (π, A) and we want to determine the original prior and penalty (Π, Λ_S) . To do so, we use the state evolution (B.1) to compute $\tau = \sqrt{\frac{\sigma^2}{1 - E(\pi, A_S)/\delta}} = 3.6337$, which uniquely defines the two-point prior via $\Pi^* = t_1 \cdot \tau = 4.9006$. We then apply the calibration (B.5) to derive Λ_S and visualize the distribution in Figure 13.

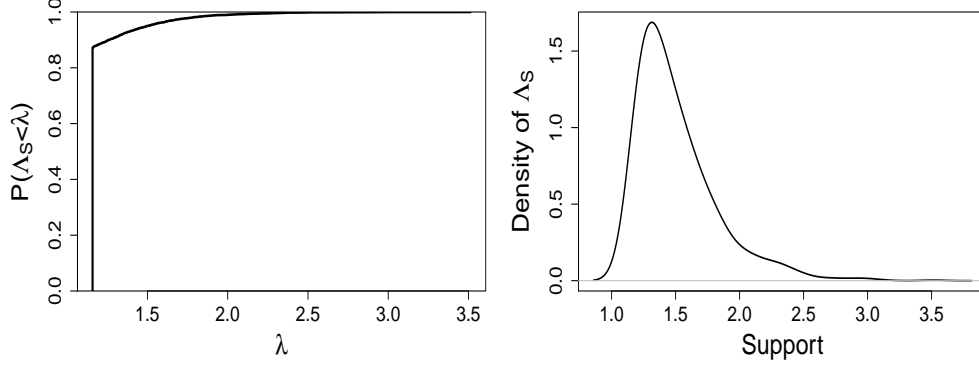


Figure 13: Cumulative distribution function of the optimal SLOPE penalty Λ_S and probability density of its non-constant component, at $(\text{TPP}^\infty, \text{FDP}^\infty) = (0.5676, 0.6216)$. Here $\delta = 0.3, \epsilon = 0.2, \sigma = 1, \Pi^* = 4.9006$.

To saturate the state evolution condition (4.1) so that $E(\pi, \Lambda_S) = \delta$, while still fixing $\text{TPP}^\infty = 0.5676$, we can increase the zero-threshold α from t^* (which is 1.19241) to 1.25672 and derive $t_1 = 1.41748$ via (3.7):

$$\mathbb{P}(|t_1 + Z| > \alpha) = \Phi(t_1 - \alpha) + \Phi(-t_1 - \alpha) = u.$$

Again, Λ_S constructed by (E.1) is increasing and optimal. This new SLOPE zero-threshold α implies $\text{FDP}^\infty = 0.5954$ which is strictly smaller than the Lasso minimum $\text{FDP}^\infty = 0.6216$.

E.4 A new TPP threshold u^\dagger

In this section, we find the minimum TPP^∞ such that we can leverage Appendix E.2 to construct SLOPE FDP^∞ below the Lasso trade-off $q_{\text{Lasso}}^*(\text{TPP}^\infty)$.

When $\text{TPP}^\infty = u$ and the zero-threshold α equals $t^*(u)$ defined in (2.6), the SLOPE penalty may have a normalized estimation error $E(\pi, \Lambda_S) < \delta$. In the above example, we increase the zero-threshold α until the state evolution constraint is binding: $E(\pi, \Lambda_S) = \delta$, thus obtaining smaller FDP^∞ . From a different angle, we can decrease u (and change $q^*(u)$ and $t^*(u)$ consequently) until $E(\pi, \Lambda_S) = \delta$.

To be specific, we test a general $\text{TPP}^\infty = u$ and set the zero-threshold α at $t^*(u)$. Then the single point $\pi^* = t_1$ can be computed via $\mathbb{P}(|t_1 + Z| > t^*(u)) = u$ and the SLOPE penalty function Λ_S is determined via (E.1). Lastly, we compute the normalized estimation error $E(\pi, \Lambda_S)$ if Λ_S is increasing.

We define the smallest u such that $E \leq \delta$ as our new TPP threshold u^\dagger :

$$u^\dagger(\delta, \epsilon) := \inf\{u \text{ s.t. } F_{t^*(u)}[\max(t^*(u), -H'_{t_1}/H_{t_1}), \rho_{t_1}] \leq \delta \\ \text{and } \max(t^*(u), -H'_{t_1}/H_{t_1}) \text{ is increasing}\}.$$

Here the function $\rho_{t_1}(t) = \delta(t - t_1)$ is the probability density function of $\pi^* = t_1$ and the functional F is defined in (G.1).

Under $\delta = 0.3, \epsilon = 0.2$, we find that $u^\dagger = 0.5283 < u_{\text{DT}}^* = 0.5676$ (visualized in Figure 14). This indicates that we can show $q_* < q^*$ for a range of u smaller than the DT power limit. We observe

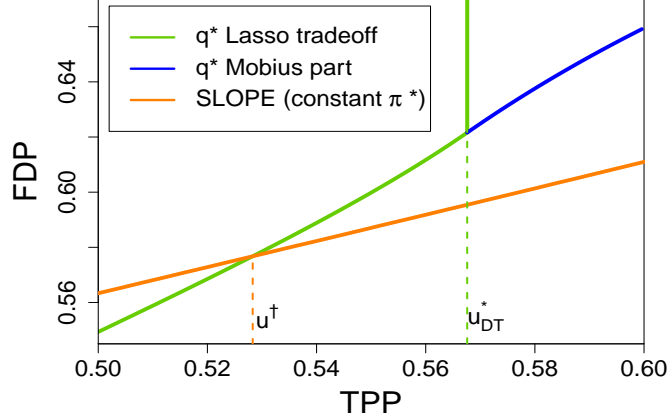


Figure 14: SLOPE $\text{TPP}^\infty\text{-FDP}^\infty$ of constant π^* and the new TPP threshold u^\dagger when $(\delta, \epsilon) = (0.3, 0.2)$. The green line is the Lasso trade-off q^* and the blue line is the Möbius part of q^* . The orange line is the $\text{TPP}^\infty\text{-FDP}^\infty$ realized by constant π^* and A_{eff} for the maximum zero-threshold α . In this example, $u^\dagger = 0.5283 < u_{\text{DT}}^* = 0.5676$.

that below u^\dagger , the Lasso penalty and the infinity-or-nothing prior achieve smaller FDP^∞ than our SLOPE penalty and constant prior, and vice versa. We further offer graphical demonstration of the difference between u^\dagger and u_{DT}^* in Figure 15.

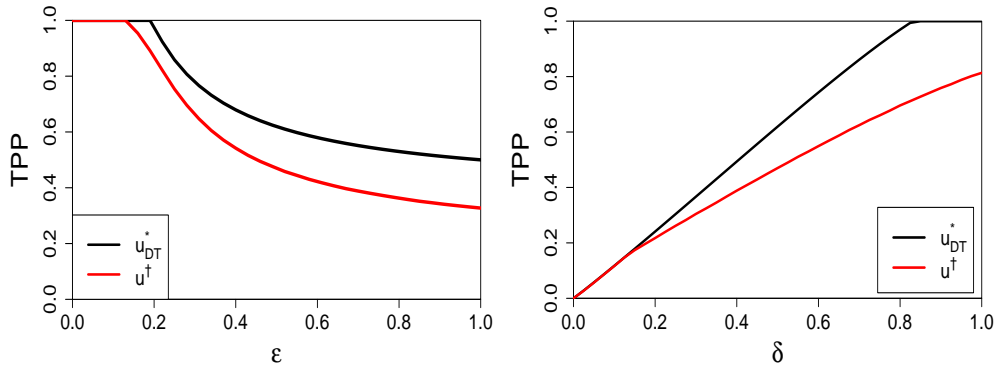


Figure 15: Comparison of u^\dagger and u_{DT}^* , fixing $\delta = 0.5$ (left) or $\epsilon = 0.5$ (right). The difference can be as large as 0.173 on the left plot and 0.282 on the right one.

F Proving SLOPE outperforms the Lasso for fixed prior

Proof of Theorem 3. The proof is broken down into three pieces: we start with the MSE, then the asymptotic TPP and lastly the asymptotic FDP ⁷.

⁷Theorem 3 can be generalized to further include certain unbounded signal prior Π as long as Equation (F.4) is satisfied. For example, for any Gaussian or Exponential Π , the SLOPE can outperform the Lasso.

SLOPE has smaller MSE Fixing any bounded prior Π and any scalar Lasso penalty λ , we can derive the corresponding (τ_L, α_L) from the calibration (B.5) and the state evolution (B.1), so as to work in the normalized regime (π_L, A_L) . The quantity τ relates to the MSE by Bu et al. (2020, Corollary 3.4):

$$\text{plim } \|\widehat{\boldsymbol{\beta}} - \boldsymbol{\beta}\|^2/p = \delta(\tau^2 - \sigma^2). \quad (\text{F.1})$$

Obviously, the SLOPE estimator has a smaller MSE than the Lasso one if and only if $\tau_S < \tau_L$, where (τ_S, A_S) is the solution to the SLOPE calibration (B.5) and the state evolution (B.1).

We now illustrate that this is always feasible by carefully designing the SLOPE penalty vector $\boldsymbol{\alpha}_S(p)$, or in the asymptotic sense, the SLOPE penalty distribution A_S . We directly work with the SLOPE AMP state evolution (B.1) instead of the Lasso AMP, since SLOPE covers the Lasso as a sub-case. In particular, we consider the two-level SLOPE of the form $A_{\ell, \alpha_L, w}$ defined in (2.3).

Our goal is to show that for any Lasso penalty $A_L = \alpha_L = A_{\alpha_L, \alpha_L, w}$, we can find a SLOPE penalty $A_S = A_{\ell, \alpha_L, w}$ for some sufficiently small w and $\ell > \alpha_L$ such that $\tau_S < \tau_L$. In other words, among all the two-level SLOPE penalties $A_{\ell, \alpha_L, w}$ with a zero-threshold α_L , we show the optimal MSE is not achieved at $\ell = \alpha_L$.

To present a clear proof, we simplify the notation of $\text{prox}_J(\mathbf{a}; \mathbf{b})$ by using $\boldsymbol{\eta}(\mathbf{a}, \mathbf{b})$, or simply $\boldsymbol{\eta}$, where $\mathbf{a} := \Pi + \tau \mathbf{Z}$ and $\mathbf{b} := \boldsymbol{\alpha} \tau$, where $\boldsymbol{\alpha} = \boldsymbol{\alpha}_{\ell, \alpha_L, w}$ (defined in (2.3)) with $\ell \geq \alpha_L$. On convergence of the state evolution (B.1), we can differentiate both sides of

$$\tau^2 = \sigma^2 + \frac{1}{\delta} \lim_{p \rightarrow \infty} \mathbb{E} \langle [\boldsymbol{\eta}(\Pi + \tau \mathbf{Z}, \boldsymbol{\alpha} \tau) - \Pi]^2 \rangle = \sigma^2 + \frac{1}{\delta} \lim_{p \rightarrow \infty} \mathbb{E} \langle [\boldsymbol{\eta}(\mathbf{a}, \mathbf{b}) - \Pi]^2 \rangle,$$

with respect to $\ell \in \mathbb{R}$. Denoting $\tau' = \frac{\partial \tau}{\partial \ell}$, we obtain

$$2\tau\tau' = \frac{\partial}{\partial \ell} \left(\sigma^2 + \frac{1}{\delta} \lim_{p \rightarrow \infty} \mathbb{E} \langle [\boldsymbol{\eta}(\mathbf{a}, \mathbf{b}) - \Pi]^2 \rangle \right) = \frac{1}{\delta} \lim_{p \rightarrow \infty} \mathbb{E} \frac{\partial}{\partial \ell} \langle [\boldsymbol{\eta}(\mathbf{a}, \mathbf{b}) - \Pi]^2 \rangle.$$

Then the chain rule leads to

$$\tau\tau' = \lim_{p \rightarrow \infty} \frac{1}{n} \sum_j \mathbb{E}(\eta_j - \Pi_j) \frac{\partial \eta_j}{\partial \ell} = \lim_{p \rightarrow \infty} \frac{1}{n} \sum_j \mathbb{E}(\eta_j - \Pi_j) \sum_k \left[\frac{d\eta_j}{da_k} Z_k \frac{\partial \tau}{\partial \ell} + \frac{d\eta_j}{db_k} \frac{\partial b_k}{\partial \ell} \right]. \quad (\text{F.2})$$

To investigate the derivative terms, we copy some important facts in Bu et al. (2020, Appendix A) here for reader's convenience:

$$\begin{aligned} \frac{d}{da_k} [\boldsymbol{\eta}(\mathbf{a}, \mathbf{b})]_j &= \mathbb{I}\{|\boldsymbol{\eta}(\mathbf{a}, \mathbf{b})|_j = |\boldsymbol{\eta}(\mathbf{a}, \mathbf{b})|_k\} \text{sign}([\boldsymbol{\eta}(\mathbf{a}, \mathbf{b})]_j [\boldsymbol{\eta}(\mathbf{a}, \mathbf{b})]_k) [\partial_1 \boldsymbol{\eta}(\mathbf{a}, \mathbf{b})]_j, \\ \frac{d}{db_k} [\boldsymbol{\eta}(\mathbf{a}, \mathbf{b})]_j &= -\mathbb{I}\{|\boldsymbol{\eta}(\mathbf{a}, \mathbf{b})|_j = |\boldsymbol{\eta}(\mathbf{a}, \mathbf{b})|_{o(k)}\} \text{sign}([\boldsymbol{\eta}(\mathbf{a}, \mathbf{b})]_j) [\partial_1 \boldsymbol{\eta}(\mathbf{a}, \mathbf{b})]_j. \end{aligned}$$

where the permutation $o: i \rightarrow j$ finds the index of the i -th largest magnitude, i.e. $|\eta|_{o(i)} := |\eta|_{(i)} = |\eta|_j$, and its inverse function is the rank of the magnitudes. In the above notation, we have used (again from Bu et al. (2020, Appendix A))

$$[\partial_1 \boldsymbol{\eta}]_j = \frac{\partial \eta_j}{\partial a_j} = \frac{1}{|\{1 \leq k \leq p : |\eta_k| = |\eta_j|\}|},$$

which converges to 1 as $p \rightarrow \infty$ if η_j is unique in the magnitudes of $\boldsymbol{\eta}$ and to 0 otherwise. In the Lasso case (i.e. $\ell = \alpha_L$), each non-zero entry in $|\boldsymbol{\eta}|$ is indeed unique, and hence we can simplify $[\partial_1 \eta]_j$ to $\mathbb{I}\{|\eta|_j \neq 0\}$. We now rewrite (F.2) as

$$\begin{aligned}
\tau \tau' &= \lim_{p \rightarrow \infty} \frac{1}{n} \sum_j \mathbb{E}(\eta_j - \Pi_j) \left[[\partial_1 \eta]_j Z_j \tau' - \text{sign}(\eta_j) [\partial_1 \eta]_j \frac{\partial b_{o^{-1}(j)}}{\partial \ell} \right] \\
&= \lim_{p \rightarrow \infty} \frac{1}{n} \sum_{j: \eta_j \neq 0} \mathbb{E}(\eta_j - \Pi_j) \left[Z_j \tau' - \text{sign}(\eta_j) \frac{\partial b_{o^{-1}(j)}}{\partial \ell} \right] \\
&= \lim_p \frac{1}{n} \sum_{j: \eta_j \neq 0} \mathbb{E}(\eta_j - \Pi_j) \left[Z_j \tau' - \text{sign}(\eta_j) (\alpha_{o^{-1}(j)} \tau' + \mathbb{I}\{o^{-1}(j) \leq wp\} \tau) \right] \\
&= \lim_p \frac{1}{n} \sum_{j: \eta_j \neq 0} \mathbb{E}(\eta_j - \Pi_j) \left[(Z_j - \text{sign}(\eta_j) \alpha_L) \tau' - \text{sign}(\eta_j) \mathbb{I}\{o^{-1}(j) \leq wp\} \tau \right].
\end{aligned}$$

To summarize, we derive that

$$\frac{\partial \tau}{\partial \ell} = \frac{\lim_p \frac{1}{n} \sum_{j: o^{-1}(j) \leq wp} \mathbb{E}(\eta_j - \Pi_j) \text{sign}(\eta_j) \tau}{\lim_p \frac{1}{n} \sum_{j: \eta_j \neq 0} \mathbb{E}(\eta_j - \Pi_j) (Z_j - \text{sign}(\eta_j) \alpha_L) - \tau}. \quad (\text{F.3})$$

The rest of the proof contains two statements: (1) We will show that the numerator term is positive for sufficiently small w ; (2) We also show that the denominator term is always negative for any Lasso penalty α_L .

To show that the numerator in (F.3) is positive for small w , we write

$$\begin{aligned}
\lim_p \frac{\tau}{n} \sum_{j: o^{-1}(j) \leq wp} \mathbb{E}(\eta_j - \Pi_j) \text{sign}(\eta_j) &= \frac{w\tau}{\delta} \mathbb{E}[(\eta_j - \Pi_j) \text{sign}(\eta_j) | o^{-1}(j) \leq wp] \\
&= \frac{w\tau^2}{\delta} \mathbb{E}[(\eta_{\text{soft}} - \pi) \text{sign}(\eta_{\text{soft}}) | |\eta_{\text{soft}}| \geq q_w],
\end{aligned}$$

in which we slightly abuse the notation for the distribution $\eta \stackrel{\mathcal{D}}{=} \eta_{\text{soft}}(\pi + Z; \alpha_L)$ and define q_w as the w -quantile of $|\eta_{\text{soft}}(\pi + Z; \alpha_L)|$ such that $\mathbb{P}(|\eta| \geq q_w) = w$.

Next, simple substitution gives that it is equivalent to show

$$\mathbb{E}\left(Z \text{sign}(\eta) \mid |\eta| \geq q_w\right) > \alpha_L. \quad (\text{F.4})$$

We notice that as $w \rightarrow 0$, $q_w \rightarrow \infty$. Hence we can always consider w small enough that the desired inequality above holds. The full proof of this fact is referred to Appendix G.

The next step is to show that the denominator in (F.3) is negative, similar to the proof in Zhang

and Bu (2021). By multiplying with the positive τ , the denominator becomes

$$\begin{aligned}
& \lim_p \frac{1}{n} \sum_{j:\eta_j \neq 0} \mathbb{E}(\eta_j - \Pi_j) [Z_j - \text{sign}(\eta_j)\alpha_L] - \tau \\
& \propto \lim_p \frac{1}{n} \sum_{j:\eta_j \neq 0} \mathbb{E}(\eta_j - \Pi_j) [\tau Z_j - \tau \text{sign}(\eta_j)\alpha_L] - \tau^2 \\
& = \lim_p \frac{1}{n} \sum_{j:\eta_j \neq 0} \mathbb{E}(\eta_j - \Pi_j)^2 - \tau^2 \\
& = \lim_p \frac{1}{n} \sum_{j:\eta_j} \mathbb{E}(\eta_j - \Pi_j)^2 - \lim_p \frac{1}{n} \sum_{j:\eta_j=0} \mathbb{E}(\eta_j - \Pi_j)^2 - \tau^2 \\
& = - \lim_p \frac{1}{n} \sum_{j:\eta_j=0} \mathbb{E}(\eta_j - \Pi_j)^2 - \sigma^2 < 0,
\end{aligned}$$

where the last equality follows from (F.1).

All in all, we finish the proof that $\frac{\partial \tau}{\partial \ell}$ in (F.3) is negative for $A_{\ell, \alpha_L, w}$ at $\ell = \alpha_L$ and small w . Along this negative gradient $\frac{\partial \tau}{\partial \ell}$, increasing the first argument of $A_{\ell, \alpha_L, w}$ from $\ell = \alpha_L$ (the Lasso case) leads to a SLOPE penalty Λ_S and reduces τ_L to a smaller τ_S . Equivalently, the SLOPE MSE is strictly smaller than the Lasso MSE.

SLOPE has higher TPP To prove the TPP result, we need the SLOPE to have smaller MSE (as shown previsouly) as well as the same zero-threshold as the Lasso. To achieve this, we claim that, for sufficiently small w and some $\ell > \alpha_L$, the SLOPE zero-threshold $\alpha(\Pi, \Lambda_S)$ is the same as the Lasso zero-threshold $\alpha(\Pi, \Lambda_L) = \alpha_L$.

In fact, the two-level SLOPE $A_{\ell, \alpha_L, w}$ by its levels must have the zero-threshold as either ℓ or α_L (see Proposition C.5), and the zero-threshold will be α_L if and only if the sparsity $\kappa(\Pi, \Lambda_S) > w$ (see Fact C.2). Therefore it suffices to guarantee $\kappa(\Pi, \Lambda_S) > w$. From $\mathbb{P}(|\Pi/\tau_S + Z| > \ell) \leq \kappa(\Pi, \Lambda_S) \leq \mathbb{P}(|\Pi/\tau_S + Z| > \alpha_L)$, it is not hard to obtain that the sparsity κ is continuous in ℓ . Hence for any $w < \kappa(\Pi, \Lambda_L)$, there exists some $\ell > \alpha_L$ but close to α_L so that the SLOPE sparsity $\kappa(\Pi, \Lambda_S) > w$.

Now that we have $\tau_S < \tau_L$ and $\alpha(\Pi, \Lambda_S) = \alpha(\Pi, \Lambda_L)$, we can finish the proof by the definition of TPP^∞ : intuitively, $\pi_S := \Pi/\tau_S > \pi_L := \Pi/\tau_L$ and $\text{SLOPE } \text{TPP}^\infty = \mathbb{P}(|\pi_S^* + Z| > \alpha_L) > \mathbb{P}(|\pi_L^* + Z| > \alpha_L) = \text{the Lasso } \text{TPP}^\infty$; formally, we show by Equation (3.7) that

$$\begin{aligned}
\text{TPP}^\infty(\Pi, \Lambda_S) &= \mathbb{P}(|\pi_S^* + Z| > \alpha(\Pi, \Lambda_S)) = \int_{-\infty}^{\infty} \mathbb{P}(|t/\tau_S + Z| > \alpha_L) p_{\Pi^*}(t) dt \\
&> \int_{-\infty}^{\infty} \mathbb{P}(|t/\tau_L + Z| > \alpha_L) p_{\Pi^*}(t) dt = \mathbb{P}(|\pi_L^* + Z| > \alpha(\Pi, \Lambda_L)) = \text{TPP}^\infty(\Pi, \Lambda_L).
\end{aligned}$$

SLOPE has lower FDP To prove the FDP result, we again use the fact that the SLOPE shares the same zero-threshold as the Lasso but has larger TPP. By Equation (3.7),

$$\begin{aligned}
\text{FDP}^\infty(\Pi, \Lambda_S) &= \frac{2(1-\epsilon)\Phi(-\alpha(\Pi, \Lambda_S))}{2(1-\epsilon)\Phi(-\alpha(\Pi, \Lambda_S)) + \epsilon \text{TPP}^\infty(\Pi, \Lambda_S)} \\
&< \frac{2(1-\epsilon)\Phi(-\alpha(\Pi, \Lambda_L))}{2(1-\epsilon)\Phi(-\alpha(\Pi, \Lambda_L)) + \epsilon \text{TPP}^\infty(\Pi, \Lambda_L)} = \text{FDP}^\infty(\Pi, \Lambda_L).
\end{aligned}$$

□

G Auxiliary proofs

Here we give some technical proofs that have been used in this work.

G.1 Derivation of F_α in Section 4

We are ready to give the explicit form of the functional F_α given that the zero-threshold is $\alpha \in \mathbb{R}_+$. Expanding the term in the integral form, we get

$$\begin{aligned} F_\alpha[\mathbf{A}_{\text{eff}}, p_{\pi^*}] &:= \mathbb{E} (\eta_{\text{soft}}(\pi + Z; \mathbf{A}_{\text{eff}}(\pi + Z)) - \pi)^2 \\ &= \int_0^\infty \int_{-\infty}^\infty \left(\eta_{\text{soft}}(t + z; \mathbf{A}_{\text{eff}}(t + z)) - t \right)^2 \phi(z) dz p_\pi(t) dt, \end{aligned}$$

where p_π is the probability density function of the normalized prior π , which is uniquely determined by p_{π^*} in a way to be explained shortly.

We further expand the quadratic term in the inner integral, by using the fact that $\eta_{\pi+Z, \mathbf{A}}(t+z) = \eta_{\text{soft}}(t+z; \mathbf{A}_{\text{eff}}(t+z)) = 0$ for $-\alpha \leq t+z \leq \alpha$, since α is the zero-threshold in Definition 4.1. We obtain

$$\begin{aligned} F_\alpha[\mathbf{A}_{\text{eff}}, p_{\pi^*}] &= \int_0^\infty \left[\int_{-\alpha-t}^{\alpha-t} t^2 \phi(z) dz + \int_{\alpha-t}^\infty (z - \mathbf{A}_{\text{eff}}(t+z))^2 \phi(z) dz \right. \\ &\quad \left. + \int_{-\infty}^{-\alpha-t} (z + \mathbf{A}_{\text{eff}}(t+z))^2 \phi(z) dz \right] p_\pi(t) dt \\ &= \int_0^\infty \left[t^2 (\Phi(\alpha-t) - \Phi(-\alpha-t)) + \int_\alpha^\infty (z-t - \mathbf{A}_{\text{eff}}(z))^2 \phi(z-t) dz \right. \\ &\quad \left. + \int_\alpha^\infty (-z-t + \mathbf{A}_{\text{eff}}(z))^2 \phi(-z-t) dz \right] p_\pi(t) dt. \end{aligned}$$

By the definition of π^* in Lemma 3.1, we use $p_\pi(t) = (1-\epsilon)\delta(t) + \epsilon p_{\pi^*}(t)$, in which $p_{\pi^*}(t)$ is the probability density function of π^* , to write

$$\begin{aligned} &F_\alpha[\mathbf{A}_{\text{eff}}, p_{\pi^*}] \\ &= 2(1-\epsilon) \int_\alpha^\infty (z - \mathbf{A}_{\text{eff}}(z))^2 \phi(z) dz + \epsilon \int_0^\infty \left[t^2 (\Phi(\alpha-t) - \Phi(-\alpha-t)) \right. \\ &\quad \left. + \int_\alpha^\infty (z-t - \mathbf{A}_{\text{eff}}(z))^2 \phi(z-t) dz + \int_\alpha^\infty (-z-t + \mathbf{A}_{\text{eff}}(z))^2 \phi(-z-t) dz \right] p_{\pi^*}(t) dt \quad (\text{G.1}) \\ &= 2(1-\epsilon) \int_\alpha^\infty (z - \mathbf{A}_{\text{eff}}(z))^2 \phi(z) dz + \epsilon \int_0^\infty \left[t^2 (\Phi(\alpha-t) - \Phi(-\alpha-t)) \right. \\ &\quad \left. + \int_\alpha^\infty \left((z-t - \mathbf{A}_{\text{eff}}(z))^2 \phi(z-t) + (-z-t + \mathbf{A}_{\text{eff}}(z))^2 \phi(-z-t) \right) dz \right] p_{\pi^*}(t) dt. \end{aligned}$$

Since Lemma 4.3 states that the optimal $p_{\pi^*}(t)$ takes the form $\rho(t; t_1, t_2) = p_1 \delta(t-t_1) + p_2 \delta(t-t_2)$

in (4.5), the above functional turns into

$$\begin{aligned}
& F_\alpha[\mathbf{A}_{\text{eff}}, \rho(\cdot; t_1, t_2)] \\
&= \int_\alpha^\infty \left[2(1 - \epsilon)(z - \mathbf{A}_{\text{eff}}(z))^2 \phi(z) \right. \\
&\quad + \epsilon p_1 \left((z - t_1 - \mathbf{A}_{\text{eff}}(z))^2 \phi(z - t_1) + (-z - t_1 + \mathbf{A}_{\text{eff}}(z))^2 \phi(-z - t_1) \right) \\
&\quad + \epsilon p_2 \left((z - t_2 - \mathbf{A}_{\text{eff}}(z))^2 \phi(z - t_2) + (-z - t_2 + \mathbf{A}_{\text{eff}}(z))^2 \phi(-z - t_2) \right) \Big] dz \\
&\quad + \epsilon p_1 t_1^2 [\Phi(\alpha - t_1) - \Phi(-\alpha - t_1)] + \epsilon p_2 t_2^2 [\Phi(\alpha - t_2) - \Phi(-\alpha - t_2)].
\end{aligned}$$

To construct the quadratic programming in problem (4.6), we can apply the left endpoint rule and approximate $F_\alpha[\mathbf{A}_{\text{eff}}, \rho(\cdot; t_1, t_2)]$ by

$$\begin{aligned}
\bar{F}_\alpha(\mathbf{A}; t_1, t_2) &= 2(1 - \epsilon) \sum_{i=1}^m (z_i - \mathbf{A}_i)^2 \phi(z_i) \Delta z \\
&\quad + \epsilon p_1 \sum_{i=1}^m \left((z_i - t_1 - \mathbf{A}_i)^2 \phi(z_i - t_1) + (-z_i - t_1 + \mathbf{A}_i)^2 \phi(-z_i - t_1) \right) \Delta z \\
&\quad + \epsilon p_2 \sum_{i=1}^m \left((z_i - t_2 - \mathbf{A}_i)^2 \phi(z_i - t_2) + (-z_i - t_2 + \mathbf{A}_i)^2 \phi(-z_i - t_2) \right) \Delta z \\
&\quad + \epsilon p_1 t_1^2 [\Phi(\alpha - t_1) - \Phi(-\alpha - t_1)] + \epsilon p_2 t_2^2 [\Phi(\alpha - t_2) - \Phi(-\alpha - t_2)].
\end{aligned} \tag{G.2}$$

G.2 Proof of Lemma 4.3

Proof. In general, ρ^* can always be approximated by a sum of Dirac delta functions, $\rho^*(t) = \sum_{i=1}^m p_i \delta(t - t_i)$. In particular, since ρ^* is a probability density function, we require $0 < p_i < 1$: otherwise if for some i , $p_i = 1$, then $m = 1$ and we are done.

We now show $m < 3$ by contradiction. The vertex principle of linear programming states that the minimum value of the linear objective function occurs at the vertices of the feasible region. Hence it suffices to show that all vertices are two-point Dirac delta functions.

The constraints in problem (4.4) lead to

$$\sum_i p_i = 1, \quad \sum_i p_i [\Phi(t_i - \alpha) + \Phi(-t_i - \alpha)] = u.$$

Suppose $m \geq 3$, then there always exists $\rho'(t) = \sum_{i=1}^m p'_i \delta(t - t_i)$ such that

- $p_i = p'_i$ for $i > 3$;
- $p_1 + p_2 + p_3 = p'_1 + p'_2 + p'_3$;
- $p_1 h_\alpha(t_1) + p_2 h_\alpha(t_2) + p_3 h_\alpha(t_3) = p'_1 h_\alpha(t_1) + p'_2 h_\alpha(t_2) + p'_3 h_\alpha(t_3)$;

where we denote $h_\alpha(t_i) := \Phi(t_i - \alpha) + \Phi(-t_i - \alpha)$. In other words, we can find ρ' such that

$$\begin{pmatrix} p'_1 \\ p'_2 \\ p'_3 \end{pmatrix} = \begin{pmatrix} 1 & 1 & 1 \\ h_\alpha(t_1) & h_\alpha(t_2) & h_\alpha(t_3) \end{pmatrix} \begin{pmatrix} p_1 \\ p_2 \\ p_3 \end{pmatrix}.$$

Since there are only two equations involving the three unknown variables p'_1, p'_2 and p'_3 , in the generic case, we can represent the infinitely many ρ' with one degree of freedom,

$$\begin{pmatrix} p'_1 \\ p'_2 \\ p'_3 \end{pmatrix} = \begin{pmatrix} p_1 \\ p_2 \\ p_3 \end{pmatrix} + s \begin{pmatrix} c_1 \\ c_2 \\ c_3 \end{pmatrix},$$

using the null vector $(c_1, c_2, c_3)^\top$ of the above matrix.

As $0 < p'_i < 1$ for $i = 1, 2, 3$, we claim that for all $s \in (-s_0, s_0)$ with some $s_0 > 0$, $(p'_1, p'_2, p'_3)^\top$ defined above is feasible for problem (4.4). In other words, suppose we explicitly define

$$\rho_s(t) = \sum_{i=1}^3 (p_i + c_i s) \delta(t - t_i) + \sum_{i>3} p_i \delta(t - t_i),$$

then there exists a range of $s \in \mathbb{R}$ such that ρ_s is feasible. However, one can easily check that

$$\rho^* = \frac{1}{2} (\rho_s + \rho_{-s})$$

is also a feasible solution. Hence ρ^* is not a vertex. Contradiction. \square

G.3 Proof of Equation (F.4)

Proof. To see that for large enough q_w , $\mathbb{E} \left(Z \operatorname{sign}(\eta) \mid |\eta| > q_w \right) \geq \alpha_L$, we write $\tilde{q}_w := q_w + \alpha_L$ and study

$$\mathbb{E} \left(Z \operatorname{sign}(\eta) \mid |\eta| \geq q_w \right) = \mathbb{E} \left(Z \operatorname{sign}(\eta) \mid |\pi + Z| \geq \tilde{q}_w \right).$$

We have

$$\begin{aligned} & \mathbb{E} \left(Z \operatorname{sign}(\eta) \mid |\pi + Z| \geq \tilde{q}_w \right) \\ &= \mathbb{E} \left(Z \mid \pi + Z \geq \tilde{q}_w \right) \frac{\mathbb{P}(\pi + Z \geq \tilde{q}_w)}{\mathbb{P}(|\pi + Z| \geq \tilde{q}_w)} - \mathbb{E} \left(Z \mid \pi + Z \leq -\tilde{q}_w \right) \frac{\mathbb{P}(\pi + Z \leq -\tilde{q}_w)}{\mathbb{P}(|\pi + Z| \geq \tilde{q}_w)} \\ &= \frac{\int_{-\infty}^{\infty} [\phi(t - \tilde{q}_w) + \phi(-\tilde{q}_w - t)] p_\pi(t) dt}{\int_{-\infty}^{\infty} [\Phi(t - \tilde{q}_w) + \Phi(-\tilde{q}_w - t)] p_\pi(t) dt}, \end{aligned}$$

in which $p_\pi(t)$ is the unknown but fixed probability density function of π .

Now we show cases where the above ratio of integrals goes to ∞ as $q_w \rightarrow \infty$ or equivalently $\tilde{q}_w \rightarrow \infty$. For bounded π (in fact for priors with bounded essential infimum and essential supreme), denoting the minimum and maximum as π_{\min} and π_{\max} , then the ratio is

$$\frac{\int_{\pi_{\min}}^{\pi_{\max}} [\phi(t - \tilde{q}_w) + \phi(-\tilde{q}_w - t)] p_\pi(t) dt}{\int_{\pi_{\min}}^{\pi_{\max}} [\Phi(t - \tilde{q}_w) + \Phi(-\tilde{q}_w - t)] p_\pi(t) dt}.$$

Using the fact that $\phi(x) + x\Phi(x) > 0$, we have

$$\begin{aligned}
& \mathbb{E} \left(Z \operatorname{sign}(\eta) \middle| |\pi + Z| \geq \tilde{q}_w \right) \\
& > \frac{\int_{\pi_{\min}}^{\pi_{\max}} [(\tilde{q}_w - t)\Phi(t - \tilde{q}_w) + (\tilde{q}_w + t)\Phi(-\tilde{q}_w - t)] p_\pi(t) dt}{\int_{\pi_{\min}}^{\pi_{\max}} [\Phi(t - \tilde{q}_w) + \Phi(-\tilde{q}_w - t)] p_\pi(t) dt} \\
& > \frac{\int_{\pi_{\min}}^{\pi_{\max}} [(\tilde{q}_w - \pi_{\max})\Phi(t - \tilde{q}_w) + (\tilde{q}_w + \pi_{\min})\Phi(-\tilde{q}_w - t)] p_\pi(t) dt}{\int_{\pi_{\min}}^{\pi_{\max}} [\Phi(t - \tilde{q}_w) + \Phi(-\tilde{q}_w - t)] p_\pi(t) dt} \\
& > \min\{\tilde{q}_w - \pi_{\max}, \tilde{q}_w + \pi_{\min}\}.
\end{aligned}$$

In summary, when $w \rightarrow 0$, all q_w, \tilde{q}_w and $\mathbb{E}(Z \operatorname{sign}(\eta) \middle| |\eta| \geq q_w) \rightarrow \infty$. Therefore we have $\mathbb{E}(Z \operatorname{sign}(\eta) \middle| |\eta| \geq q_w) > \alpha_L$ for sufficiently small w . \square

H Computation of SLOPE AMP quantities

In order to compute α and τ , e.g. for the AMP calibration or for computing the estimation error, we need to estimate the SLOPE proximal operator in the state evolution (B.2). Despite that the Monte Carlo method is easy to implement, it is often unstable nor efficient for high-dimensional SLOPE problems, say when p is in the order of thousands. Here we demonstrate how to approximate the normalized estimation error $E(\Pi, \Lambda)$ in a way that matches the truth asymptotically and has satisfactory approximation error in the finite dimension (see bottom-right plot in Figure 17).

Notice in this section, the prior distribution Π is general and does not necessarily satisfy the sparsity assumption $\mathbb{P}(\Pi \neq 0) = \epsilon$.

H.1 Approximating state evolution and calibration with quantiles

In state evolution (B.2), the expectation term can be difficult to evaluate because of the ordering and the non-separability of the sorted norm. In addition, the convolution between Π and Z also makes the estimation difficult.

We propose the following method for estimation: denote q_D as discretized quantile function of distribution D at $\{\frac{1}{p}, \frac{2}{p}, \dots, \frac{p-1}{p}\}$. Denote Π as the true distribution of β , $\mathbf{\Pi}_p$ as p -variate Π with i.i.d. entries; π as Π/τ and $\boldsymbol{\pi}_p$ as p -variate π with i.i.d. entries accordingly. Similarly denote standard normals Z and \mathbf{Z}_p . Assume $\alpha \in \mathbb{R}^p$ is p -variate A with i.i.d. entries (in decreasing order). We can decompose

$$\begin{aligned}
& \mathbb{E}\langle [\operatorname{prox}_J(\mathbf{\Pi}_p + \tau \mathbf{Z}_p; \alpha\tau) - \mathbf{\Pi}_p]^2 \rangle \\
& = \mathbb{E}\langle [\operatorname{prox}_J(\mathbf{\Pi}_p + \tau \mathbf{Z}_p; \alpha\tau)]^2 \rangle + \mathbb{E}\langle \mathbf{\Pi}_p^2 \rangle - \frac{2}{p} \mathbb{E}[\operatorname{prox}_J(\mathbf{\Pi}_p + \tau \mathbf{Z}_p; \alpha\tau)^\top \mathbf{\Pi}_p] \\
& = \mathbb{E}\langle [\operatorname{prox}_J(\mathbf{\Pi}_p + \tau \mathbf{Z}_p; \alpha\tau)]^2 \rangle + \mathbb{E}\Pi^2 - \frac{2}{p} \mathbb{E}[\operatorname{prox}_J(\mathbf{\Pi}_p + \tau \mathbf{Z}_p; \alpha\tau)^\top \mathbf{\Pi}_p] \tag{H.1} \\
& \approx \langle [\operatorname{prox}_J(q_{\Pi+\tau Z}; q_{A\tau})]^2 \rangle + \frac{1}{p} q_\Pi^\top q_\Pi - \frac{2}{p} \operatorname{prox}_J(q_{\Pi+\tau Z}; q_{A\tau})^\top \mathbb{E}[\mathbf{\Pi}_p | \mathbf{\Pi}_p + \tau \mathbf{Z}_p = q_{\Pi+\tau Z}].
\end{aligned}$$

Such approximation for (H.1) is consistent and can be visualized in Figure 17. This is due to the fact that the ordering and the signs do not affect the sum of squares and the property of Riemann Stieltjes integral (see Johnsonbaugh and Pfaffenberger (2012); Kolmogorov; Rudin et al. (1976)).

Fact H.1 (Existence of Riemann Stieltjes integral). *Suppose f is continuous and g is of bounded variation. For every $\epsilon > 0$, there exists $\delta > 0$ such that for every partition $P := (a = x_0 < x_1 < \dots < x_p = b)$ with $\text{mesh}(P) < \delta$, and for every choice of points c_i in $[x_i, x_{i+1}]$, we have*

$$\left| S(P, f, g) - \int_a^b f(x) dg(x) \right| < \epsilon,$$

where $S(P, f, g) := \sum_{i=1}^{p-1} f(c_i)(g(x_{i+1}) - g(x_i))$.

We start with the simplest second term in (H.1). Set $f(x) = x^2$ and $g(x)$ to be cumulative distribution function of Π . Denote q_i as $\frac{i}{p}$ -th quantile. Setting $c_i = q_i$ and $P = (q_1, \dots, q_{p-1})$, then we have the approximate sum as

$$\begin{aligned} \frac{1}{p} q_{\Pi}^{\top} q_{\Pi} &= S(P, f, g) = q_1^2 \mathbb{P}(q_1 < \Pi < q_2) + \dots + q_{p-1}^2 \mathbb{P}(q_{p-1} < \Pi < q_p) \\ &= \sum_i \int_{q_i}^{q_{i+1}} q_i^2 dg(x) \rightarrow \int_{-\infty}^{\infty} x^2 dg(x) = \mathbb{E} \Pi^2. \end{aligned}$$

Similarly, for the first term in (H.1), denote the distribution to which the empirical distribution of $\text{prox}_J(\mathbf{\Pi} + \tau \mathbf{Z}; \boldsymbol{\alpha} \tau)$ converges as $\widehat{\Pi}$. By approximating the Riemann Stieltjes integral twice, we have

$$\langle [\text{prox}_J(q_{\Pi+\tau Z}; q_{A\tau})]^2 \rangle \rightarrow \mathbb{E} \widehat{\Pi}^2 = \text{plim} \mathbb{E} \langle [\text{prox}_J(\mathbf{\Pi} + \tau \mathbf{Z}; \boldsymbol{\alpha} \tau)]^2 \rangle.$$

For the last term in (H.1), we transform the term via the law of total expectation,

$$\begin{aligned} &\text{plim} \frac{1}{p} \mathbb{E}[\text{prox}_J(\mathbf{\Pi} + \tau \mathbf{Z}; \boldsymbol{\alpha} \tau)^{\top} \mathbf{\Pi}] \\ &= \lim \frac{1}{p} \mathbb{E}[\text{prox}_J(\mathbf{\Pi} + \tau \mathbf{Z}; q_{A\tau})^{\top} \mathbf{\Pi}] \\ &= \lim \frac{1}{p} \mathbb{E}_{\Pi+\tau Z} \left[\mathbb{E}_{\Pi, Z} [\text{prox}_J(\mathbf{\Pi} + \tau \mathbf{Z}; q_{A\tau})^{\top} \mathbf{\Pi} | \mathbf{\Pi} + \tau \mathbf{Z}] \right] \\ &= \lim \frac{1}{p} \mathbb{E}_{\Pi, Z} [\text{prox}_J(q_{\Pi+\tau Z}; q_{A\tau})^{\top} \mathbf{\Pi} | \mathbf{\Pi} + \tau \mathbf{Z} = q_{\Pi+\tau Z}] \\ &= \lim \frac{1}{p} \left(\text{prox}_J(q_{\Pi+\tau Z}; q_{A\tau})^{\top} \mathbb{E}_{\Pi, Z} [\mathbf{\Pi} | \mathbf{\Pi} + \tau \mathbf{Z} = q_{\Pi+\tau Z}] \right). \end{aligned}$$

Before we move on to the next section where we look at the conditional expectation term above, we pause to remark that the approximation via quantiles can be also used for computing the calibration (B.4): the calculation of $\mathbb{E} \|\text{prox}_J(\mathbf{\Pi} + \tau \mathbf{Z}; \mathbf{A} \tau)\|_0^*$ can be approximated by the number of unique values in $|\text{prox}_J(q_{\Pi+\tau Z}; q_{A\tau})|$.

H.2 Closed-form of conditional expectation

The challenge remains on computing the vector $\mathbb{E}[\mathbf{\Pi} | \mathbf{\Pi} + \tau \mathbf{Z} = q_{\Pi+\tau Z}]$. We will derive its closed-form by applying the inverse transform sampling on each entry. The effect of approximation using our explicit form is demonstrated in Figure 16.

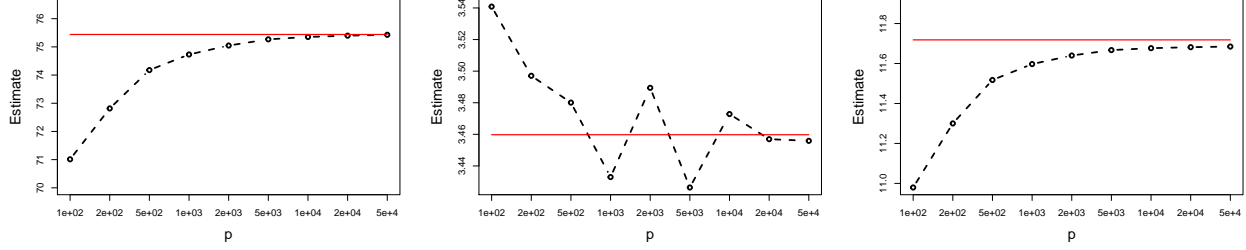


Figure 16: $\mathbb{E}\langle \text{prox}_J(\mathbf{\Pi} + \tau \mathbf{Z}; \mathbf{A}\tau)^\top \mathbf{\Pi} \rangle$ estimated by the quantiles and the closed-form conditional expectation (black dotted) against true expectation (red solid). Here $\delta = 0.3$ and $\mathbf{A} \sim \text{Exp}(0.2)/10$. Left: $\mathbf{\Pi} \sim \text{Exp}(0.1)$. Middle: $\mathbf{\Pi} \sim 10 \cdot \text{Bernoulli}(0.1)$. Right: $\mathbf{\Pi} \sim \mathcal{N}(2, 25)$.

For any $q \in \mathbb{R}$, denoting the support of $\mathbf{\Pi}$ as supp and the probability density function as $p_{\mathbf{\Pi}}$, we get

$$\mathbb{E}[\mathbf{\Pi} | \mathbf{\Pi} + \tau \mathbf{Z} = q] = \frac{\int_{\text{supp}(\mathbf{\Pi})} x \cdot \frac{1}{\sqrt{2\pi\tau}} \exp\left(-\frac{(q-x)^2}{2\tau^2}\right) p_{\mathbf{\Pi}}(x) dx}{\int_{\text{supp}(\mathbf{\Pi})} \frac{1}{\sqrt{2\pi\tau}} \exp\left(-\frac{(q-x)^2}{2\tau^2}\right) p_{\mathbf{\Pi}}(x) dx}.$$

Substitute $u = q - x$,

$$\mathbb{E}[\mathbf{\Pi} | \mathbf{\Pi} + \tau \mathbf{Z} = q] = q - \frac{\int_{\text{supp}(q-\mathbf{\Pi})} u \exp\left(-\frac{u^2}{2\tau^2}\right) p_{\mathbf{\Pi}}(q-u) du}{\int_{\text{supp}(q-\mathbf{\Pi})} \exp\left(-\frac{u^2}{2\tau^2}\right) p_{\mathbf{\Pi}}(q-u) du}.$$

Denote $s_q(u) := p_{\mathbf{\Pi}}(q-u) \exp\left(-\frac{u^2}{2\tau^2}\right)$, $S_q := \int_{-\infty}^{\infty} s_q(u) du$. Then $h_q(u) = s_q(u)/S_q$ is a normalized density of s_q . It can be viewed as a posterior density $h(u|q)$ with a Gaussian prior of u and $p_{\mathbf{\Pi}}(q-u)$ as evidence. Then

$$\begin{aligned} \mathbb{E}[\mathbf{\Pi} | \mathbf{\Pi} + \tau \mathbf{Z} = q] &= q - \frac{\int_{\text{supp}(q-\mathbf{\Pi})} u \cdot s_q(u) du}{\int_{\text{supp}(q-\mathbf{\Pi})} s_q(u) du} \\ &= q - \frac{\int_{\text{supp}(q-\mathbf{\Pi})} u \cdot h_q(u) du}{\int_{\text{supp}(q-\mathbf{\Pi})} h_q(u) du} = q - \mathbb{E}[U_q | U_q \in \text{supp}(q - \mathbf{\Pi})], \end{aligned}$$

where U_q is a univariate random variable with the density h_q .

Here we derive explicit formulae when the priors are Gaussian, exponential and Bernoulli. Two types of special generalization are worth mentioning: (1) when the support of $\mathbf{\Pi}$ is $(-\infty, \infty)$, the conditional expectation $\mathbb{E}[U_q | U_q \in \text{supp}(q - \mathbf{\Pi})]$ is indeed unconditional and the computation is simplified; (2) the cases of discrete priors can be easily derived in general besides the Bernoulli case.

Gaussian distribution When $\mathbf{\Pi} = \mathcal{N}(\mu, \sigma^2)$, we have $\mathbf{\Pi} + \tau \mathbf{Z} = \mathcal{N}(\mu, \sigma^2 + \tau^2)$, and $h_q(u)$ is the density of $\mathcal{N}\left(\frac{(q-\mu)\tau^2}{\sigma^2 + \tau^2}, \frac{\sigma^2\tau^2}{\sigma^2 + \tau^2}\right)$. Hence

$$\mathbb{E}[\mathbf{\Pi} | \mathbf{\Pi} + \tau \mathbf{Z} = q] = q - \mathbb{E}[U_q] = q - \frac{(q-\mu)\tau^2}{\sigma^2 + \tau^2} = \frac{q\sigma^2 + \mu\tau^2}{\sigma^2 + \tau^2}.$$

Exponential distribution When $\mathbf{\Pi} = \text{Exp}(c)$, we have $\mathbf{\Pi} + \tau \mathbf{Z}$ being an exponentially modified Gaussian (EMG) distribution. Then

$$s_q(u) = c \exp\left(-cq + \frac{c^2\tau^2}{2}\right) \left[\frac{1}{\sqrt{2\pi\tau}} \exp\left(-\frac{(u-c\tau^2)^2}{2\tau^2}\right) \right],$$

and h_q is the density of $N(c\tau^2, \tau^2)$. And, denoting $\xi = \frac{q-c\tau^2}{\tau}$, we get

$$\mathbb{E}[\Pi|\Pi + \tau Z = q] = q - \mathbb{E}[U_q|U_q \in (-\infty, q)] = q - \mathbb{E}[U_q|U_q < q] = \tau \left(\xi + \frac{\phi(\xi)}{\Phi(\xi)} \right).$$

Discrete distribution We begin with $\Pi = k \cdot \text{Bernoulli}(\epsilon)$ and then generalize to any discrete priors. Writing the density as $(1 - \epsilon)\delta(x) + \epsilon\delta(x - k)$, we have

$$\begin{aligned} h_q(u) &\propto [\epsilon\delta(q - u - k) + (1 - \epsilon)\delta(q - u)] \exp\left(-\frac{u^2}{2\tau^2}\right) \\ &= [\epsilon\delta(u - (q - k)) + (1 - \epsilon)\delta(u - q)] \exp\left(-\frac{u^2}{2\tau^2}\right). \end{aligned}$$

The last equality is true since the Dirac delta function is an even function. Hence

$$U_q = \begin{cases} q & \text{w.p. } (1 - \epsilon) \exp\left(-\frac{q^2}{2\tau^2}\right)/C \\ q - k & \text{w.p. } \epsilon \exp\left(-\frac{(q-k)^2}{2\tau^2}\right)/C \end{cases}$$

where $C = (1 - \epsilon) \exp\left(-\frac{q^2}{2\tau^2}\right) + \epsilon \exp\left(-\frac{(q-k)^2}{2\tau^2}\right)$. We get

$$\begin{aligned} \mathbb{E}[\Pi|\Pi + \tau Z = q] &= q - \mathbb{E}[U_q|U_q \in \{q, q - k\}] = q - \mathbb{E}[U_q] \\ &= q - q \mathbb{P}[U_q = q] - (q - k) \mathbb{P}[U_q = q - k]. \end{aligned}$$

where both probabilities are given above.

Remark H.2. It is easy to derive the conditional expectation for any discrete priors by writing the probability mass function as a sum of Dirac delta functions. In general, suppose the prior takes values in a_1, \dots, a_n with probability p_1, \dots, p_n , then U_q takes values $(q - a_i)$ with probability $\mathbb{P}_i = p_i \exp\left(-\frac{(q-a_i)^2}{2\tau^2}\right)/C$ where C is normalizing constant and the conditional expectation is $q - \sum_i (q - a_i) \mathbb{P}_i$.

H.3 Algorithm for state evolution term

Taking the quantile method and closed-form conditional expectation described in the previous sections, we present the following algorithm to compute the state evolution term efficiently.

Algorithm 2 Calculating $\mathbb{E}\langle [\text{prox}_J(\mathbf{\Pi} + \tau \mathbf{Z}; \mathbf{A}\tau) - \mathbf{\Pi}]^2 \rangle$ given $\mathbf{A}, \mathbf{\Pi}, \tau$

1. Derive quantiles $q_{\mathbf{A}}, q_{\mathbf{\Pi}}$
 2. Derive $D = \mathbf{\Pi} + \tau \mathbf{Z}$ by convolution and compute q_D
 3. Compute $G = \text{prox}_J(q_D; q_{\mathbf{A}\tau}) \in \mathbb{R}^p$, (notice that $q_{\mathbf{A}\tau} = \tau q_{\mathbf{A}}$)
 4. Compute $H = \mathbb{E}[\mathbf{\Pi}|\mathbf{\Pi} + \tau \mathbf{Z} = q_D] \in \mathbb{R}^p$
 5. Return $\frac{1}{p} [G^\top G + q_{\mathbf{\Pi}}^\top q_{\mathbf{\Pi}} - 2G^\top H]$
-

We give some simulation results on different dimensions. Since all three priors show similar patterns, only the exponential prior case is plotted.

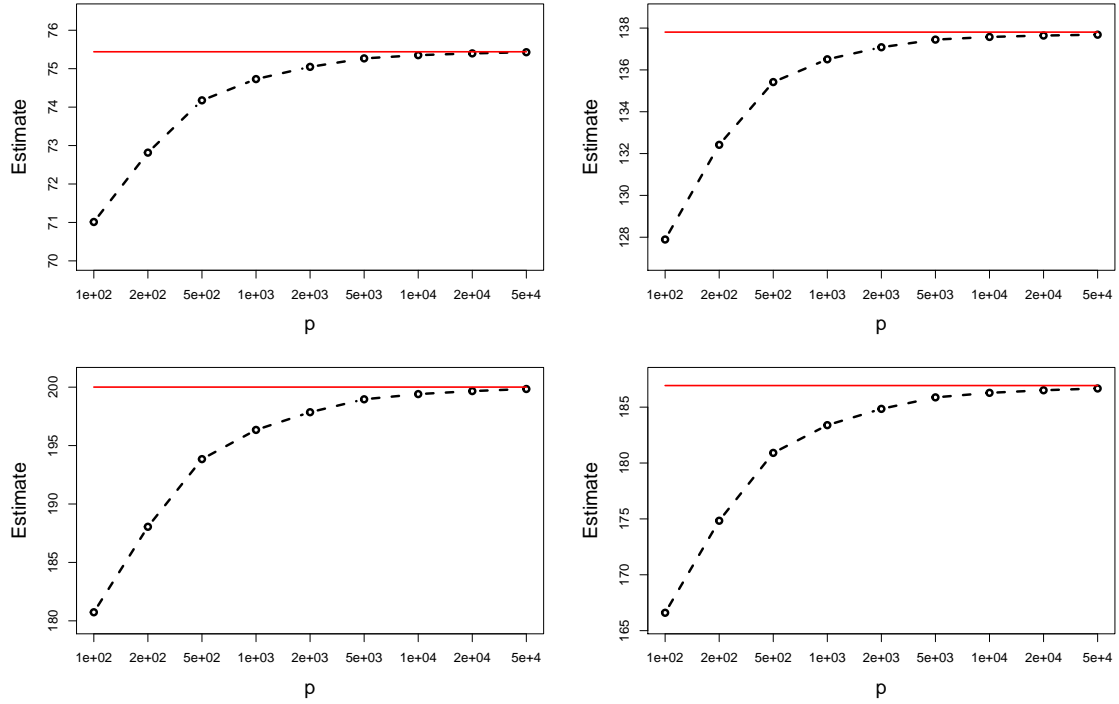


Figure 17: $\mathbb{E}\langle \text{prox}_J(\mathbf{\Pi} + \tau \mathbf{Z}; \mathbf{A}\tau)^\top \mathbf{\Pi} \rangle$ (top-left), $\mathbb{E}\langle [\text{prox}_J(\mathbf{\Pi} + \tau \mathbf{Z}; \alpha\tau)]^2 \rangle$ (top-right), $\mathbb{E}[\mathbf{\Pi}^2]$ (bottom-left) and $\mathbb{E}\langle [\text{prox}_J(\mathbf{\Pi} + \tau \mathbf{Z}; \mathbf{A}\tau) - \mathbf{\Pi}]^2 \rangle$ (bottom-right) estimated by the quantiles (black dotted) against true expectation (red solid). Here $\sigma = 0$ (no noise), $\mathbf{X} \sim \mathcal{N}(0, 1/n)$, $n/p = \delta = 0.3$, $\mathbf{A} \sim \text{Exp}(0.2)/10$, $\mathbf{\Pi} \sim \text{Exp}(0.1)$.